PASSIVE AND ACTIVE CONTROL DESIGN AND SIMULATION OF MICROCHANNEL HEAT SINK

A thesis

submitted

by

B. INDULAKSHMI

(Reg. No.4727)

for the award of the degree

of

DOCTOR OF PHILOSOPHY IN ENGINEERING

Under the guidance of

Prof. (Dr.) G. Madhu

SCHOOL OF ENGINEERING

COCHIN UNIVERSITY OF SCIENCE AND TECHNOLOGY,

KOCHI - 682 022

December 2017

PASSIVE AND ACTIVE CONTROL DESIGN AND SIMULATION OF MICROCHANNEL HEAT SINK

Ph. D Thesis under the Faculty of Engineering

Author

B. INDULAKSHMI

(Reg. No.4727)

Research Scholar

School of Engineering

Cochin University of Science and Technology.

E-mail: indulakshmi.d@gmail.com

Under the supervision of

Prof. (Dr.) G. MADHU

SCHOOL OF ENGINEERING

COCHIN UNIVERSITY OF SCIENCE AND TECHNOLOGY,

KOCHI - 682 022

December 2017

THESIS CERTIFICATE

This is to certify that the thesis entitled **PASSIVE AND ACTIVE CONTROL DESIGN AND SIMULATION OF MICROCHANNEL HEAT SINK** submitted by **B. Indulakshmi** to the Cochin University of Science and Technology, Kochi for the award of the degree of Doctor of Philosophy is a bonafide record of research work carried out by her under my supervision and guidance at the Division of Chemical Engineering, School of Engineering, Cochin University of Science and Technology. The contents of this thesis, in full or in parts, have not been submitted to any other University or institute for the award of any degree or diploma.

I further certify that the corrections and modifications suggested by the audience during the pre-synopsis seminar and recommended by the doctoral committee are incorporated in the thesis.

Kochi-682 022

Date 22-12-2017

Research Guide

Prof. (Dr.) G. Madhu
Professor
Division of Chemical Engineering
School of Engineering

DECLARATION

I hereby declare that the work presented in the thesis entitled **PASSIVE AND ACTIVE CONTROL DESIGN AND SIMULATION OF MICROCHANNEL HEAT SINK** is based on the original research work carried out by me under the supervision and guidance of **Prof. (Dr.) G. Madhu**, Professor, Division of Chemical Engineering, School of Engineering, for the award of the degree of Doctor of Philosophy with Cochin University of Science and Technology. I further declare that the contents of this thesis in full or in parts have not been submitted to any other University or Institute for the award any degree or diploma.

Kochi – 682 022

Date 22-12-2017

B. Indulakshmi

Research Scholar

ACKNOWLEDGEMENT

I would like to express my profound gratitude to Prof. (Dr.) G. Madhu, Professor, Division of Chemical Engineering, School of Engineering for his valuable guidance, timely advice and suggestions as research supervisor and also for being a source of constant inspiration and motivation during the course of my research work. I express my sincere thanks to him for the support given to me during each phase of my research work. I also extend my sincere gratitude to the doctoral committee, faculty members and staff of the School of Engineering, Cochin University of Science and Technology, for their support and help during my period of research.

My sincere thanks also to all my colleagues for supporting me during the period my research. I am thankful to the International Centre for Heat and Mass Transfer for providing a travel grant to attend and present my research paper in the International Symposium, held in Napoli, Italy.

I am very much grateful to the anonymous reviewers of my submissions to journals and conferences for providing constructive criticism for the improvement of my research work.I am greatly indebted to my family members for their motivation, encouragement, support and care extended throughout the course of the study. I was also benefited from the support and encouragement extended by a number of individuals during the course of this research work. My wholehearted thanks to all of them.

Last but not least, I thank God, The Almighty, for all the blessings bestowed upon me.

B. Indulakshmi

ABSTRACT

KEYWORDS: Heat transfer in microchannels, Phase changing materials, Electronics cooling, Dynamic thermal model, Control system modelling and simulation

Passive and active control design, modelling, and simulation of electronics cooling module employing microchannel heat exchanger are presented. Electronic systems used in various mission-critical applications such as high-performance computing devices, directed-energy weapons and communication systems of spacecraft call for the requirements to dissipate high heat flux in limited space. Dynamic thermal models for heat transfer processes in cooling modules used in typical electronic devices, dissipating heat to a coolant in microchannel array as well as to ambient by natural convection, have been developed. The model successfully accounts for the effect of the variation in operating atmospheric conditions which are significant in systems employed in harsh thermal environments. These heat transfer models can also be adapted to take care of the heat stored in the phase changing material storages introduced for the passive control of cooling modules. Simulations have been performed for a wide range of heat generation rates and appropriate coolant flow rates being set for a prescribed safe operating temperature of the processor. Passive control simulation of electronics cooling module with phase changing materials embedded within the available heat spreader shows that it can provide stable operation of electronic systems during peak heat loads as well as in extreme ambient conditions. Active control simulations for the thermal management in the similar electronics cooling module have been carried out using H_∞ controller and PIDcontroller for single phase cooling.A cascadecontroller is designed and simulated for the two-phase heat transfer in the microchannel.The

effectivenessof control actions are compared andthe maintenance of stable operating conditions are ensured.

The excessive power densities in electronic chips due to microminiaturization calls for dissipation of high heat flux in limited space which brings about multifaceted challenges for the development of electronics cooling solutions. This essentially necessitates the development of control strategies of heat exchanging devices used in such devices to maintain safe and reliable temperature levels while overcoming the peak heat flux removal demand. Nowadays microchannel heat exchangers are widely used for heat flux removal in limited space. Single phase liquid cooling microchannel heat exchangers have also limitations with escalating heat dissipation demand, wherein internal flow boiling of coolant in the microchannel is being projected as a promising option for dissipation of high heat flux in modern electronic cooling applications. Though it can provide an effective solution for high heat flux thermal management, limitations imposed by their support systems, excessive pressure drop and flow instabilities and critical heat flux bring challenges in its implementation in devices used in harsh environments. Passive cooling solution based on PCM storagesanalyzed in this work is a promising self-contained cooling solution to achieve efficient cooling. Active control endeavours in which the developed dynamic thermal models have been used for designing and simulating $H_\infty$and PID control strategies for single-phase forced convection in microchannels. Whereas, flow boiling in microchannel results in system instability due to pressure drop and oscillations.A cascade controller involving control loops for both pressure and temperature are designed and simulated for controlling boiling heat transfer in a microchannel-based cooling module.

TABLE OF CONTENTS

CHAPTER 1 INTRODUCTION

CHAPTER 2 LITERATURE REVIEW

CHAPTER 3 THEORETICAL MODELS AND CORRELATIONS

CHAPTER 4 DYNAMIC THERMAL SYSTEM DESIGN, MODELLING, AND ANALYSIS OF COOLING MODULES

CHAPTER 5 ACTIVE CONTROL SYSTEM DESIGN, MODELLING AND SIMULATION

CHAPTER 6 CONCLUSIONS

LIST OF TABLES

LIST OF FIGURES

ABBREVIATIONS

Computational Fluid Dynamics	CFD
Complementary Metal Oxide Semiconductor	CMOS
Carbon nanotubes	CNT
Critical Heat Flux	CHF
Chemical Vapour Deposition	CVD
Electrical Discharge Machining	EDM
Hybrid Electric Vehicles	HEV
Integrated Chip	IC
Integral of the square error	ISE
Integral of the Absolute value of the Error	IAE
Integral of the Time-weighted Absolute Error	ITAE
Joint Engineering Device Council of the Electronic Industries Alliance	JEDEC
Linear Quadratic Regulator	LQR
Microelectromechanical systems	MEMS
Microchannel heat sink	MCHS
Model Predictive Control	MPC
Network Equipment Building System	NEBS
Onset of boiling	ONB
Printed Circuit Board	PCB
Phase Changing Material	PCM
Perfluorocarbon	PFC
Proportional Integral Derivative	PID
Photo Voltaic	PV

Right-hand side	RHS
Robust Model Predictive Control	RMPC
Root Mean Square	RMS
Selective Laser Melting	SLM
Thermal Conductivity Enhancer	TCE
United States	US
Very Large Scale Integration	VLSI

NOTATIONS

English Letters

$\mathbf{A}$		Coefficient matrix
A_c	m^2	Area of cross section
a	m	The height of the rectangular microchannel
$\mathbf{B}$		Input matrix
Bg		Boiling number
b	m	The width of the rectangular microchannel
$\overline{C}$	W/K	Thermal conductance
C	J/K	Heat capacity
c	kJ/kgK	Specific heat
C_a		Capillary number
C_f		Friction coefficient
D_h	m	Hydraulic diameter
f		Fanning friction factor
G	kg/ m^2	Mass flux
Gr		Grashof number
g	m/s^2	Acceleration due to gravity
H	m	The height of the microchannel
h	W/m^2K	The convective heat transfer coefficient
h_{LV}	kJ/kgK	Latent heat of vaporisation
h_x	W/m^2K	The local convective heat transfer coefficient
h_{tp}	W/m^2K	The two-phaseheat transfer coefficient
K		Gain value

k	W/mK	Thermal conductivity
$k(x)$		Incremental pressure defect
$k(\infty)$		Hagenbach's factor
L	m	Length of fin
L^*	m	Half-length of fin
L_f	kJ/kgK	Latent heat of fusion
l	m	Length of the microchannel
M		The coefficient in correlation for boiling heat transfer
n		Number of fins in an array
Nu		Nusselt number
Nu_x		Local Nusselt number
P	m	The perimeter of microchannel cross section
Po		Poiseuille number
Pr		Prandtl number
p	N/m^2	Pressure
q	W/m^2	Heat flux
q_{ONB}	W/m^2	Heat flux at the onset of boiling
q_s	W/m^2	Surface heat flux
Re		Reynolds number
S	m	Spacing between fins
T	K	Temperature
t	s	Time
u	m/s	Axial velocity of the fluid

$\hat{U}$		Dimensionless velocity
W		Weight for PID control design
We		Weber number
w	m	The width of the microchannel
X		Martinelli parameter
x		Vapour fraction
y		Liquid fraction

Greek Letters

α		The aspect ratio of the rectangular microchannel a/b
μ	Ns/m^2	Viscosity
ξ		Dimensionless length factor
ρ	Kg/m^3	Density
σ	N/m^1	Surface tension
τ		Dimensionless time factor
Θ		Dimensionless temperature
ω	Rad/s	Frequency

Subscripts

CHF		Critical heat flux
e		Exit of the channel
i		Inlet of the channel
L		Liquid
S		Spacing between fins
s		Saturated vapour
tp		Two-phase

v	Vapour
$3W$	Three walls
$4W$	Four walls
∞	Ambient condition

CHAPTER 1

INTRODUCTION

Modern technical advancements call for the packaging of energy exchange in smaller device volumes, thereby necessitating high flux in the transfer process to carry out across the limited area. The emergence of Micro-Electro-Mechanical Systems (MEMS) requires increased heat flux dissipation in limited space. Thermal management is essential for the electronic devices to maintain their expected performance, to ensure reliability, and to safeguard from failure. Microchannel heat exchangers, with fluid flow passages of hydraulic diameter below 1 mm, have been widely used to cool electronics that dissipate significant amounts of heat. Usage of smaller dimension channels brings about better heat transfer performance amidst the various hurdles of realization and operational difficulties such as pressure drop. Effective operation of any heat exchanging devices needs an optimum control of the fluid outlet temperature, mass flow rates and maximization of heat transfer across fluid streams without incurring CHF. Towards this, the dynamic thermal modelling and simulation of microchannel heat sinks with multimode heat transfer have been carried out in the present work and are extended to explore various options of both passive and active control of heat exchangers. A typical microchannel heat sink (MCHS) dissipating the heat generated in an electronic chip to a coolant passed through an array of the microchannel as well as to ambient through an array of the fin by convection is shown in Fig. 1.1.

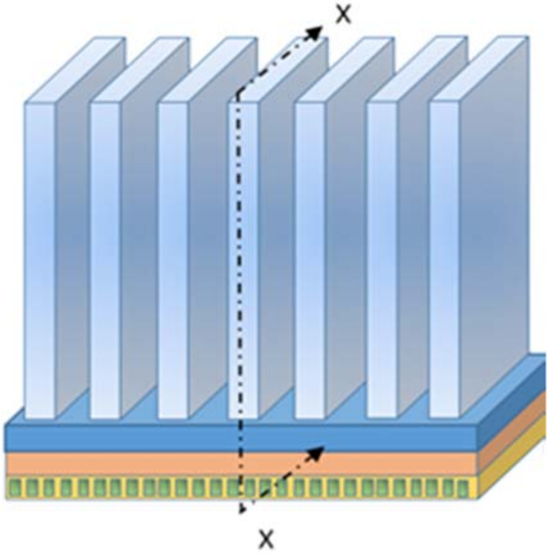

Fig. 1.1 A typical microchannel heat sink

1.1 AN OVERVIEW OF ELECTRONICS COOLING MODULES AND COOLING STRATEGIES

The operational reliability of electronic devices has been a challenge ever since its inception. Literature focusing on electronics cooling based on conduction cooled module (Oktay and Kammer 1982) can be found even in the era of vacuum tubes. Later the complementary metal oxide semiconductor (CMOS) based circuits were in practice for computing devices and endeavors to improve their clock frequencies demanded cooling levels beyond that air cooling can achieve. A desirable chip operating temperatures of CMOS device has a significant impact on device performance and reliability. Traditional electronics cooling methods include air cooling, liquid cooling, evaporation cooling, thermoelectric cooling, and jet impingement cooling. The MCHS has significant potential in electronics cooling arena ever since the pioneering work of Tuckerman and Pease (1981) which were designed to handle a heat flux of

790 W/cm^2 by maintaining substrate temperature at 71°C. Integration of MCHS into the chip has brought down the resistance in interfaces of heat dissipation path. Colgan(2007) demonstrated a single-phase Si microchannel for the single chip modules using fluorinated fluid for direct cooling. This maintains a low thermal resistance and providesa significant improvement in CMOS performance. The escalating heat generation rates in Very-large-scale integration (VLSI) circuits lead to the development of closed-loop two-phase microchannel cooling system (Jiang 2002) using electroosmotic pumping. Three-dimensional circuit integration of logic with memory, radio-frequency devices, optoelectronic devices, and MEMS on a single chip are under development. Koo (2005) proposed an integrated microchannel based 3D circuit and simulated the thermal model for the cooling system network. Microstructure heat exchangers (Brandner, 2007) fabricated using chemical etching or micromachining on metal, ceramics, and polymers foils can outperform conventional MCHS. Recently nanofluid microchannel heat exchangers(Wang, 2007) are being developed for a variety of applications due to enhanced thermal properties of such coolants. Heat transfer enhancement methods such as surface modifications of channels (Ahn, 2012) with special nanoparticle coatings, dimples, and protrusions can improve the performance of boiling in MCHS. Kandlikar (2012) summarized the status and research needs heat transfer research in microchannels in electronics cooling. Murshed (2017) recently reviewed the emerging techniques and fluids used for electronics cooling. Intel co-founder Gordon Moore made an observation in 1965 that the number of transistors per square inch on integrated circuits had doubled every year since their invention and power density of advanced microcircuits may reach several hundred W/cm^2. The peak power dissipation and heat flux from the high-performance microprocessors can reach about 360 W and 190 W/cm^{2}respectively, according to International Electronics

Manufacturing Initiative technology roadmap (Fig. 2). Development of an appropriate thermal model for fluid thermal transport processes in MCHS is essential in characterizing the performance and its enhancement.

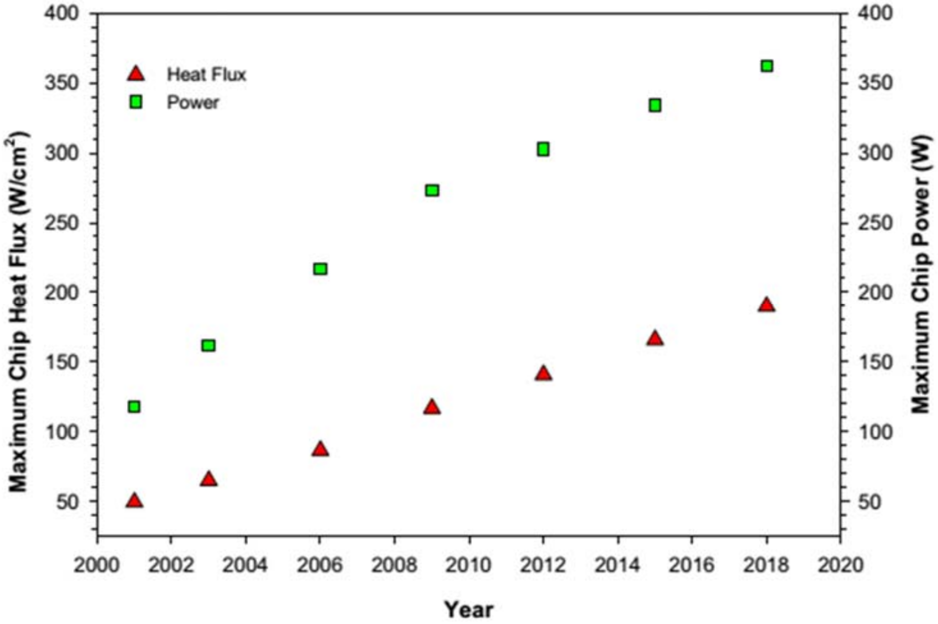

Fig. 1.2 Peak heat flux and power dissipation projections for the microprocessor (Murshed,2017))

1.2 CHALLENGES IN THE DEVELOPMENT OF EFFICIENT COOLING SOLUTIONS FOR HIGH HEAT FLUX APPLICATIONS

Need of adequate cooling to maintain the stability of electronic devices by avoiding overheating possibilities has been established in the preceding discussions. Air cooling has been widely used in most of the applications (Incropera, 1988) and direct liquid cooling maintaining direct contact between coolant and chips were developed towards the end of the 1980s. Single-phase cooling can only depend on the sensible heat of the coolant and there are inherent limitations posed for achieving the necessary heat dissipation effect. This essentially led to the development of two-phase cooling solutions which can make use of both sensible and latent heat to absorb a higher amount of heat than a single phase coolant can do. A large number of parallel mini/microchannel cooling circuits are established to circumvent the heat dissipation requirements that came up with advents in semiconductor lasers, hybrid electric vehicles, aviation electronics,and telecommunication devices. There are many challenges in the development of two-phase cooling solutions due to the lack of availability of reliable physical models that can accurately represent the phase changing phenomena and flow behavior in miniature passages. Mudawar (2013) summarized the challenges associated with two-phase cooling solutions for high heat flux applications.

Though two-phase microchannel heat sinks are suitable for electronics cooling solutions, there are many practical challenges imposed by boiling instabilities microchannels. Pressure oscillations generated in two-phase flow regimes inside microchannel can lead to severe pressure drop which in turn can adversely affect the functioning of the entire flow delivery system. CHF sets a thermal limit during the phase change occurs associated with heat dissipation beyond which efficiency of heat transfer drastically comes down. The occurrence of premature CHF is often triggered by two-phase flow instabilities due to the low mass flow rates of the coolants available in microchannels. Flow regimes during flow boiling and the development of unstable features during the occurrence of premature CHF conditions are shown in Fig. 1.3

Apart from the difficulties associated with two-phase systems during flow boiling, there are many challenges even in single-phase liquid cooling systems. Higher freezing points of commonly available eco-friendly coolants, such as water, prevents their use in electronics cooling. Glycol based antifreeze agents are essential to bring down the freezing points to the present industry requirement. This shall open up another difficulty in providing additional pumping power to overcome the pressure drop offered by viscous organic coolants. Usage of antifreeze agents may adversely affect the thermal properties and thereby bring down heat transfer effectiveness of the entire cooling system. The development of microchannel exchangers with improved heat transfer efficiency and minimized pressure drop has been a challenging task.

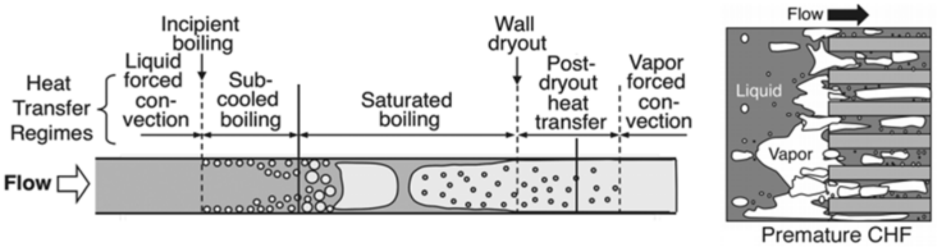

(a)Flow regimes during the flow boiling in a microchannel (b) Instability at CHF

Fig. 1.3. Challenges associated with two-phase flow in a microchannel (Mudawar,2013))

High fidelity experimentation of microchannel heat transfer leading to the revelation of multifaceted aspects of the involved physics is inherently difficult and expensive. Real-time in-situ measurements of heat flux, temperature,and pressure inside the miniature channel, to characterize the evolution of process during the high heat flux transfer, are essentially challenging due to size limitations (Kandlikar, 2006). Often temperature rise and pressure drop across the inlet and outlet plenums connecting an array of microchannels are only measured. Two-phase flow regimes in the presence of high heat flux transferring surface pose challenges in the visualization of the flowfield due to difficulties in providing optical access. Mixed overlap of flow regimes and intermittent wavy interfaces (Winkler, 2012) sets trouble in identifying flow regimes in two-phase flow. Expansion of gas, in microchannels using gaseous coolants, creates difficulties in measurement of mass flow rates in limited space by either constant pressure or volume methods. Estimation of heat transfer coefficients in flowfields with marginal temperature rise may become inaccurate. Not only in experiments, but deviation from continuum behavior also necessitates involved analytical methods. Lack of availability of reliable theoretical models and correlations leads to inaccurate estimates of heat transfer rates, which in turn affect control strategies for improving the performance of microchannel heat exchangers.

1.3 OBJECTIVES OF THE PRESENT RESEARCH

The objective of a dynamic thermal analysis of an electronics packaging is to model and simulate the heat transfer physics from the available theoretical/experimental models/correlations for each subsystem and characterize thermal behavior of components and coolant when the chip is subjected to various kinds of transient heat generation. Objectives of the present research include,

- To perform an extensive survey of available literature in the field of microchannel heat exchanger analysis and control. A state of the art comprehensive review of research publications in this very active research field is required to identify and develop the control strategies that are essential for efficient heat dissipation in modern electronic packages.

- To develop dynamic thermal models of electronic cooling modules which uses multimode heat dissipation methods. Most appropriate heat transfer models for each component of electronic cooling modules are to be identified from existing literature so as to bring together to analyze the multimode heat dissipation from the heat generating electronic chip.

- Thermal models that take care of variations in ambient conditions are essential for the analysis of cooling systems used in harsh environments. Dynamic thermal models are to be developed that accounts for the variations in ambient conditions.
- To analyze the performance of self-contained passive cooling solutions based on phase changing materials. Extensive simulations are essential to ensure the effectiveness of the proposed cooling solutions for various operating conditions of the equipment.
- To design the control strategies for active control systems to arrive at stable operating conditions for electronics cooling module and perform simulations for various states of its real-time functioning.
- To characterize the fluid flow and heat transfer in miniature channels, which forms the backbone of advanced cooling systems of the modern era, based on the various operating conditions.

1.4 OVERVIEW OF METHODOLOGY AND APPROACH

It is essential to identifythe appropriate physical model for heat transfer in various internal and external sub-systems of electronic cooling modules that are present in the heat dissipation passages. This includes resistances of single phase/two-phase flow and heat transfer in microchannels, natural convection/forced external convection in fin arrays, and various interfaces of components. Similarly, heat capacities of each sub-system are also accounted. Thermal circuits corresponding to the heat dissipation path with constituent components are to be framed. Energy balance is applied at each node of the thermal circuits. Resulting differential equations for each node are simultaneously solved to obtain the transient response of constituent components.

Effective self-contained cooling methods for high heat flux management in electronics cooling systems based on PCM are introduced in the present work, in order to circumvent issues associated with peak heat dissipation. Thermal circuits corresponding to the heat dissipation path are suitably modified for incorporating the presence of latent heat encapsulations. As mentioned before, differential equations based on the principle of energy balance are simultaneously solved and analyzed the effectiveness of PCMs in negotiating peak heat flux. This concept is augmented to introduce a variable area latent heat storage along the flow direction in the microchannel in order to check CHF.Active control strategies are also attempted to facilitate real-time control of system variables based on established practices in modern control theory. These control system designs, modelling, and analyses are carried out using the dynamic thermal system developed for MCHS. Controllers are designed for the various type of MCHS and analyzed the system stability to establish the robustness of controllers for various kinds of transient heat responses from the chip. A systematic study of cooling strategies adopted for electronic packaging based on passive self-contained mode and active real-time control mode are presented here. Matter presented in this thesis is as follows.

1.5 ORGANIZATION OF THE THESIS

Last few decades have witnessed unprecedented growth in research and development of MCHS for high heat flux applications. A comprehensive review covering the progress of cooling solutions of electronics and survey of associated experimental and analytical heat transfer, dynamics and control research is presented in chapter two. Reliability of the dynamic thermal system model developed for electronic packaging depends on the accuracy of the theoretical models for sub-systems. Chapter three provides a conscientious presentation of existing heat transfer theory and models associated with internal forced convection and flow boiling in mini and microchannels. Fourth chapter presents the progressive development of a dynamic thermal model for a self-contained cooling system based on PCM encapsulation. Transient response of various system components for various heat generation patterns have been assessed for various passive control strategies proposed in the present work. Developed thermal models finds application in real-time control applications also. Chapter 5 presents active control system design and simulations for single-phase internal convection as well as flow boiling in microchannel used in electronic cooling solutions. The concluding chapter (Chapter 6) of the thesis presents the summary of findings in the present work and the scope for further research. The bibliography is presented towards the end of the thesis.

CHAPTER 2

LITERATURE REVIEW

2.1 INTRODUCTION

Last few decades have witnessed unprecedented technological advancements in the field of electronics cooling. The overwhelming quest for increasing power densities, improving reliability, and bringing down the cost of electronic devices has been maintaining this as an evergreen field of research. With the advancing trends in miniaturization together with the capability advances in nano/micro-manufacturing processes have posed multifaceted challenges in heat removal from limited space. Though air cooling has been conventionally used to cool electronic devices, efficient cooling cannot be achieved from small surfaces with limited heat transfer coefficients. Liquid cooling systems based on mini/microchannel passages are introduced to negotiate the escalating cooling demand. But the extreme heat flux dissipation requirements encountered in communication systems, power electronics, and high-performance computing systems cannot be met by the possible sensible heat absorption in single-phase liquid cooling systems. Evaporative cooling methods have the advantages in terms of both heat removal capability as well as maintenance of uniform temperature while responding to fluctuating and high heat flux cooling demands. Development of support systems for two-phase cooling systems such as pumping devices to overcome excessive pressure drop and instabilityis inherently difficult due to the minimal size of the overall domain. Porous media flow and jet impingement cooling are also emerging as heat removal methods in direct cooling applications. Nanoparticle additives in base coolants have proven to improve heat transfer characteristics.

Thermal management using latent heat storage systems containing PCMs is now getting wide attention in the development of modern heat sinks for electronic components, Li-ion batteries,and PV cells, due to their capability to absorb heat and maintain the safe working temperature. A critical review of recent advancements, challenges and research opportunities in the field of thermal management of electronic devices, as well as heat exchangers in other high heat flux applications, are presented.

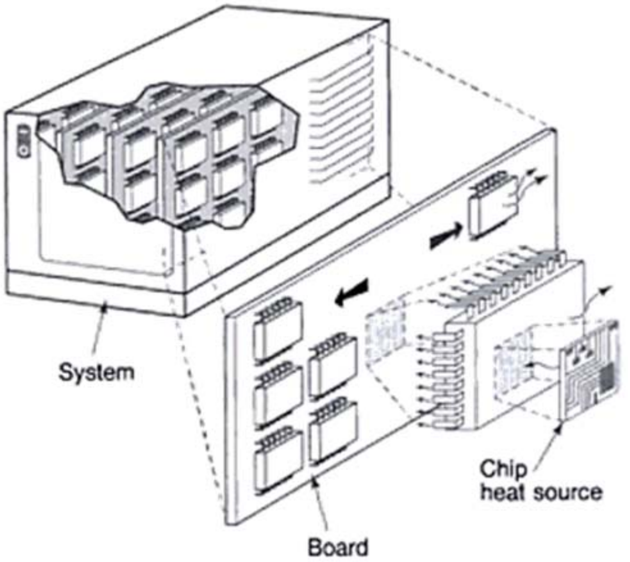

Fig. 2.1 Conventional architecture of an electronic system (Azar,1997)

The major objective of any thermal management system and its design consideration is to maintain the device temperature below a critical limit which can ensure safe and reliable performance under various operating and ambient conditions. Heat removal technology has been advancing to deal with evolving demands in functional density and speed of electronic devices so as to avoid heat-induced failure of devices.

The electronic chip is a small piece of silicon crystal embedded with multiple miniature electronic circuits. A package or a module has many such chips and their interconnections and are mounted on Printed Circuit Board (PCB). An electronic system may have multiple PCBs. A conventional architecture of an electronic system is given in Fig. 2.1. Heat generated in chips gets dissipated to local ambient through any path of least thermal resistance including the moulding material and leads used for signal transmission. Thus heat transferred to boards on which chips are mounted also suitably thermally coupled so as to enable necessary heat transfer. The system frame in which multiple boards mounting many electronic chip communicates with ambient by both convection and radiation. Azar (1997) gives various design considerations and strategies for conventional electronics cooling. Three important factors attribute to the cooling in electronics chips are the following (Azar, 2000)

- Dynamic switching current: -The current used in charging and discharging gate capacitance and interconnect capacitance in circuits
- Short-circuit current: -The current that flows between the power supplies during signal transitions.
- Leakage current: -The current that generated by sub-threshold conduction heat generation

Power dissipation is proportional to the capacitance of the logic elements, the square of the operating voltage swing, and the operating frequency (Hannemann, 2003). The evolution of heat flux generation in module levels for mainframe computers over the previous century (Chu, *et al.*1999), is given in

Fig. 2.2. If the number of components packed on a chip was about only few hundreds during 1960s, now it has grown up to the order of 109 components in chip of about a square inch. This, in turn, resulted in an escalation of cooling demand from 0.1 W/cm^2 to 100 W/cm^2. Lack of proper cooling arrangements may lead to failure of processors employed in critical applications because the failure rate of an electronic equipment is found to increase exponentially with temperature. The temperature of junctions in silicon semiconductor devices has to be limited to about 125°C for ensuring their safe operation. Often processors are subjected to drastic variations in operating conditions. This may lead to creep and associated damages due to thermal load cycling.

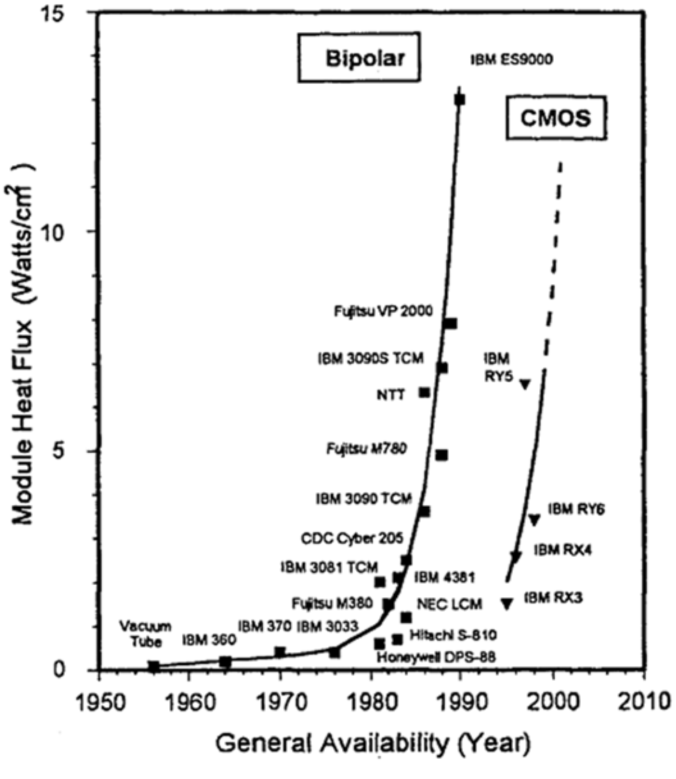

Fig. 2.2 Module level heat generation in mainframe computers developed during the previous century (Chu*et al.*, 1999)

2.2 ELECTRONICS COOLING METHODS AND RECENT TECHNOLOGY ADVANCEMENTS

It is already established in the preceding discussion about the need of advanced cooling applications for new generation electronic systems due to overwhelming hike in density integration, processing requirements, and miniaturization. The scientific community has been very keen in technology development associated with cooling of the electronics system due to technical issues and failure associated with overheating of components. According to an earlier study conducted by US Airforce, about fifty percent of malfunctioning issues associated with electronic devices are due to undesirable temperature build up. Vibration, humidity and dusty environments are the other major reasons for failure. Choice of a cooling method naturally depends on nature and extent of heat production in the chip and the heat transferring capability of the cooling method. Conventional cooling methods such as air cooling are not enough to meet the excessive cooling demand in modern electronics packaging. Whereas,the liquid cooling methods need heavier and complicated subsystems which require continuous performance monitoring. A comprehensive review on historical developments over the years, as well as the recent advances in electronics cooling technology, is presented to highlight the current status of the state-of-the-art cooling technology.

Various cooling methods for electronic devices include:

- Air cooling
    - Natural convection
    - Forced convection
- Liquid cooling
    - Natural convection (immersion)
    - Forced convection

  - Forced convection using nanofluids
- Two-phase cooling
  - Immersion in fluorocarbons
  - Cooling using solid phase changing materials
  - Flow boiling
- Spray and jet impingement cooling
- Heatpipes
- Thermoelectric cooler

Air cooling has been an attractive option during the inception period of semiconductor technology development due to ease of implementation and operation. Natural convection using air is preferred when cooling demand is minimum. This method does not require any auxiliary forcing mechanism for the movement of coolant as temperature induced density gradient to enable natural circulation. Hence troubles associated with noise, vibration, wear and tear of components of air blower can be avoided. About 10 times higher cooling rates than natural air convection systems can be achieved when air blowers are used with a penalty of increased costs, power, and complexity. A state of the art technology roadmap of earlier developments in air cooling, including theoretical and practical consideration in the design of cooling systems, has been compiled by Kim and Lee (1996). Industry requirements for cooling system design and performance evaluation shall conform to the regulations of the Network Equipment Building System (NEBS). Joint Engineering Device Council of the Electronic Industries Alliance (JEDEC) has also provided thermal characterization standards for packages. Often electronic package consists of vertically stacked PCBs, being cooled by an air stream. Researchers have attempted to provide optimum design of spacing to facilitate free convection through board interspace. Though air-cooling is a green technology, ever increasing heat dissipation demand has motivated researchers to explore more effective cooling methods.

Liquid cooling has been emerged as an alternative for limited capable air-cooling during the 1980s and became popular after its successful implementation in cooling of mainframe computers. Here the dielectric coolant fluids or hydrofluoroethers are in direct contact with the heat sources. Some applications such as aircraft electronics require complete isolation from local ambient and are often placed in enclosures to avoid the effects of varying ambient conditions. Liquid cooling offer higher convection heat transfer coefficients than air cooling systems. The components are immersed in dielectric fluids in direct cooling systems, whereas there exist a physical separation of coolant and component to be cooled in indirect cooling systems. Supercomputers evolved during that period such as ETA 10, Cray 2, Cray Y-MP, etc. used immersion cooling methods. Bar Cohen (1993) has provided a review of earlier inventions in immersion cooling methods using dielectrics like perfluorinated (PFC) fluids. Boiling of coolants is desirable with excessive heat dissipation demands. Recently various surface modification techniques have been evolved for the enhancement of boiling heat transfer with dielectric fluids. Leong *et al.* (2017) provided a comprehensive review of the pool and flow boiling enhancing surface features for dielectric fluids. Surface features that enhance boiling heat transfer can be created using advanced manufacturing techniques such as Selective Laser Melting (SLM) Chemical vapour deposition (CVD), Electrochemical deposition, and Electrical discharge machining (EDM). Typical surface features that enhance boiling on chip surface is given in Fig. 2.3.

Water is often used as coolant in indirect cooling systems employing heat exchangers due to its free availability, high thermal capacity, and low viscosity.

Though turbulent flows in forced convection systems can offer high heat transfer rates, high amounts of pressure drops also must be negotiated to establish the flow. Miniature pumping systems must be capable of overcoming the resistance offered by viscous effects. Additives to these coolants are used to avoid the possibilities of corrosion and freezing.

Fluorocarbon coolant encapsulated electronics modules make use of boiling at the exposed chip surfaces which can offer heat transfer coefficients of the order of 10^4 W/m^{2}K. Flow boiling in microchannel heat exchangers offer possibilities of even higher heat removal capabilities but flow instabilities and larger pressure drop in channels necessitate improved miniature pumping systems. Kandlikar (2012) presents a comprehensive review of single-phase liquid flow and flow boiling in microchannels which addresses their uses in high heat flux removal applications. Since work presented in this thesis focus on flow and heat transfer in microchannels, a review highlighting on technology advancements in microchannel heat exchangers is given later in this chapter.

(a) Particle sintering method (Sarangi*et al.*, 2015)

(b) Selective laser melting (Ho*et al.,* 2017)

Fig. 2.3. Advanced surface featuring for heat transfer enhancement

Improved heat transfer capabilities associated with nanofluids (a base fluid suspended with nano-sized particles) has open up an active research area in microelectrionics cooling. Nanoparticles made up of metals, dielectric, and semiconductors have size of the order of 1–100 nm. These particles are stably suspended in small volumes inside base heat transfer fluids, thereby remarkable improvement in thermal properties can be achieved. Nanoparticles/tubes/fibers in the form of dry powder is manufactured by inert gas condensation or chemical vapor deposition, thereafter it is dispersed in the base liquid. Choi (2009), who coined the term nanofluids, provides a state-of-the-art review of fundamental and applied research associated with its heat transfer enhancement. Jang and Choi (2004) introduced the concept of nanoconvection created by Brownian motion of nanoparticles which enhances the transport properties. Bang *et al.*(2005) demonstrated a remarkable enhancement of CHF in nanofluids. Thus nanofluids are ideally suited for high heat removal applications in limited space. Nguyen *et al.* (2007) demonstrated the application of Al_2O_3–water nanofluid for a microprocessor liquid cooling system. Jang and Choi (2006) found that heat transfer performance enhances by 10% in a microchannel heat sink with water-based nanofluids compared with that of a microchannel heat sink with water alone. Recently Bahiraei and Heshmatian (2017) demonstrated the use of biological nanofluid containing the silver nanoparticles electronic processor cooling application.

Jet impingement cooling makes use of liquid or gaseous high-speed jets impinging directly on the chip to be cooled so as to enable single-phase or two-phase heat transfer depending on surface condition and thermal properties of fluid used. Jet impingement can be classified as free-surface jet, submerged jet and confined submerged jet depending on the environmental condition of the interaction of jet with the surface to be cooled. These methods offer very high heat transfer coefficients and localised cooling on hot spots on electronic chips. Webb and Ma (1995) gave a comprehensive review of single-phase liquid jet impingement heat transfer.

The microjet cooling device proposed by Kercher *et al.* (2003) uses a vibrating diaphragm to transfer momentum to the surrounding fluid as shown in Fig. 2.4 This offer localized cooling for the hot spots and comparable cooling performance with that of conventional fans are obtained.

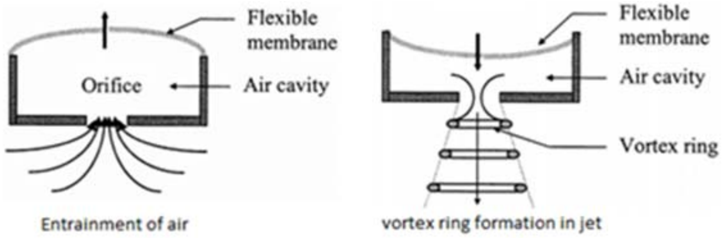

Fig. 2.4. The microjet cooling device (Kercher*et al.* (2003)

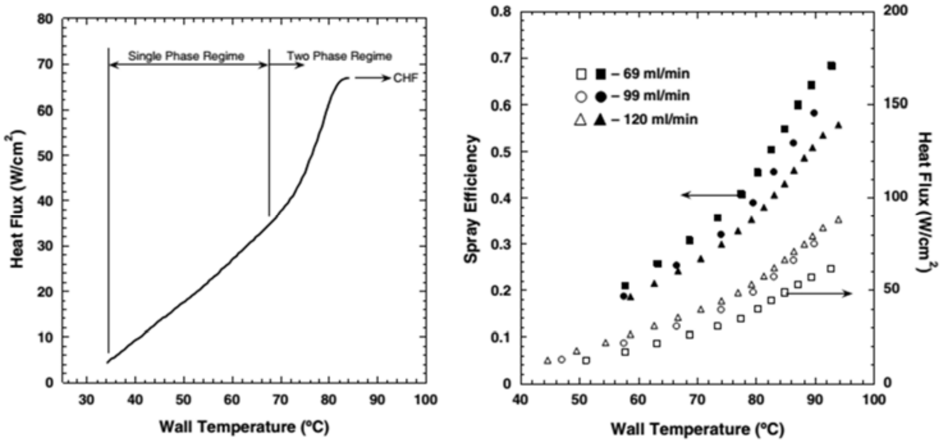

Fig. 2.5. Heat transfer characteristics for spray cooling system using FC72 (Kim, 2007).

Spray cooling offers higher heat dissipation due to the two-phase heat transfer enabled by microdroplets while impinging on a hot surface. Droplets of fluorocarbons are formed in fine nozzles by the larger pressure drop which can remove heat fluxes up to 200 W/cm^2 (Martínez-Galván*et al.,* 2013). The thermo-fluidbehaviour of droplet impingement is quite difficult to model due to the complex processes involved. Kim (2007) provides an overview of spray cooling for electronic cooling applications. Typical heat transfer characteristics obtained using spray cooling with FC72 is shown in Fig. 2.5. Higher wall temperature on surfaces enable droplets to undergo a phase change and thereby high amount of heat flux can be removed. Kandlikar and Bapat (2007) presents a comprehensive summary of the developments in jet impingement and spray cooling for high heat flux removal applications.

A heatpipe (Reay*et al.*, 2013) is an effective passive two-phase heat transferring device consisting of an evaporator, adiabatic section, and condenser. The working fluid is sealed inside a vacuum container and it evaporates when heat is added in evaporator region. Subsequently, it gets advected to condenser region due to the pressure difference and gives out its latent heat. Thereafter the capillary effect in wick brings the condensate to the evaporator again, thereby heat removal rates of the order of 10^2 W/cm^2 can be achieved without the involvement of any external driving mechanism. Howard and Peterson (1995) presentthe performance of a vertical array of heatpipes to cool a semiconductor base plate. Cotter (1984) introduced the concept of wickless microheatpipes for electronics cooling. He defined the micro heatpipe as *"channels which are so small, that the mean curvature of the vapor-liquid interface is comparable in magnitude to the reciprocal of the hydraulic radius of the flow channel"*.

Micro heatpipes offer very high thermal conductance even for feeble temperature gradients. Micro heatpipes are having the advantage of higher heat transfer coefficient as well as higher heat transferring surface area per unit fluid volume. Being a passive heat transferring device, this is ideally suited for microelectronics cooling applications. Sobhan*et al.* (2007) present a review and analysis of various types of micro heatpipe geometries. Nanofluids find application in high-performanceheatpipes used for high heat flux management. Tsai *et al.* (2004) used gold nanoparticles in base fluid for improving the thermal performance of heatpipe.

Solid state cooling devices make use of heat pumps that function based on thermoelectric (Peltier) effect which can provide cooling below the ambient temperature. Heat is transferred when an electric current passed between thermoelectric couple elements. Chein and Huang (2004) analysed the performance of thermoelectric cooler employed in the electronic cooling device using a microchannel heat sink. Li *et al.* (2005) claimed that nanostructured solid-state cooling devices can make use of the advantage of dispersion modification and quantum confinement can enhance thermal transport.

Venkatasubramanian*et al.* (2001) established that localized heat flux removal of up to 700 W/cm^2 is possible with thin-film thermoelectric devices made up of Bi_2Te_3 alloys. Chowdhury *et al.* (2009) integrated nanostructured Bi_2Te_3 thermoelectric coolers on electronic packages and achieved heat flux removal up to 1300 W/cm^2. Zebarjadi (2015) suggested that thermoelectric materials can be embedded in the fin geometry and is quite ideal for electronic cooling applications. Rowe (1994) compared various potential thermoelectric materials for electronic cooling. The non-dimensional figure of merit ZT of materials that are relevant to electronic cooling is given in Fig. 2.6

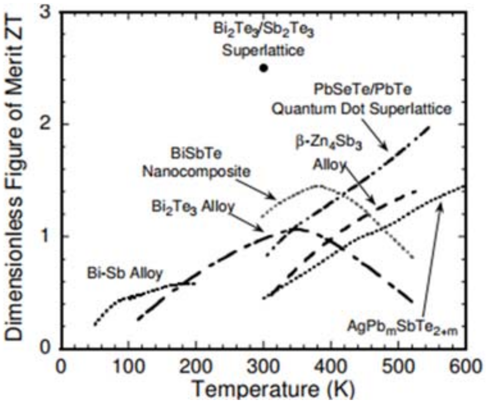

Fig. 2.6. Performance of thermoelectric materials for electronic cooling (Rowe, 1994)

An overview of various active and passive cooling strategies employed for electronics cooling are presented. A detailed review focus on the state-of-the-art advances in PCM based heat sinks is presented later in this chapter of the thesis since the present work primarily focuses on passive thermal control using PCM encapsulation. With the recent advent of novel methods, heat dissipation capability has been improved considerably. Fig. 2.7 provides an overall perspective of heat transfer coefficients and possible heat dissipation that can be achieved within a safe limit of temperature rise (say a minimum of 50°C) for major cooling options.

With the ever-increasing trend of heat dissipation, future technological research and development in electronics cooling shall focus on

- Material with higher heat spreading characteristics.
- Fluids with improvised thermal properties for single-phase liquid cooling.
- Phase changing fluids with quick response to absorbing high transient cooling demands.

- Microheatpipes that can be directly embedded for chip-level thermal management.
- Miniature jet impingement and spray coolers that can be installed for chip-level thermal management.

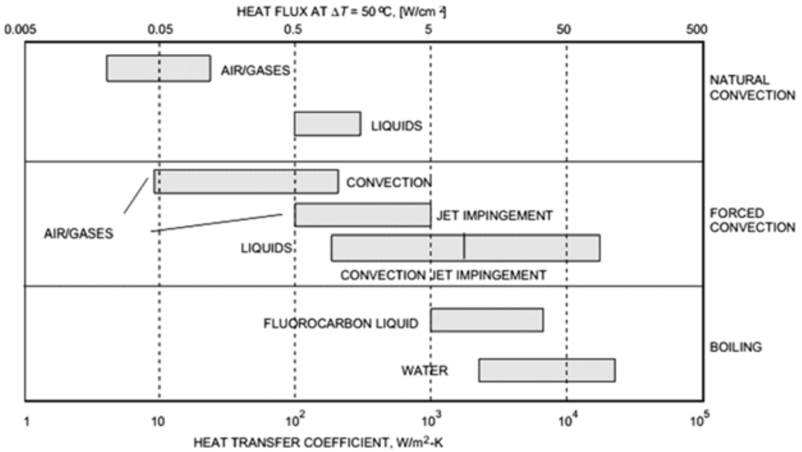

Fig. 2.7 Heat transfer coefficient for various heat removal/cooling techniques ZbigniewJ. Staszak (The electronics handbook / edited by Jerry C. Whitaker. — 2nd ed. 2005)

2.3 MICROCHANNEL HEAT EXCHANGERS

Unprecedented progress in micromachining technology enabled the technological advancements in microchannel heat exchangers for various engineering applications (Kandlikar and Grande, 2003). These technology developments complement the ever increasing demands on heat flux removal and temperature control arose due to the aggressive microminiaturization in modern MEMS devices and electronic packages. Microchannel heat sinks have an array of fluid passages, having hydraulic diameters of the order of few microns, which enable the dissipation of heat by either single phase forced convection or flow boiling without direct contact of the heat source with the coolant. Direct integration of coolant channels brings down the further addition of contact resistances in interface materials. An ultrathin heat sink design of Fu *et al.* (2012) fabricated using carbon nanotubes that can be directly integrated on-chip is shown in Fig 2.8.

Single phase cooling method depends only on sensible heat development of coolant whereas flow boiling options have the advantage of absorbing a greater amount of heat in the form of both sensible heat and latent heat. Coolant flow is subjected to a substantial pressure drop while carried through miniature passages. Therefore, fluid pumping systems integrated with microchannel heat exchangers should be able to negotiate such large resistances to flow. Though phase change of coolants offers larger heat removal capability and temperature control of heat developing surfaces, flow boiling initiates instabilities in fluid passages leading to enormous pressure surge and flow reversal. Kandlikar (2005) reviewed the major issues associated with high heat flux removal and formulated design procedure for single phase and two-phase microchannel heat exchangers. The descriptionon the physics of microchannel heat exchanging process is essential since the present work focuses on modelling, simulation, and development of various passive and active control strategies in high heat flux removal applications. A review on the advances in the area of fluid flow and heat transfer in microchannel heat sinks for electronic packaging applications is presented.

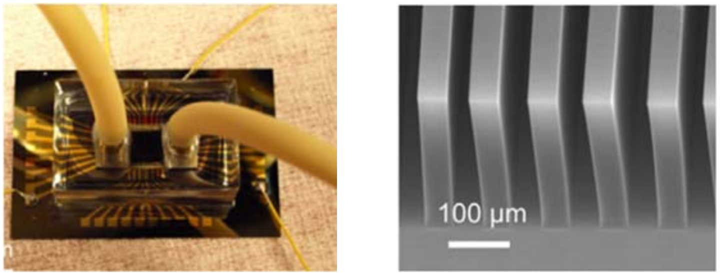

(a) Packaging (b) CNTmicrochannel cooling fins

Fig. 2.8 Ultrathin heat sink (Fu *et al.*, 2012)

2.3.1 Single Phase Internal Forced Convection in Microchannels

Ever since Tuckerman and Pease (1981) at Stanford University introduced the concept of microchannel heat sink with parallel coolant channels etched on a silicon substrate, great advances have come up in the last four decades about the enhancement of heat transfer from limited space using this technique. Though high heat transfer rates can be achieved using microchannels due to the fact that the heat transfer coefficient is inversely proportional to the hydraulic diameter of the channel; fluid flow in them is subjected to enormous pressure drop. Schematic of a simple microchannel array heat sink is shown in Fig. 2.9.

Microchannel heat sinks may have multiple parallel channels placed as an array and heat is absorbed in coolants while carried through these channels. Many experimental, analytical, and numerical simulation work have been reported in the recent past. These are aiming at design improvements of channels that can maximise heat transfer rate by maintaining minimum pressure drop.

According to an earlier dimension based criteria of Mehendale*et al*. (2000) channels above 6 mm are conventional channels and those below 100µm are called microchannels. They termed channels dimensions between 100 µm to 1 mm as meso-channels whereas those in the 1–6 mm range are compact passages. Often channels with hydraulic diameters between 200 µm and 3mm are termed as minichannels and those having hydraulic diameters between 10µm and 200 µm are termed as microchannels based on microscale effects observed in miniature channels (Kandlikar and Grande, 2002). The distinction between smaller diameter channels, minichannels, and microchannels is not universal across the available literature.

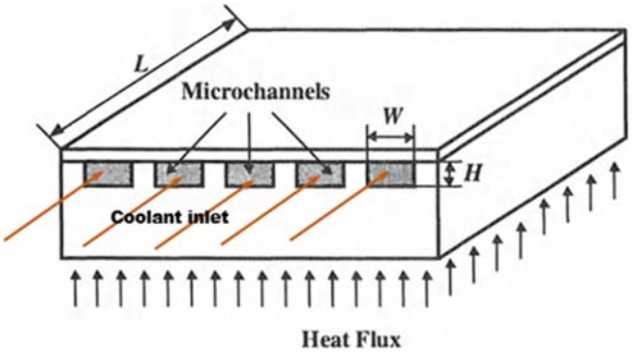

Fig. 2.9. Schematic of a simple microchannel array heat sink

Unlike the analysis of conventional scale channels, in microchannel flows, the characteristic dimensions tend to the same dimensions of hydrodynamic and thermal boundary layer thickness. This creates gradients in directions other than streamwise direction. Asthe characteristic dimension of flow shrinks, the effect of surface area dominates over volume and this enhance all transfer processes. Microscale gaseous flows exhibit local rarefaction near solid walls which bounds the flow, leading to velocity slip and temperature jump at the interface. Entrance effects dominate in miniature channels due to the reduced size. Surface features and roughness on channel walls are of the same order of dimension as of flow characteristics, factors such as friction factors must account for this size effects. There does not exist any fixed transition Reynolds number above which fluid turbulence is observed. Needless to say that aspect ratio and geometry of cross section of microducts also influence transport processes. Therefore, the entire theoretical and experimental considerations in the microchannel flow differ considerably from that of conventional channels. The anomaly of data across various experimental studies is quite common in this area of research. This also can be attributed by the difficulties encountered in measurements in microscale ducts. According to Palm (2001), classical theory on thermo-fluid dynamics cannot be applied for estimating friction and heat transfer effects in microchannels. A review of research articles published in the area of Fluid flow and single phase internal forced convection in microchannels is presented here to outline enhanced transport effects achieved in such geometries so as to make them ideal for high heat flux removal applications.

Peng *et al.* (1995) experimented the heat transfer characteristics of stainless steel plates containing rectangular microgrooves. They found that the heat transfer coefficient is independent of the wall temperature beyond a mode transition condition for transport phenomena of single-phase flow through the microchannel. Papautsky and Ameel (2001) present a systematic study of the results compiled out of various microscale single-phase internal flows. This includes measurements of flow rate, pressure drop, and friction factors estimated in microchannel flows of various kinds of fluids. Shen *et al.* (2004) also provide a summary of friction factors from salient studies of microchannel liquid flows. Wu and Cheng (2003) carried out experiments in various trapezoidal cross-section microchannels to assess the laminar pressure drop and convective heat transfer. They found that fluid flow and heat transfer characteristics are primarily influenced by geometric parameters, surface roughness and surface hydrophilic properties. Owhaib and Palm (2004) studied the heat transfer in single-phase flow of R134a through circular microchannels and compared their microscale and existing macroscale correlations. Gunnasegaran*et al.* (2010) numerically investigated the geometrical effect of microchannels such as size, geometry and aspect ratio on their thermal performance for various flow conditions. Experimental and numerical investigations of Chiu *et al.* (2011) has established that the channel aspect ratio is significant to the thermal performance (Fig. 2.10) and found that the thinner channels are performing better under high pressure drop.

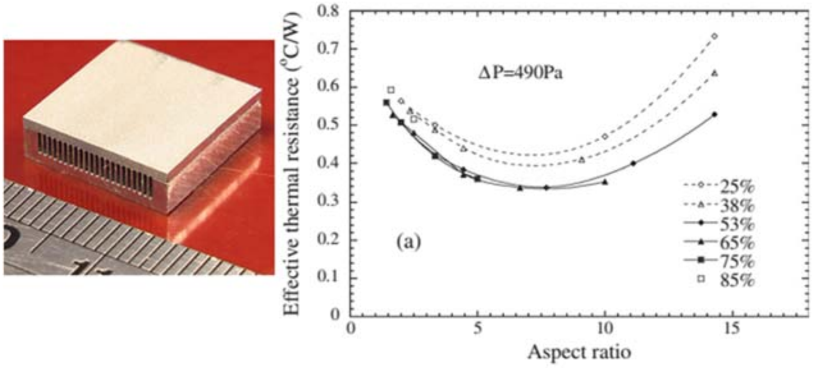

(a) Prototype of microchannel (b) Effect of aspect ratio on thermal resistance

Fig. 2.10.Studies on the effect of aspect ratio (Chiu *et al.*,2011)

Microscale gaseous flows exhibit different flow and heat transfer characteristics due to flow rarefaction. Rostami*et al.* (2002) summarizes the findings of experimental and theoretical works in the area of microscale gas flows and highlighted the effect of slip in solid-gas interfaces in various experimental conditions. Mala *et al.* (1997) hypothesised the presence of an interfacial electric double layer wherein an electrical surface potential alters the flow dynamics due to the restriction of the motion of ions. Hetsroni*et al.* (2005) found that the axial conduction in the fluid significantly influences the heat transfer in micro-channels. Morini (2004) outlined the deviations between the behaviour of fluids through microchannels and conventional sized channels and suggested for systematised study for arriving at suitable correlations.

The focus of microchannel heat exchange research has shifted towards heat transfer enhancement earlier in the current century. This aim at efficiency augmentation of single-phase heat transfer by a variety of passive and active methods to cater the imminent escalating cooling demands. Steinke and Kandlikar (2004a) reviewed the established practices of heat transfer enhancement techniques that can be brought in to the microchannel. Passive techniques create secondary flows by typical geometrical features that are intentionally provided on ducts. This includes rough surfaces, re-entrant boundaries, curvatures, and flow disruptions. These are capable of disrupting the developing thermal boundary layer and thereby enhance the thermal gradient at heat transferring boundaries. Active techniques include the forceful creation of pulsating flows, surface vibrations, and agitation using electrostatic fields. Bergles (2002) proposed to combine passive and active methods of enhancements for improved performance.

Many convoluted flow passages have also been experimented during the past decade to improve the thermo-hydraulic performance of microchannels. This is aimed at maintaining chaotic advection in fluid passages to improve transfer processes. Sui *et al.* (2010) experimented to assess the thermo-hydraulic performance of wavy microchannels. Centrifugal force generated while fluid is taken through curved passages leads to the generation of dean vortices that enhance heat transfer by sequentially thinning the developing thermal boundary layer. Wavy channels have higher heat transfer performance than straight counterparts and it maintains lower friction factors. Heat transfer performance in serpentine channels is dependent on geometry factors such as amplitude and wavelength as well as flow conditions (Al-Neama*et al.*, 2017).

Analytical modelling of flow and heat transfer in a straight microchannel of regular geometries and established correlations for estimating friction factor and heat transfer coefficient will be discussed later in this thesis.

2.3.2 Flow Boiling in Microchannels

Advantages of creating high heat transfer coefficients with the two-phaseflow in microchannels, due to possibilities of both sensible and latent heat absorption, has already been discussed in the preceding section along with the hurdles in implementing it as a feasible cooling solution. A comprehensive literature review on application of flow boiling in microducts for ultra-high heat flux removal applications is presented here. This includes an overview of available research work pertaining to visualization of complex two-phase flow patterns in microchannels, in situ measurements of flow variables, theoretical models and correlations. Thome (2006) presents a critical review of boiling and two-phase flows in microchannels.

Bowers and Mudawar (1994) presented an experimental study of pressure drop, the effect of subcooling, and critical heat flux (CHF) achieved in channel size of about 510μm and developed correlations. Boiling pattern depends on geometry, coolant flow rates, and extent of subcooling. Boiling in microchannels involves a cascade of events from bubble nucleation to slug flow, annular flow and forced convection of vapour before complete dryout as shown in Fig. 2.11. Mudwar (2001) observed significant changes in this sequence when mass velocity and subcooling at the inlet is reduced, formed due to Liquid film dryout, leading to very low CHF.

Smaller dimension of channels used in high heat flux removal applications brings substantial changes in physics of flow boiling than in conventional size channels. This will reflect in the extent of overall pressure drop and heat transfer. This highlights the requirement of theoretical models, flow pattern maps and correlations exclusively for flow boiling in microchannels. Triplett *et al.* (1999) observed slug and churn flow to be dominant in microchannel flow boiling for a wide range of operating conditions due to enhanced surface tension effects. Kandlikar (2002) observed that the acceleration pressure drop developed at higher heat fluxes is quite high. Cornwell and Kew (1992) performed experiments with R-113 in narrow rectangular channels and observed an annular-slug region dominant flow pattern through a glass window

Fig. 2.12 (a). Kasza*et al.* (1997) observed nucleating bubbles in the thin liquid films attached to the microchannel wall surface as shown in Fig. 2.12 (b). Vlasie*et al.* (2004) suggested that correlations developed for nucleate boiling in two-phase flow has reasonable agreement with the boiling of pure fluids in microchannels. There are contradictions across observation of flow pattern across available research publications.

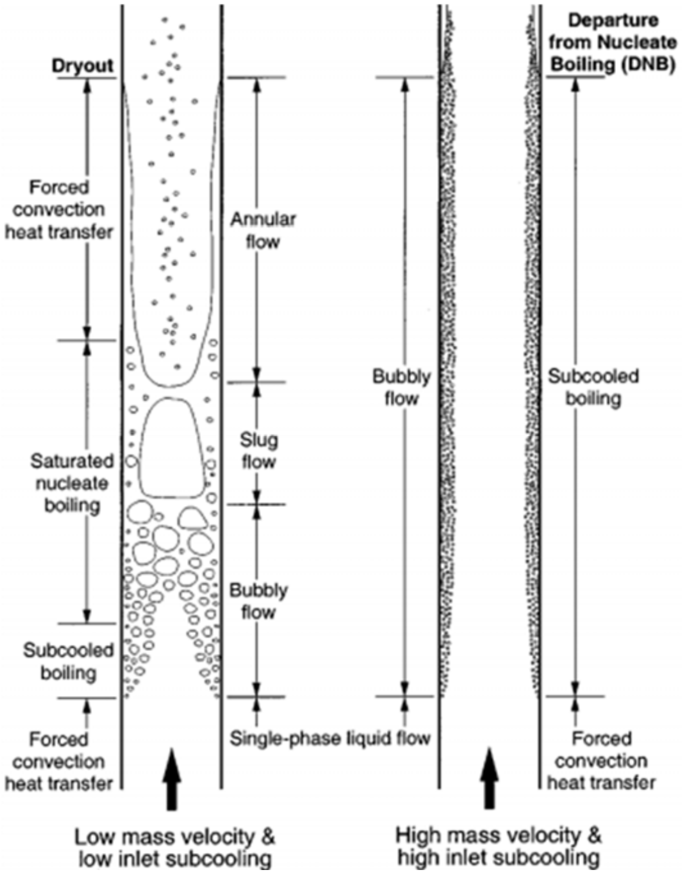

Fig. 2.11. Flow regimes during flow boiling in microchannles with various inlet fluid conditions. Mudwar (2001)

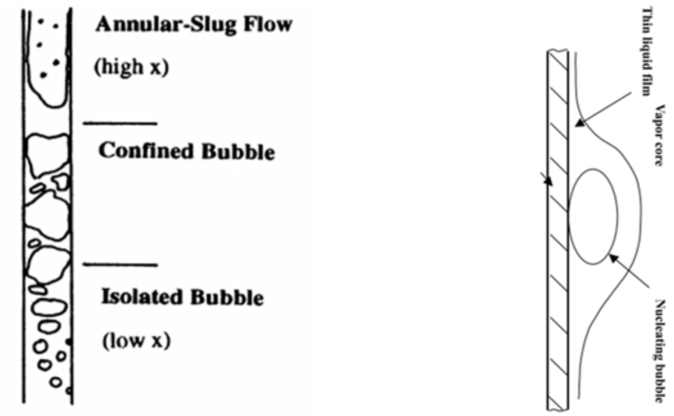

(a) Flow patterns (Cornwell and Kew,1992)

(b) Nucleation of thin liquid film in microchannels (Kasza*et al.*, 1997)

Fig. 2.12 Physics of flow boiling in microchannel

Instabilities created during the flow boiling in microchannels bring in multifaceted challenges in implementing it as a promising and reliable heat dissipation method in microsystems. Instabilities result in excessive pressure drop, wall temperature, mass and heat flux oscillations, and finally set in dryout. Sustaining oscillations creates may induce instabilities in subsystems due to excessive vibration and undesirable flow conditions. Control of such hostile situations will also be difficult due to fluctuations in all salient parameters involved. Huh*et al.* (2007) experimentally studied the aforementioned instability generation during flow boiling in a single microchannel. They visualized flow transitions across patterns of slug flow and semi-annular flow with the change in flow and heating conditions as well as extent of subcooling. Recently Saha and Celata (2016) compiled pioneering research advances in the field of instability in flow boiling in microchannels. Qu and Mudawar (2002) performed experiments with flow boiling of water in a set of parallel microchannels by applying heat flux up to 1.3MW/m^2. They observed vapour backflow induced flow instabilities (Fig. 2.13) which sets in early CHF condition. Bergles and Kandlikar (2005) provided an overview of the occurrence of CHF in microchannels.

During the recent past, the focus of research on flow boiling in microchannels has shifted towards exploring various methods that can bring down the instability and enhancement of heat transfer. Ebadian and Lin (2011) reviewed and suggested performance improvement for two-phase flow boiling heat transfer. Special surface features such as finned surface (Krishnamurthy and Peles, 2010) made of various kinds of geometries have experimented. Kandlikar*et al.* (2006) introduced the idea of providing artificially manufactured nucleation sites for stabilizing the flow boiling process. This has been effective in controlling the backflow phenomenon and significant control over pressure drop has been attained. Addition of nanoparticles also provides significant enhancement in flow boiling performance and improvement in CHF (Lee and Mudawar, 2007)).

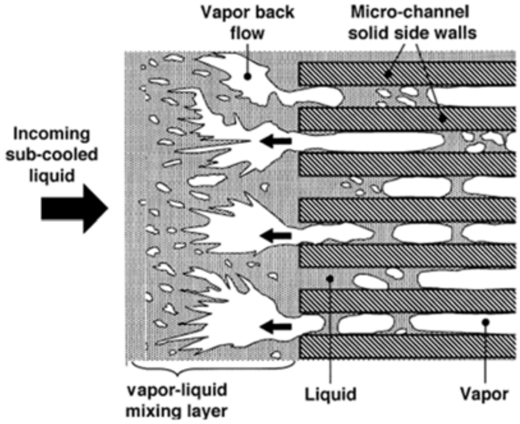

Fig. 2.13. Observation of Qu and Mudawar (2002) on backflow in near CHF condition

A complete revelation of the physical mechanisms involved in flow boiling is still imprecise. Analytical modelling of flow boiling in microchannels and established correlations for estimating heat transfer coefficient and CHF will be discussed later in this thesis.

2.4 TECHNOLOGY ADVANCEMENTS IN PCM BASED COOLING SOLUTIONS

Conventionally Phase change materials (PCM) are used in latent heat storage systems associated with renewable energy harvesting devices and waste heat recovery systems (Zalba*et al.*, 2003; Farid*et al.*, 2004; Sharma *et al.*, 2009). Abhat (1982) initiated the study on low temperature (0-120°C) latent heat storage materials and systematic approach towards the development of various latent heat storage systems. Thermal cycling tests are suggested to ensure the long-term stability of PCM. PCMshave also employed in typical electronic cooling applications wherein other conventional cooling methods are ineffective. This includes missiles and other airborne guidance systems, high energy weapon systems, and satellite systems. New innovative approaches to bring down sudden heat dissipation demands incorporates PCMs also in electronic packaging cooling solutions as well as component level thermal control. Cooling using latent heat absorption in solid phase changing materials have been proposed to circumvent the rapid cooling demand in portable devices. A concise review of the latest trends in latent heat storage system has been presented here.

Pal and Joshi (1998) used a honeycomb core filled with an organic PCM for the thermal management of an avionics module. Wirtz*et al.* (1999) demonstrated that the latent heat storage capacity of solid paraffin can be usedfor the development of PCM based hybrid heat sinks having efficient thermal control. Application of high-end processors in handheld devices (Wirtz, 2012, Ge*et al.* 2013,) have also mooted recent research interest in this field. Kandasamy*et al.* (2007) experimentally studied the feasibility of paraffin wax based PCM package for thermal management of portable electronic devices. These studies are extended (Kandasamy*et al.* 2008) for a heat sink used for the transient thermal management of plastic quad flat electronic package as shown in Fig. 2.14. Lei Shao *et al.* (2014) studied the application of a low melting temperature metallic alloy based PCM heat sink within a smartphone and proved that it can negotiate the thermal buffer during intermittent computations.Though PCMs can offer better cooling and maintenance of thermal stability during latent heat absorption, poor rate of heat diffusion in these materials calls for state-of-the-art techniques to improve heat transfer in latent heat storages. Various thermal conductivity enhancement methods have emerged in the recent past which synergistically complements the development of effective and compact PCM based thermal control solutions for electronics. Thermal conductivity enhancer (TCE) has become inevitable in developing quick acting, compact, and effective PCM based cooling solutions.

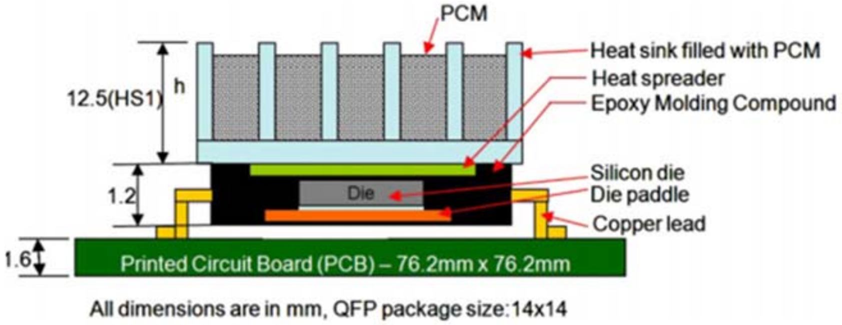

Fig. 2.14. Schematic of PCM filled heat sink (Kandasamy*et al.* 2008)

The effectiveness of operation of a TCE-PCM based heat sink depends on the extent of distribution of the TCE in PCM, fin geometry, material, and distribution pattern, geometry and volume of PCM storage, amount and type of heat dissipation demand from the heat source. Four categories of TCE-PCM options are shown in Fig. 2.15. Chintakrinda*et al.* (2011) compared the transient thermal performance of various enhancement options for PCM when they are exposed to high heat fluxes. The limited thermal conductivity of PCMs may affect the performance of heat spreaders. Fan *et al.* (2011) provided an overview of existing methods in thermal conductivity enhancement. Recently Sahoo*et al.* (2016) reviewed and presented the outcomes from studies on PCM based heat sinks used for electronics cooling. A summary of recent advances in TCE-PCM cooling solutions for electronics is given in Table 2.1.

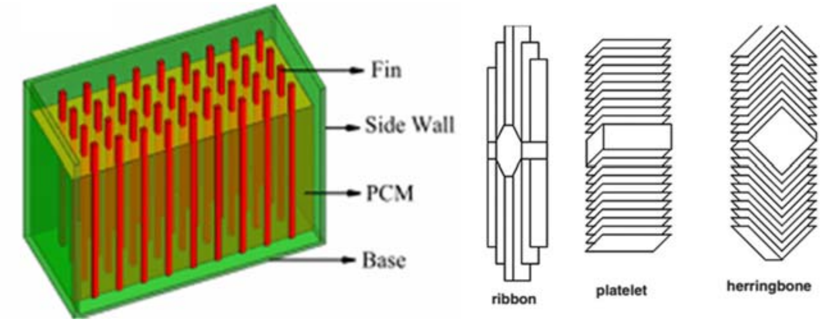

(a) PCM-based pin fin heat sink (Pakrouh*et al.*, 2015)

(b) Graphite nanofibers (Weinstein *et al.*, 2008)

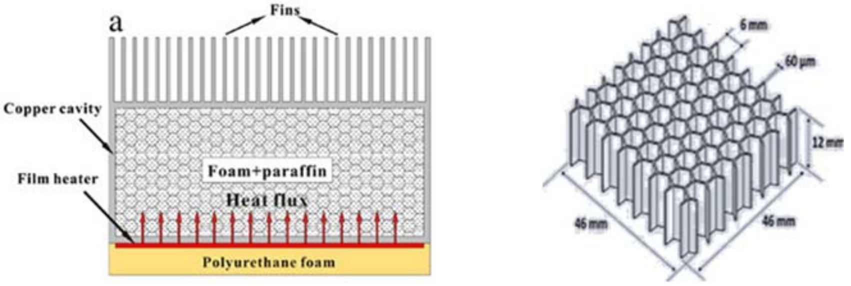

(c) Metal foam–PCM composite (Qu*et al.*, 2012)

(d) Honeycomb inserts (Mahmoud *et al.*, 2013)

Fig. 2.15 Thermal conductivity enhancers used for PCM based cooling

Table 2.1 Studies on thermal conductivity enhancement in PCM based electronics cooling systems.

Enhancement method	**Reference**	**Salient research outcome**
Internal fins	Shatikian*et al.* 2005	Numerical parametric studies to optimise height and thickness of fin to be distributed in PCM.
	Saha*et al.* 2008	Volume fraction of enhancer for thermal performance is found to be about 8% for Al pin fin placed in Eicosane
	Hosseinizadeh*et al.* 2011	Internal fins help to create convective fluid motion within the heat sink resulting in a higher melting rate
	Baby &Balaji 2012	The latent heating duration is more for the pin fin heat sinks.
	Levin *et al.* 2013	Optimal PCM percentages are inversely related to the range of temperature distribution in the PCM
	Fan *et al*. 2013	Use of internal fins could lower the maximum temperature inside the heat sink.
	Pakrouh*et al.* 2015	Addition of fins results in a lower melting time and base temperature
Additives in PCM	Khodadadi*et al.* 2007	Dispersion of nanoparticles enhances the thermal conductivity, lower the latent heat of fusion, and provide higher heat release rate
	Weinstein *et al.* 2008	Graphite Nanofibers enhance the performance of a paraffin PCM by improving the heat conduction and delaying the steady state
	Sanusi*et al.* 2011	Graphite nanofibers enhance heat diffusion, reduce the maximum temperature in the thermal containment unit and shortens solidification time.
	Chintakrinda *et al.* 2012	Rayleigh-Benard convection currents are supressed at higher nanofiber loading level and obtained control of the heatedbase.
Metal matrix composites and foams	Lafdi, 2008	Decreasing the foam porosity improves the performance of the heat sink
	Qu *et al.* 2012	copper metal foam with reduced porosity brings down the surface temperature and the time required to reach the melting point of PCM
	Mahmoud *et al.* 2013	Light weight honeycomb inserts give comparable thermal performance like fins placed in PCM
	Yang 2015	The metal foam placed in PCM enhance the melting process, alter the nature of melt front propagation
Hybrid methods	Weng 2011	Heatpipe placed in tricosane PCM improves the performance of an air cooled module

2.5 ESTABLISHED PRACTICES IN ACTIVE CONTROL OF HEAT EXCHANGERS

Heat exchange process automation is essential in developing efficient standalone cooling systems, wherein time-varying cooling demand and evolving process barriers, such as CHF, are to be successfully negotiated. Control techniques are to be developed for the proper manipulation of process variables such as the temperature of heat developing surfaces, the flow rate of coolants, and pressure drop in heat exchanger channels, so as to maintain the effective heat exchanging process. This essential to upkeep the reliability, operability, and safety of various subsystems involved in the system.

Mathematical models derived based on conservation principles can describe entire basic dynamic characteristics of heat exchangers. Transfer functions based on the solutions of the systems of partial differential equations governing the heat-exchange process are inherently difficult to analyse. Assumptions such as one-dimensional heat transfer and constant fluid properties are often invoked to simplify the governing equations so as to enable the development of model solutions that provide dynamics of thermal state variables. Real-time control strategies can be developed based on this time domain behaviour of the heat exchanger system. Models for microchannel heat exchanger control needs appropriate adaptation since classical thermo-fluid dynamic theories does not hold for heat exchangers with the miniature fluid passage. Khan and Fartaj (2011) reviewed theory and models available for the analysis of microchannel heat exchangers.

Conventional heat exchanger models can be broadly classified as distributed and lumped. An idealized plug flow without any mixing of particles of fluid is often considered in distributed models. Whereas, the heat exchanger is subdivided in to numerous volume units in the lumped type of approach. Past few decades have witnessed considerable progress in research in the field of control of conventional industrial heat exchangers. An early attempt to reduce the order of the system ismade by Shoureshi*et al.* (1978) where the infinite parallel and counter heat exchanger model is reduced to simple fourth order compartmental models. Mathisen*et al.* (1994) examine the important features of model accommodated by order of the model. The model features such as heat transfer coefficients, model order, temperature driving force, wall capacitance, flow configuration, fluid compressibility and pipe residence time are evaluated. Simpler models are found to fail in identifying inherent control limitations such as zeros in the right half plane. Different types of models of heat exchangers with distributed parameter are discussed by Abbasov*et al.* (2006). Different models with lower-order parameters are also proposed. Bilir (2002) conducted a numerical study on heat transfer in pipes under conjugated transient condition. A parametric study based on finite difference method has been carried out to investigate Peclet number, wall-to-fluid thermal conductivity ratio, wall-to-fluid thermal diffusivity ratio and wall thickness to inner radius ratio. The study concludes that the parameters have less effect on time to reach the steady state and the thermal inertia of the system depends mainly on flow conditions than on the wall characteristics. Nevriva*et al.* (2009) has also attempted similar method, wherein a set of the partial differential equations is solved numerically to simulate the steam superheaters of thermal power stations for the purpose of the steam temperature control system.

Taler (2015) developed a new method for numerical modelling of tubular cross-flow heat exchangers and applied for a row of tubes in a car radiator. This method is based on a control volume method in which as integral averaging of gas temperature has been implemented. This model is found to be appropriate for modelling of a plate fin and tube heat exchangers with gas temperature differences. A control mechanism is also developed to regulate the water temperature at the heat exchanger outlet. A model-based controller is developed to control the water outlet temperature by adjusting the fan revolutions number. This is compared with digital PID and found to have shorter settling time. Burns *et al.* (2014) developed numerical approximation methods based on an averaging scheme for optimal control of counterflow heat exchangers. A linear–quadratic regulator (LQR) problem is considered to check the convergence of the approximation method. Alotaibi*et al.* (2002) conducted a numerical simulation of thermal control of single-pass water-to-air cross-flow heat exchangers, where the temperature of outlet air is controlled by changing the water flow rate, using a proportional-integral (PI) controller. They simulated the control behaviour numerically and found to be an effective control methodology. An Input/output linearizing controllers are derived for full model and the reduced model by Heo*et al.* (2011) for a heavy duty counter-current heat exchanger. The heat exchanger is modeled by stiff hyperbolic PDEs with multi-time scale dynamics. The controller derived on the reduced model found to be robust to the modeling errors than the full model.

Maidi*et al.* (2008) developed a linear proportional–integral fuzzy controller for a shell-and-tube heat exchanger represented by partial differential equations and approximated by a finite-dimensional model of high order. An unconstrained optimization problem is formulated from the simplification of a formulated constrained optimization, where an integral error forms the objective function and the relationships between fuzzy and conventional PID gains forms the constraints. The proposed design approach provides a good approximation of the PDE and good tuning of the scaling factors. A similar effort is attempted by Pacheco-Vega *et al.* (2009) by developing an on-line fuzzy-logic-based temperature control for a concentric-tube heat exchanger.

The results are compared with the conventional PID controllers and found to provide smoother changes in the control actuators with similar performance.

Vinaya*et al*. (2012) attempted to develop a robust model predictive control (RMPC) for a shell and tube heat exchanger for controlling the temperature of a fluid flowing out of the heat exchanger. The performance of Model predictive control (MPC) is found to be superior to the PID controller. Bakošová*et al*. (2012) also used the same controller for tubular heat exchanger use in pre-heating petroleum by hot water, to control the output temperature of the heated stream at a reference value and minimize the energy consumption needed for petroleum heating. The study showed that the RMPC approach increases the quality of the control performance and decreases energy supplied to the heating medium.

The present review focused only on control of conventional industrial heat exchanger due to the lack of specific literature on microchannel heat exchanger control. An attempt has been made to develop models based on microchannel thermo-fluid dynamics in the present study and the evaluation of control strategies is carried out in line with the conventional approach.

2.6 SUMMARY

The unprecedented growth of microminiaturization in all facets of technology together with an augmentation of processing capabilities has fostered research in heat transfer in microscale and development of associated ancillaries. The present review figured out the need of cooling in electronic packaging in view of its inherent architectural constraints in heat dissipation. Ever growing heat dissipation demands calls for effective heat transferring methods that can dissipate more amount of heat by maintaining required surface temperature. Technology advancements from conventional air cooling to the microjet cooling have been reviewed to depict the underlying concepts and direction of impending research. A detailed survey of existing literature in a single phase as well as two-phase heat transfer in microchannel heat transfer has been carried out as it is an imperative theme of the present research. Physical evolution of complex flow features in two-phase flow is compiled from existing pioneering research publications. These are vital in the present subject point of view since it can result in functional difficulties as well. Research advancements in the phase changing material have been proven to synergistically complement not only cooling but also to assist conventional heat transfer methods. This has motivated towards the development of the idea of PCM assisted flow boiling for passive control of electronics cooling, which is one of the prime objectives of the present research. Finally, the background of control strategies of conventional heat exchangers is also appraised so as to extend the fundamental principles involved towards implementation of active control of microchannel heat exchanger envisaged in the present work.

CHAPTER 3

THEORETICAL MODELS AND CORRELATIONS

3.1 INTRODUCTION

The needof miniature flow passages in accomplishing higher amounts of heat transport rates, while carrying out cooling in limited space, has already established in the preceding chapter. Advantages of a higher surface to volume ratio in smaller diameter channels enable intimate contact with the heat transferring solid boundary. Often channel dimensions within a few hundred microns are termed as microchannel and the classification based on the size of the channel is quite arbitrary. Since the physics of thermo-hydraulics in such channels differ considerably from their larger counterpart, the term "microscale" has been coined to classify the studies belong to this scale. This is vital in the case of microscale gas flows in which electrokinetic effects and gas rarefaction effects brings in significant changes. Liquid flows though microducts above 1μm can be resolved with continuum theories. But specific issues, such as the transition from laminar to turbulent flow, are geometry and fluid dependent in microscale. Two-phase flow in microchannels exhibits distinct features in comparison with its conventional size counterpart. Therefore, specific models deduced out of rigorous experimentation/specific theories for the flow conditions have to be employed to ensure accuracy in analysis. Physical models and empirical correlations, that are available in the open literature for microchannels, are compiled and presented here for the purpose of developing specific dynamic models for simulation and control of heat exchangers employed in high heat flux removal applications.

3.2 SINGLE PHASE INTERNAL FORCED CONVECTION IN MICROCHANNELS

Theoretical models and correlations available for fluid flow and heat transfer in laminar single phase one dimensional steady incompressible Newtonian flows in microducts are presented. There is always a trade-off between internal forced convection heat transfer in ducts and the net pressure drop that the fluid is subjected to while transferred through it. These aspects become crucial in the case of microchannel heat exchanger. Because tiny pumps, that can transfer fluids through miniature fluid passages by overcoming excessive pressure drops, needs to be realised for achieving high heat transfer rates. Both pressure drop and heat transfer enhancement are evolved by the high surface to volume ratio effects. It is very convenient to extend from the well-developed theories of thermo-fluid mechanics of conventional channels towards the development of the accurate models and correlations applicable for fluid flow and heat transfer in microchannels.

3.2.1 Hydrodynamics of single phase microchannel flows

The frictional pressure drop (Δp) in a fully developed flow of an incompressible fluid in a pipe can be estimated by equating to frictional force experienced by the shear stress on its wall.

$$\Delta p = \frac{2(f\,\mathrm{Re})l\mu u}{D_h^{\,2}} \tag{3.1}$$

where μ is the viscosity of the fluid, l is the length of the duct, u is the mean velocity of the fluid, f is the Fanning friction factor and D_h is the hydraulic diameter $D_h = 4A_c/P$. Here A_c is the cross-sectional area of the channel and P is the wetted perimeter.

The Poiseuille number (Po) is the product of friction factor and Reynolds number and it depends on the channel cross section. This product takes the value 16 for circular ducts. But the rectangular cross section is often preferred in microchannel heat exchangers due to the expediency of manufacturing. Shah and London (1978) proposed the following polynomial for determining the Poiseuille number for rectangular microchannels as a function of aspect ratio (α, the ratio of height to width of the channel),

$$\begin{aligned} Po = 24(1 - 1.3553\alpha + 1.9467\alpha^2 - 1.7012\alpha^3 \\ + 0.9564\alpha^4 - 0.2537\alpha^5) \end{aligned} \tag{3.2}$$

Often the length of the microchannel in practical applications are kept minimum due to excessive pressure drop. This brings in the considerable effect of entrance length effects, as it extends to a significant length in the ducts. Overall pressure drop by combining the entrance and fully developed region, Equation (3.1) can be modified as

$$\Delta p = \frac{2(f\,\mathrm{Re})l\mu u}{D_h^2} + K(x)\frac{\rho u^2}{2} \tag{3.3}$$

Here $K(x)$ is the incremental pressure defect which is introduced to account the additional pressure drop in the entrance region. This will attain a constant value beyond the entrance length, known as Hagenbach's factor $K(\infty)$. Steinke and Kandlikar (2005) proposed a curve fit for this factor for rectangular channels as follows

$$\begin{aligned} K(\infty) = 0.6796 + 1.2197\alpha + 3.3089\alpha^2 - 9.5921\alpha^3 \\ + 8.9089\alpha^4 - 2.9959\alpha^5 \end{aligned} \tag{3.4}$$

Poiseuille number and Hagenbach's factor for fully developed laminar flow in rectangular channels (Shah and London, 1978) is given in Fig. 3.1. Laminar flow in sub-millimeter rectangular channel depends on its aspect ratio. Pengand

Peterson (1996) suggested the following empirical correlations for friction factor, a dimensionless quantity used to express friction losses in channels.

$$f = \frac{C_f}{\mathrm{Re}^n} \tag{3.5}$$

Here C_f is the empiricalfriction coefficient for laminar/turbulent flow. Value of n=1.98 for laminar flow and n=1.72 for turbulent flow. A comparison of friction factor estimates based on this empirical formula and experiments is given in Fig. 3.2. Peng*et al.* (1995) shown that laminar to turbulent transition happens in 200≤Re≤700 and is influenced by the aspect ratio of the channel.

3.2. 2 Heat transfer in single phase microchannel flows

Convective heat transfer characteristics also deviate considerably from conventional theoretical estimates, in which the Nusselt number in fully developed laminar flow is a constant. Deviations are also attributed to the real thermal and flow boundary conditions, surface roughness, entrance and exit effects, and axial conduction effects. Modelling of convective heat transfer in rectangular microchannel carried out in the present study assumes that the wall surface of the channel is provided with a constant heat flux condition both circumferentially and axially (often termed as H2 boundary condition). Shah and London (1978) proposed the following polynomial for determining the Nuselt number in rectangular microchannels as a function of aspect ratio.

$$\begin{aligned} Nu_{4w} = 8.325(1 - 10.6044\alpha + 61.1755\alpha^2 \text{-} 155.1803\alpha^3 \\ + 176.9203\alpha^4 - 72.9236\alpha^5) \end{aligned} \tag{3.6}$$

Dharaiya and Kandlikar (2012) carried out a numerical simulation to study heat transfer in developing and fully developed a laminar flow. The nusselt number in rectangular microchannels of various aspect ratios with H2 boundary condition obtained in the simulationare compared with correlation suggested by Shah and London (Fig. 3.3).

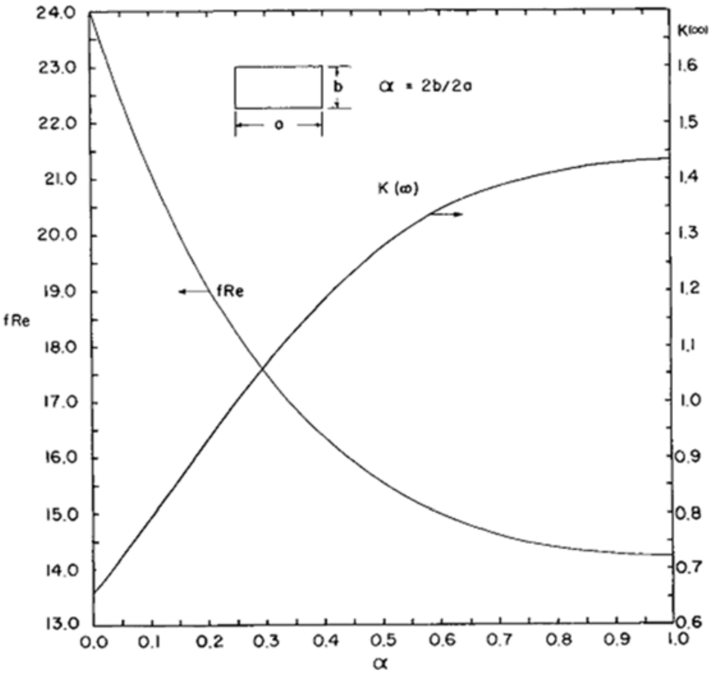

Fig. 3.1. Poiseuille number and Hagenbach's factor for fully developed laminar flow in rectangular channels (Shah and London,1978)

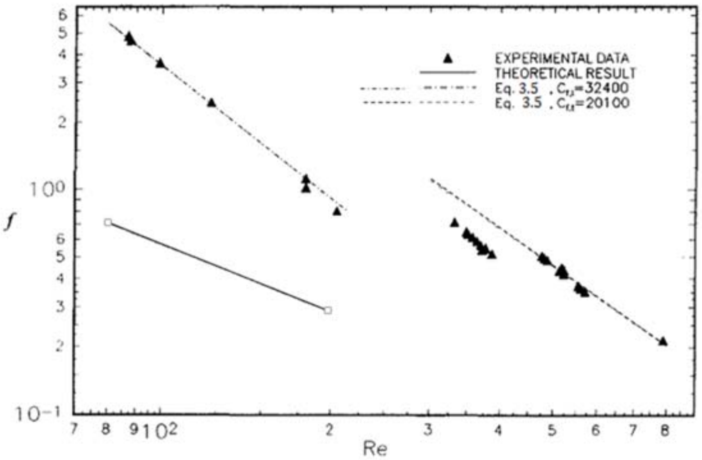

Fig. 3.2. A comparison of friction factor estimates in microchannel (Peng and Peterson,1996)

Dharaiya and Kandlikar (2012) suggested following correlation for rectangularmicrochannel with three walls heated under H2 boundary conditions based on their numerical simulation.

$$Nu_{3w} = 2.464(1 - 0.4319\alpha + 2.40355\alpha^2 - 1.708\alpha^3 + 0.4477\alpha^4 - 0.04864\alpha^5 + 0.001861\alpha^6) \quad (3.7)$$

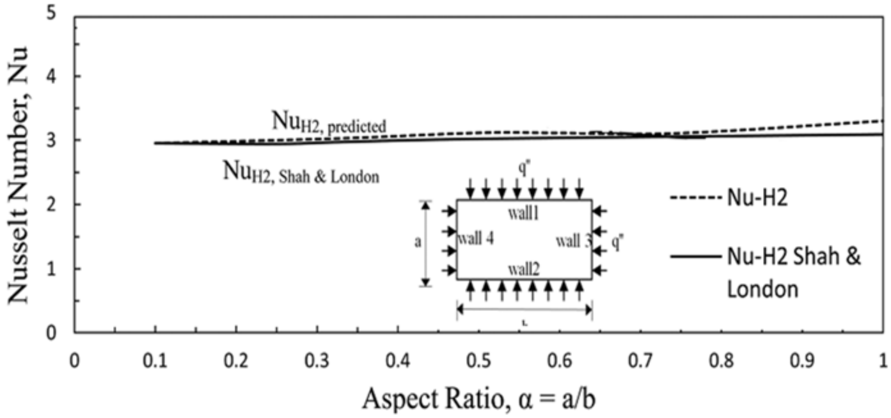

Fig. 3.3. Comparison of Nusselt number estimates in rectangular microchannels (Dharaiya and Kandlikar, 2012)

As discussed earlier, a considerable effect of entrance length in short microchannel also can influence heat transfer estimates. Philips (1987) studied this effect in thermally developing flow and worked out the localNusselt number in the entrance region of rectangular channels (Table 3.1). Philips (1987) suggested that the local Nusselt number in the entrance region of rectangular channels of (various aspect ratios) given with three side heating can be obtained from the data of four side heating (Table 3.1) and the ratio of fully developed Nusselt numbers of three side heating and four side heating as

$$Nu^*_{3w} = Nu^*_{4w} \frac{Nu_{3w}}{Nu_{4w}} \quad (3.8)$$

Axial length parameter used for expressing local Nusselt number is

$$x^* = \frac{x/D_h}{\mathrm{Re}\,\mathrm{Pr}} \quad (3.9)$$

Fig. 3.4 shows the axial variation of the localNusselt number obtained by Dharaiya and Kandlikar (2012) from their numerical simulation. The difference in local Nusselt number in the entrance region of the smooth and abrupt entrance is compared. It is evident that both types of entrance condition lead to the extension of the entrance region into the duct significantly.

Table 3.1 Nusselt number for thermally developing flow in rectangular channels (Philips, 1987))

$1/x^*$	$1/\alpha = 1$	$1/\alpha = 2$	$1/\alpha = 3$	$1/\alpha = 4$
1	3.6	4.11	4.77	5.35
10	3.71	4.22	4.85	5.45
20	3.91	4.38	5	5.62
40	4.45	4.84	5.39	5.87
80	5.33	5.7	6.21	6.63
100	5.69	6.05	6.57	7
140	6.32	6.68	7.22	7.63
160	6.6	6.96	7.5	7.92
200	7.1	7.46	8.02	8.44
400	8.9	9.2	9.9	10.4
10000	25.2	23.7	27	26.7

Peng and Peterson (1996) experimented with about a dozen different rectangular microchannel geometry and correlated laminar convective heat transfer for water as

$$Nu = 0.1165\left(\frac{D_h}{W_c}\right)^{0.81}\left(\frac{H}{W}\right)^{-0.79}\mathrm{Re}^{0.62}\,\mathrm{Pr}^{1/3} \tag{3.10}$$

Salient geometrical parameters involved in the above correlations are W - the width of microchannel, W_c - the centre-to-centre distance of microchannel, and H- height of microchannel. A comparison of the experimental results with correlation for Nusselt number (Eqn 3.10) is given in Fig. 3.5

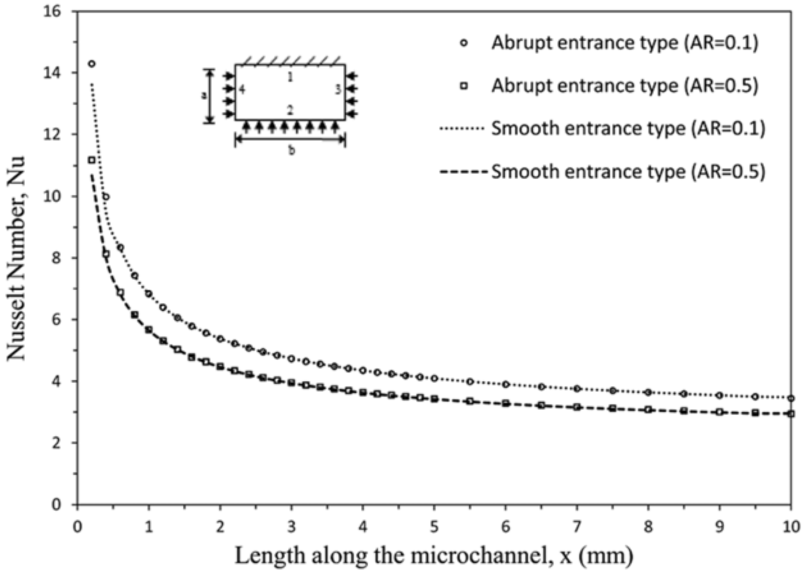

Fig. 3.4 Axial variation of localNusselt number in three side heated channel(Dharaiya and Kandlikar, 2012)

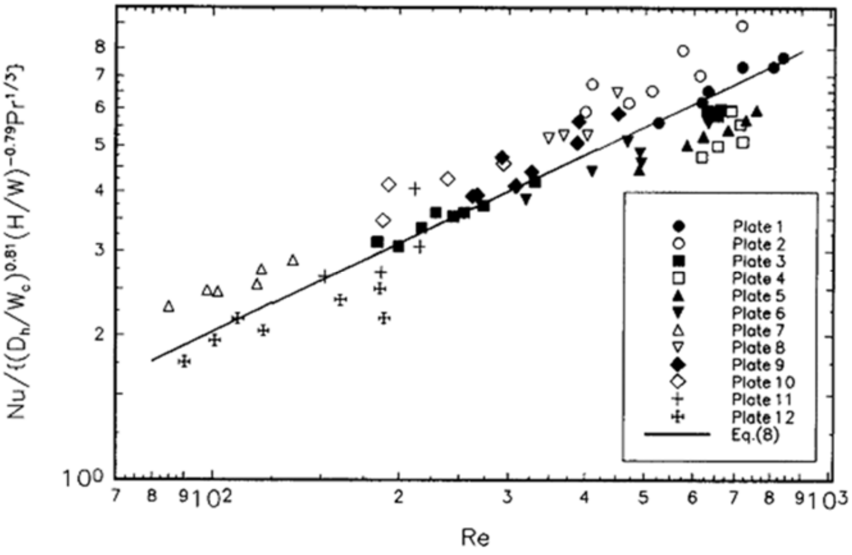

Fig. 3.5 Comparison of the experimental results with correlation (Eqn 3.10) of laminar heat transfer (Peng and Peterson, 1996)

3.3 FLOW BOILING IN MICROCHANNELS

Flow boiling in the microchannel is often preferred to meet requirements of heat dissipation as well as uniform surface temperature. Higher heat transfer can be achieved in flow boiling even with larger size ducts and it requires less pumping power. Researchers have achieved heat transfer coefficients of the order of few MW/m^{2}K (Steinke and Kandlikar (2004b), Qu and Mudawar (2004) Kennedy *et al.* (2000), Inasaka*et al.* (1989)) during the flow boiling in microchannels. Flow boiling systems necessitates continuous liquid flow to dry out avoid and further interruption in higher heat dissipation during the process. Critical heat flux (CHF) restrains the thermal limit of the boiling phenomenon, hence it sets the upper design limit for the phase-change cooling system. Present work envisages to model and simulates flow boiling in rectangular microchannels and its control. Therefore, the theories and correlations associated with estimates of CHF, pressure drop and heat transfer are abridged from the monographs (Yarin*et al.* ,2009; Kandlikar*et al.*, 2014; and Sobhan and Peterson, 2008) as well as relevant research publications.

3.3.1 Estimates for the onset of nucleate boiling

Subcooled liquid entry is preferred in two-phase heat transfer systems as it can offer high heat transfer rates and possibilities of rapid bubble growth can be avoided. The initiation of nucleation in flow boiling has to be identified for further requirements in the analysis of flow boiling. Hsu (1962) proposed a fundamental approach based on Clausius-Clapeyron equation applied to a spherical bubble formed in an artificial nucleation cite (cavity) together with the one-dimensional energy balance between solid surface and adjoining fluid medium. This analysis assumes that a bubble will grow outside the cavity if the bulk liquid is heated to achieve force balance at the bubble interface. At the onset of nucleate boiling (ONB), the difference in minimum vapour temperature in the vapor bubble (T_b) and saturation temperature (T_s) can be obtained as

$$T_b - T_s = \frac{2\sigma T_s}{r_b \rho_v h_{LV}} \tag{3.11}$$

Here $r_b$is the bubble radius, h_{LV} is the latent heat of vaporization, $\rho_v$is the vapour density, and σ is the surface tension.

Qu and Mudawar (2002) observed that small bubbles nucleate, grow and collapse near to its location of initiation and suggested to improve the aforementioned theory to take care of bubble growth as well as departure. Some of the earlier pioneering works (Bergles and Rohsenow, 1964; Sato and Matsumara, 1964) as well as recent work (Liu *et al.* ,2005)) suggested the wall superheat at the inception of nucleate boiling ($\Delta T_{s,ONB}$) for the initiation of boiling in forced convection for a given heat flux can be expressed in the form

$$q_{ONB} = M \frac{\rho_v h_{LV} k_L}{\sigma T_s} \left(\Delta T_{s,ONB} \right)^2 \tag{3.12}$$

where k_L is the thermal conductivity of the liquid.

Value of M may vary from 0.083 (Hsu, 1962) to 0.125 (Sato and Matsumura, 1964). Kandlikar (2006) carried out visualization experiments of flow boiling in microchannel and suggested for the application in rectangular microchannel

$$\Delta T_{s,ONB} = \sqrt{\frac{8.8 g \sigma T_s q_{ONB}}{\rho_v h_{LV} k_L}} \tag{3.13}$$

Dependence of saturation pressure on $\Delta T_{s,ONB}$ given in Eqn. (3.12) can be modelled in the form

$$\Delta T_{s,ONB} = M p^{\alpha} \left(q_{ONB} \right)^{\beta} \tag{3.14}$$

where the value of exponents are $\alpha \approx -0.5$ and $\beta \approx 0.5$

3.3.2 Correlations for frictional pressure drop and heat transfer

Total pressure drop in a horizontal microchannel, wherein a liquid undergoes a phase transition in a constant area duct, is attributed by pressure drops in a single-phase (including entrance effects), two-phase region, and acceleration due to evaporation. Fluid available at inlet regions may be in liquid phase and the correlations discussed in sec. 3.2.1 is valid till the ONB criteria are met. Similarly, this approach also can be used when the entire fluid has converted to vapour. Axial pressure drop at any location in the microchannel can be found in terms of liquid phase pressure drop and a two-phase multiplier as

$$\left(\frac{dP}{dz}\right)_{2ph} = \left(\frac{dP}{dz}\right)_{l} \times \left[1 + \frac{C\left(1-e^{-319D_h}\right)}{X} + \frac{1}{X^2}\right] \tag{3.15}$$

Above correlation suggested by Mishima and Hibiki (1996) is a modification of formulation suggested by Chisholm (1983). Here the value of C to be taken as five if both phases are laminar. The Martinelli parameter(X) for two-phase flow calculated based on frictional pressure drop based in each phase is

$$X = \sqrt{\left(\frac{dP}{dz}\right)_{L} \Big/ \left(\frac{dP}{dz}\right)_{V}}$$

Acceleration pressure drop for a homogeneous two-phase flow in which condition at entrance is only liquid

$$\left(dP\right)_{ac} = G^2 x_{exit}\left(v_V - v_L\right) \tag{3.16}$$

where x_{exit} is the exit quality of two-phase mixture, G is the mass flux of the working fluid, and the term inside parenthesis represents the specific volume difference between vapour and liquid specific volume. Quality at any section towards exit side is determined from inlet conditions based on energy balance as

$$x_e = x_i + \frac{4q''L}{GD_h h_{LV}} \tag{3.17}$$

where h_{LV} is the latent heat of vaporization.

Often, in practical applications, the microchannel is fed from an inlet plenum and the vapour expands towards a higher area at exit. Pressure drop due to these effects are not considered in the present study as inlet and exit plenums are absent. Lee and Mudawar (2005a) proposed a homogeneous equilibrium model (HEM) based on the assumption that there exist pseudo single-phase fluid (with mean properties) inside microchannels. This model could also account for the effects of kinetic energy changes, flashing, and compressibility during two-phase heat transfer. Therefore, a model which accounts for the liquid inertia, viscous, and surface tension can realistically portray the two-phase heat transfer process in a microchannel. Lee and Mudawar (2005a) modified Eqn. (3.15) to take care of these effects, applicable for laminar liquid and vapour, as

$$\left(\frac{dP}{dz}\right)_{2ph}=\left(\frac{dP}{dz}\right)_{l}\times\left[1+\frac{2.16\left(GD_h/\mu_L\right)^{0.047}\left(v_L G^2 D_h/\sigma\right)^{0.6}}{X}+\frac{1}{X^2}\right] \qquad (3.18)$$

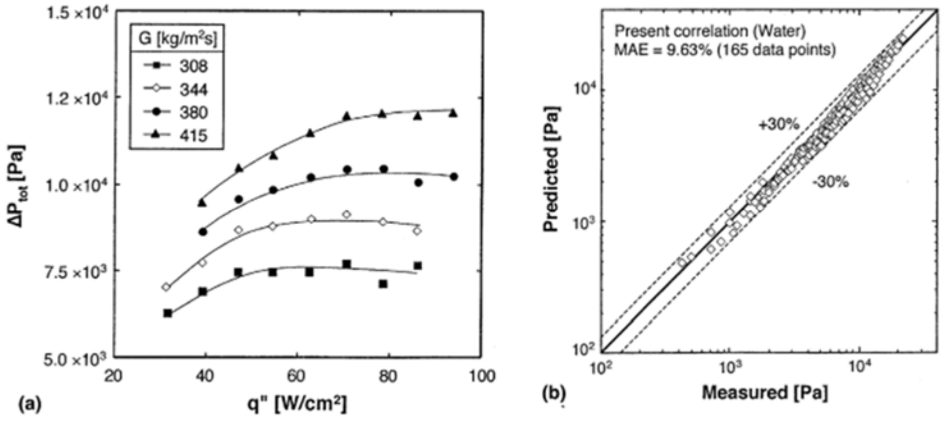

(a) Total pressure drop with heat flux (b) Comparison with experiment

Fig. 3.6 Pressure drop predictions in two-phase microchannelflow(Lee and Mudawar,2005a)

Terms cited in the numerator of the second term of RHS in parenthesis (Eqn. (3.18)), are respectively the Reynolds number and Weber number based on liquid properties. Pressure drop predictions and their comparison with experiments are given in Fig. 3.6. The accuracy mapped for the developed correlations are considered to be satisfactory due to the inherent instability and the difficulty in measurement in the miniature channel.

Prediction of two-phase heat transfer coefficient for flow boiling in microchannels has been attempted by many researchers. A summary of such correlations can be found in Qu and Mudawar (2004) as well as Steinke and Kandlikar (2004b). Kandlikar and Balasubramanian (2004) proposed a correlation for of two-phase heat transfer coefficient for Reynolds numbers below 100

$$h_{tp} = 0.6683 \frac{(1-x)^{0.8}}{\left\{\left[(1-x)/x\right]^{0.8}\sqrt{\rho_V/\rho_L}\right\}^{0.2}} h_L + 1058\left(\frac{q''}{Gh_{LV}}\right)^{0.7}(1-x)^{0.8} h_L F_{FS} \quad (3.19)$$

where h_L is the liquid only heat transfer coefficient described in Sec. 3.2.2., F_{FS} is the fluid surface parameter identified for a given fluid surface combination. This fluid surface parameter is taken as unity in the present analysis for water in microchannels.

Lee and Mudawar (2005b) suggested a general modification to be done for correlations for circular channels with uniform circumferential heating for adapting to use them for rectangular channels,

$$h_{tp} = h_{tp,c}\frac{Nu_{3W}}{Nu_{4W}} \quad (3.20)$$

Here Nu_3 and Nu_4 are the single-phase Nusselt numbers (Shah and London, 1978) for laminar flow with three-sides and four-sides wall heating respectively,

$$Nu_{3W} = 8.235\left(1 - 10883\,\alpha + 3.767\alpha^2 - 5.814\alpha^3 + 5.361\alpha^4 - 2\alpha^5\right)$$

$$Nu_{4W} = 8.235\left(1 - 2.042\alpha + 3.085\alpha^2 - 2.477\alpha^3 + 1.058\alpha^4 - 0.186\alpha^5\right)$$

A comparison of two-phase heat transfer coefficient predicted for rectangular channels with experiment is given in Fig. 3.7.

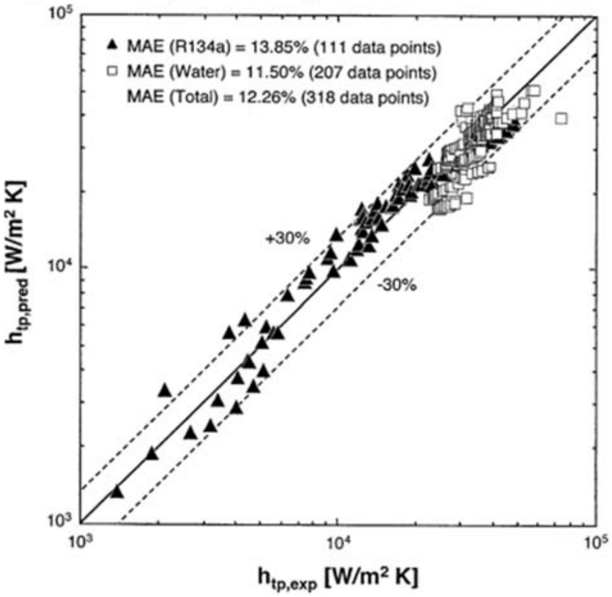

Fig. 3.7. Comparison of prediction of two-phase heat transfer coefficient with experiment (Lee and Mudawar,2005b)

3.3.3 Correlations for critical heat flux

Critical heat flux (CHF) indicates the upper heat transfer limit of a boiling equipment resulted by a sudden decrease in the heat transfer coefficient which leads to its failure due to uncontrolled rise in the wall temperature. Specific models and correlations developed based on extensive experimentation are essential to estimate CHF in microchannels. This is attributed to the typical flow boiling physics exhibited owing to the size constraints and enhanced wall effects experienced in microchannels. Correlations are developed based on the relative effects of various forces present in the boiling process. Dimensionless groups that appear in CHF formulations are boiling number $Bg = q_{CHF}/(h_{LV}G)$, Weber Number $We = G^2 D_h/\sigma\rho_L$, and Capillary number $Ca = G\mu_L/\rho_L$.

Kandlikar (2011) observed that bubble occupies the whole channel as soon as it nucleates. This aspect is identified as a limiting factor in the heat transfer during flow boiling in microchannels. He hypothesized that the stability of the flow depends on the balance of the inertia force of the liquid $\left(G^2 D_h / \rho_L\right)$ and the evaporation momentum force $\left[\left(q_{CHF}/Gh_{LV}\right)\times\left(D_h/\rho_V\right)\right]$ at the liquid-vapor interface between the vapour bubble and liquid. Kandlikar introduced a parameter $K_1 = \left(\frac{q_{CHF}}{Gh_{LV}}\right)^2\left(\frac{\rho_L}{\rho_V}\right)$ by taking the ratio of these forces.

Hall and Mudawar (2000) proposed the following statistical correlation for CHF in microchannels with subcooled liquid entry, as

$$Bg = \frac{C_1 We^{C_2}\left(\rho_L/\rho_V\right)^{C_3}\left[1 - C_4\left(\rho_L/\rho_V\right)^{C_5} x_i\right]}{1 + 4C_1C_4We^{C_2}\left(\rho_L/\rho_V\right)^{C_3+C_5}\left(L/D_h\right)} \tag{3.21}$$

Values of the constants in the above formulation are C_1=0.0722, C_2 = 0.312, C_3 = 0.644, C_4 = 0.900, and C_5 = 0.724.

x_i is the quality at the inlet of the channel. This formulation is developed using 4860 data points and predicted CHF with an RMS error 14.3% when compared with experimental results (Fig. 3.8).

Zhang *et al.* (2006) evaluated the existing models for CHF in smaller size channels and reliability in their prediction capability are analysed. They proposed the following correlation for saturated flow boiling by performing artificial neural network and parametric trend analyses,

$$\begin{aligned} Bg = 0.0352\left[We + 0.0119\left(L/D\right)^{2.31}\left(\rho_V/\rho_L\right)^{0.361}\right]^{-0.295} \times \\ \left(L/Dh\right)^{-0.311}\left[2.05\left(\rho_V/\rho_L\right)^{0.17} - x_i\right] \end{aligned} \tag{3.22}$$

This correlation has claimed to have a total mean deviation of 16.8% in comparison with experimental database of small-diameter channels (Fig. 3.9).

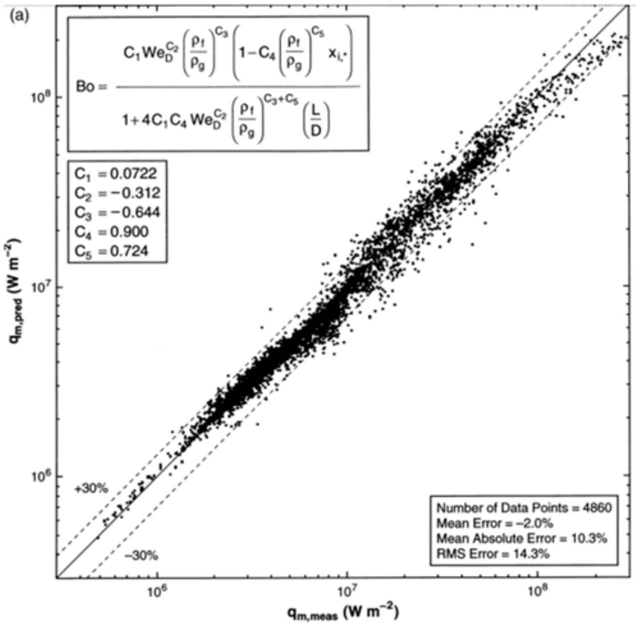

Fig. 3.8 Comparison of predicted and measured values of CHF Hall and Mudawar (2000)

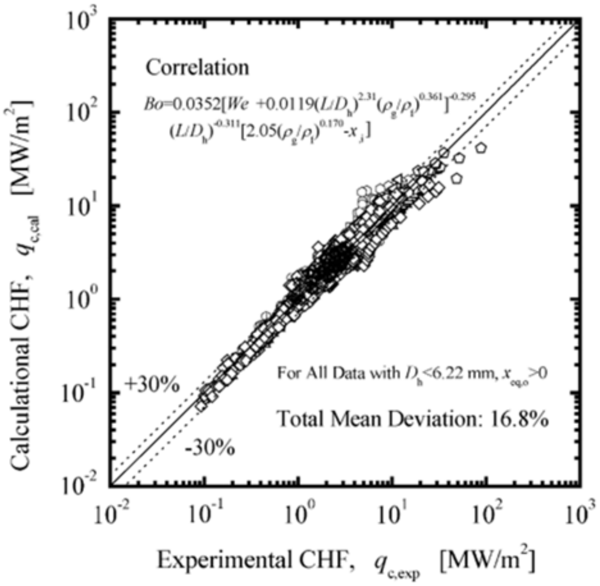

Fig. 3.9 Comparison of predicted values of CHF with a database of smaller diameter channels (Zhang *et al.*,2006)

3.4 MATHEMATICAL MODEL OF A TUBULAR HEAT EXCHANGING SYSTEM

Microchannel heat exchanging system for high heat flux removal applications dealt in the present work consists of several individual tubular heat-exchanging modules transferring heat from the bound solid surface to a liquid passing through it. It is assumed that the thermos-physical properties, the velocity of the fluid and the heat transfer coefficient remain constant for the infinitesimally small control volume. A fundamental governing equation for such tubular heat exchanging systems can be formulated based on the energy balance of an infinitesimally small control volume considered inside the duct as shown in Fig. 3.10.

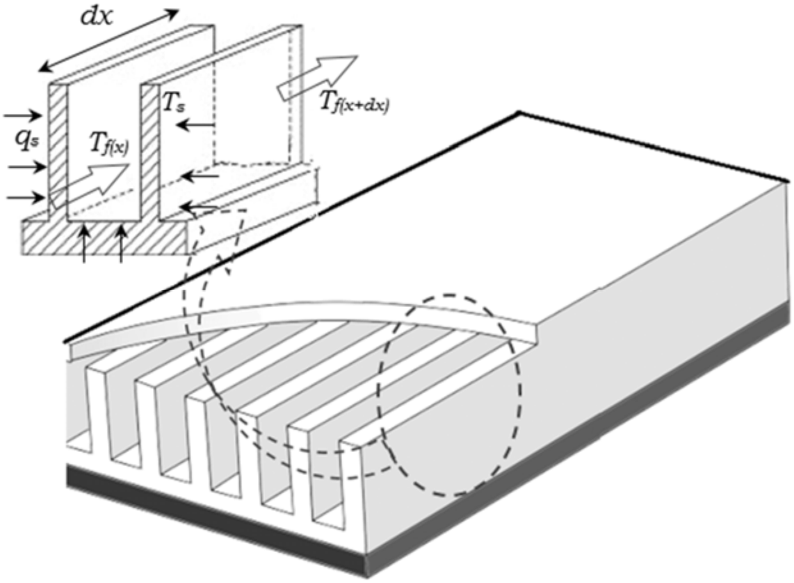

Fig. 3.10. Control volume considered inside a microchannel

Let q_s be the uniform surface heat flux given from the channel surface whose cross-sectional area is A_c and perimeter is P. T_s is the surface temperature of the channel. Coolant fluid enters the control volume with a steady velocity u, temperature $T_{f(x)}$and leaves at $T_{f(x+dx)}$at a distance dx from the inlet. For a given time period dt, the increase in enthalpy of the coolant enters the control volume is attributed by the difference in enthalpy of the coolant at its inlet and outlet as well as the enthalpy addition from its surface. Mathematically,

$$(\rho c A_c dx)\left[T_{f_{(t+dt)}} - T_{f_{(t)}}\right] = \left[(\rho c u A_c)T_{f_{(x)}} - (\rho c u A_c)T_{f_{(x+dx)}}\right] + q_s P dx dt$$

Dividing by $dxdt$and rearranging,

$$\rho c A_c \frac{dT_f}{dt} + \rho c u A_c \frac{dT_f}{dx} = q_s P \tag{3.23}$$

or $$\rho c A_c \frac{dT_f}{dt} + \rho c u A_c \frac{dT_f}{dx} = h_x P\left(T_s - T_f\right)$$

Here the local surface heat transfer coefficient h_x is estimated based on an appropriate theory for the specific situation; viz. single phase internal forced convection and flow boiling, discussed in the preceding section.

In reality, the heat transfer in microchannel array is a conjugate one. The thermal resistance offered by the coolant in the microchannel can be modelled more accurately as a finned surface extending to the coolant Qu and Mudawar (2002). One unit element considered here for the analysis consists of few such rectangular microchannels of the cross-section with identical spacing (t_c) between them.

$$R_F = \frac{1}{n_c \eta_c \, h_x \, (2ldx)} \tag{3.24}$$

where n_c is the number of rectangular microchannels in one unit element, h_x is the convection heat transfer coefficient for the internal forced convection within the rectangular microchannel, l is the height of a rectangular microchannel and the efficiency of the fin array considered here to model the microchannel is given by

$$\eta_c = \frac{\tanh(m_c l)}{m_c l}$$; in which the parameter $m_c = \sqrt{\frac{2h_x\left(dx + t_c\right)}{k_c t_c dx}}$

where $k_c$is the thermal conductivity of the material used to fabricate rectangular microchannel and t_c is the thickness of the microchannel wall.

Resistance for the remaining one more horizontal internal surface of microchannel is given by

$$R_H = \frac{1}{n_c h_c \, s_c dx} \tag{3.25}$$

Another horizontal side of rectangular microchannel at the bottom is assumed to be insulated in certain test cases analysed in the present work.

3.5 NATURAL CONVECTION IN FIN ARRAYS

Theory and correlations of natural convection from rectangular fin array, whose base is held horizontal, are presented. This arrangement of fins forms one of the heat dissipation element in a typical electronic packaging analysed in the present study. The orientation of fin placement (viz. vertical, horizontal, and inclined), the presence of a base, and the spacing between individual fins influence the free convective fluid flow. Therefore, the basic theory of natural convection from a vertical surface is inadequate in modelling heat transfer from finned array extending from the horizontal base. It is evident that increasing number of fins (by decreasing fin spacing) on a base surface increases heat transfer from it. But this will adversely affect the heat transfer coefficient due to the restriction in free convective fluid flow. Geometrical features of a fin array with horizontal base is given in Fig. 3.11. Estimations of heat transfer coefficient and optimum fin spacing for maximising heat transfer from various research publications are summarized below.

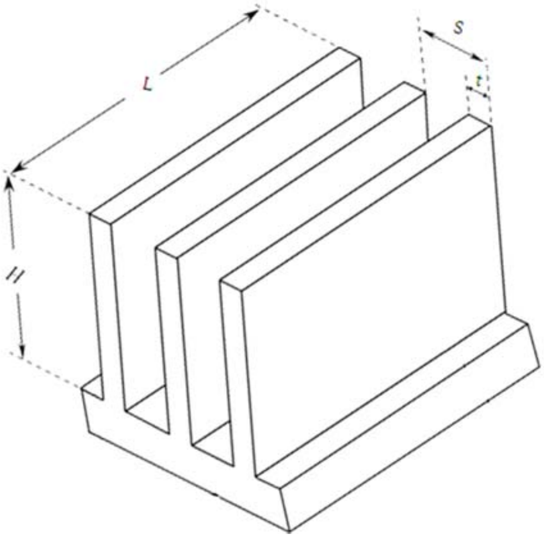

Fig. 3.11. The arrangement of a horizontal fin array

A widely accepted correlation for natural convection from the vertical surface is

$$\mathrm{Nu_S} = 0.54\mathrm{Gr_S}\ \mathrm{Pr} \tag{3.26}$$

Here the characteristic dimension used for estimating the Nusselt number and Grashof number is taken as fin spacing (*S*).

Jones and Smith (1970) visualized the flow pattern in fin interspaces using Mach-Zehnder interferometer and found that above found that the above correlation can be applied if the fin spacing is more that 5cm. For a small amount of fin spacing, they suggested using the correlation

$$\mathrm{Nu_S} = 6.7\times10^{-4}\mathrm{Gr_S}\ \mathrm{Pr}\left[1-\exp\left(0.746\times10^{4}/\mathrm{Gr_S}\ \mathrm{Pr}\right)^{0.44}\right]^{1.7} \tag{3.27}$$

From the results of an earlier study performed by Harahap and McManus (1967), it is suggested to use the correlation

$$\mathrm{Nu}_{L*} = C\left[\mathrm{Gr}_{L*}\mathrm{Pr}\frac{Sn}{H}\right]^{\mathrm{a}}\left(\frac{H}{L*}\right)^{0.656}\left(\frac{S}{L*}\right)^{0.412} \tag{3.28}$$

Here the characteristic dimension $L*$ used to estimate non-dimensional factors is one half of the length of the fin (L). n is the number of spacing in the fin array. Values of the correlation constant $C = 5.22\times10^{-3}$ and $a = 0.57$ for experimental conditions in the range $10^6 \le \left(\mathrm{Gr}_{L*}\,\mathrm{Pr}\frac{Sn}{H}\right) \le 2.5\times10^7$. The value of constant $C = 2.787\times10^{-3}$ and $a = 0.745$ for another experimental condition in the range $2.5\times10^7 \le \left(\mathrm{Gr}_{L*}\,\mathrm{Pr}\frac{Sn}{H}\right) \le 1.5\times10^8$.

Baskaya*et al.* (2000) and Shen*et al.* (2014) verified the applicability of these correlations based on finite volume based computational fluid dynamics (CFD) analysis and suggested minor corrections to the estimates. A comparison of heat transfer coefficient estimations based on the aforementioned studies is presented in Fig. 3.12.

Bar-Cohen and Rohsenow (1984) developed a correlation for the heat transfer from vertical two-dimensional channels formed by fins. Convection heat transfer coefficient for natural convection within the fin array is evaluated as

$$Nu_S = \left[\frac{576}{\left(Ra_S\,S/L\right)^2} + \frac{2.873}{\left(Ra_S\,S/L\right)^{0.5}}\right]^{-0.5} \tag{3.29}$$

Rayleigh number is $Ra = \dfrac{2g\left(T_M - T_\infty\right)S^3\,\mathrm{Pr}}{\left(T_M + T_\infty\right)\mu_\infty{}^2}$

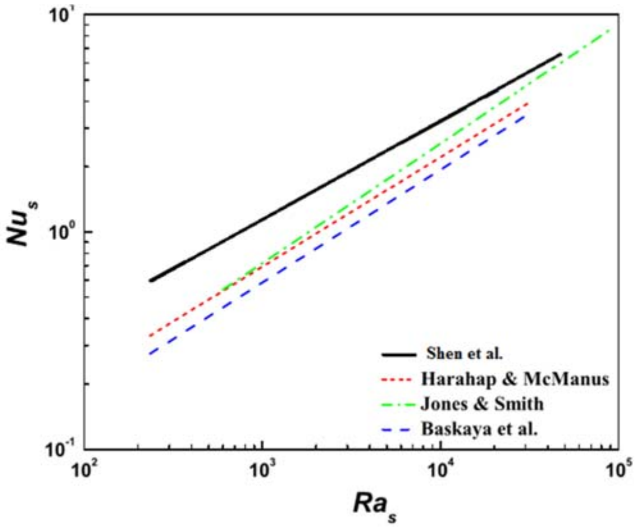

Fig. 3.12. Comparison of heat transfer estimates for a horizontal fin array (adapted from Shen*et al.*(2014))

Prandtl Number is $\quad \mathrm{Pr} = \mathrm{Ra}_S \dfrac{L^3}{S^3}$

Heat transfer coefficient for the natural convection in the finned array is

$$h_S = \frac{\mathrm{Nu}_S \times k_\infty}{S} \tag{3.30}$$

Here all the thermal properties of ambient air are evaluated for the average value of surface and ambient temperature.

Thermal resistances encountered in the heat dissipation through fin array exposed to ambient can be estimated as,

$$R_F = \frac{1}{\eta_e \; h_S \; L_c dx} \tag{3.31}$$

where L_c are the corrected length of the fin and the efficiency of the external fin is

$\eta_e = \dfrac{\tanh(mL_c)}{mL_c}$ in which the parameter $\quad m = \sqrt{\dfrac{2h_S\left(t_f + dx\right)}{k_s t \; dx}}$

3.6 MODELLING OF LATENT HEAT STORAGE SYSTEMS

Heat transfer in the phasechange materials for control of passive cooling and flow boiling are envisaged in the present work. It is assumed that the heat transfers in the phase changing material are majorly controlled by the heat conduction alone and the effect of convection due to density difference at phase interface is negligible in miniature encapsulations. The fundamental governing equation for one-dimensional conduction controlled phase change problems (Voller and Swaminathan, 1991) is

$$\rho c_m \frac{\partial T}{\partial t} = k_m \frac{\partial^2 T}{\partial x^2} + S \tag{3.32}$$

Here the mixture thermal properties are found using property values of solid and liquid phases as

Mixture conductivity $k_m = (1-y)k_S + yk_L$

Mixture specific heat $c_m = (1-y)c_S + yc_L$;

Here y is the volume fraction of liquid. The source term arising due to latent heat storage is

$$S = \rho[(c_S - c_L)T + L]\frac{\partial y}{\partial t} \tag{3.33}$$

The value of volume fraction of liquid (y)is evaluated as

$$y = 0 \qquad \text{if } T < T_{solidus}$$

$$y = \frac{T - T_{solidus}}{T_{liquidus} - T_{solidus}} \text{ if } T_{solidus} \le T_{liquidus}$$

$$y = 1 \qquad \text{if } T > T_{liquidus}$$

Thermal properties of phase changing materials considered in the present study are summarized in Table 3.2.

Table 3.2 Thermal properties of the phasechange materials

Property	**Eicosane**	**α-naphthol**	**Sorbitol**
Melting point [K]	309	369	373
Conductivity [W/mK]	0.39	0.135	0.1
Specific heat [kJ/kgK]	2.46	1.5	1.325
Latent heat of fusion [kJ/kg]	266	163	217
Density [Kg/m^3]	800	1100	450

3.7 OVERVIEW OF CONTROL SYSTEM DESIGN AND MODELLING

The theoretical background that is required to create a dynamic model of single phase and two-phase heat exchanging systems involving microchannels have been discussed in the preceding sections. Various active control solution methods are implemented and simulated based on the dynamic heat exchange process models with an objective to maintain safe operating conditions of the device to be cooled. Dynamic behaviour of the microchannel based heat exchanging system are assessed by analysing the responses of system variables obtained for various types of disturbances imposed. Three basic control methods are employed in the present study viz; H_∞ optimization, PID controller, and cascade controller. H_∞ controller is applied for the heat transfer in single-phase laminar flow in microchannel.System response of H_∞controller is compared with a conventional PID controlled system. Though boiling in microchannel offers excellent heat removal capabilities, rapid fluctuations and immense pressure drop raise serious concern about the system stability. A cascade controller is designed and implemented to overcome thesedrawbacks of two-phase flow heat exchanging systems. An H infinity controller keeps the temperature of the chip intact while a PID controller maintains the pressure inside the microchannel steady.

3.7.1 H_∞method

H_∞ control theory, presented by Zames (1979), forms one of the most innovative methods to deal with complex systems and processes. It generates controllers to realize stabilization with an assured performance and disturbance rejection. The H_∞ control problem can be defined based on a generalised model shown in Fig. 3.13, where P represents the plant transfer function and K represents the controller function. The inputs to the plants are an exogenous signal (w) and control input (u). The output signal z forms the output error and y represents the measured signal from the plant.

H_∞ optimization states to minimize the closed loop norm from *w* to *z*, by forming an optimal controller K, which counteracts the influence of w on z, given by (Skogestad and Postlethwaite, 2005) minimize $\|T_{w\to z}(P,K)\|_\infty$, subject to K stabilizes P internally ($T_{w\to z}$ denotes closed loop mapping of outside influence to regulated variables). The state space representation of the plant P is given by,

$$P \Rightarrow \begin{cases} \dot{x} = Ax + B_1 w + B_2 u \\ z = C_1 x + D_{11} w + D_{12} u \\ y = C_2 x + D_{21} w + D_{22} u \end{cases} \tag{3.34}$$

where x is the state of the system.

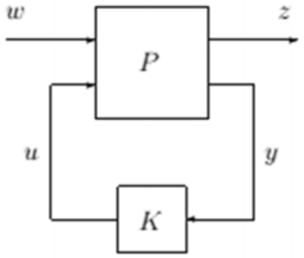

Fig. 3.13 Generalised feedback model for H_∞ control problem

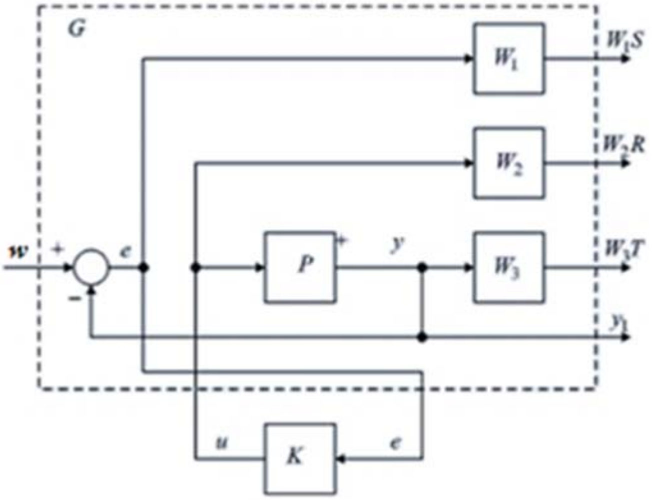

Fig. 3.14 Detailed feedback control model using mixed sensitivity approach

Two popular methods of controller design for H$_\infty$ optimization are mixed sensitivity approach and loop-shaping approach. In mixed sensitivity approach, frequency-domain loop shaping is done through suitable weighting strategies with frequency dependent weights W_1 to W_3. The detailed control model of the plant using mixed sensitivity approach is shown in Fig.3.14.

The mixed sensitivity cost function is given by [2]: $\|T_{w\to z}\|_\infty \le 1$, where $T_{w\to z} = \begin{bmatrix} z_1 \\ z_2 \\ z_3 \end{bmatrix} = \begin{bmatrix} W_1S \\ W_2R \\ W_3T \end{bmatrix}$. S and T are sensitivity and complementary sensitivity functions given by $S = (1+PK)^{-1}$ and $T = K(1+PK)^{-1}$. R is the control effort which indicates the transfer function from reference input to plant input, given by $R = PK(1+PK)^{-1}$. The resulting controller K should be such that it should satisfy the following inequalities.

$$\left.\begin{aligned}\bar{\sigma}S(jw) &< \gamma\ \underline{\sigma}W_1^{-1}(jw)\\ \bar{\sigma}R(jw) &< \gamma\ \underline{\sigma}W_2^{-1}(jw)\\ \bar{\sigma}T(jw) &< \gamma\ \underline{\sigma}W_3^{-1}(jw)\end{aligned}\right\}, \forall w,$$ where $\bar{\sigma}(\cdot)$ and $\underline{\sigma}(\cdot)$ are maximum and minimum singular values of a matrix, and γ is the minimum H infinity norm, ideally less than one. For noise rejection, W_1should be small in the frequency range of noise (as $w \to \infty$).Similarly, For good disturbance rejection, W_3 should be small for the frequency range of disturbance (as $w \to 0$).

In loop shaping design approach (McFarlaneand Glover, 1992), the shape of the plant is reformed using two filters W_1 and W_2 on either side of the plant transfer function, such that, $P_s=W_2PW_1$. A stabilizing controller K_∞ is computed using the normalisedcoprime factor of the plant *P,* by minimising $\left\| \begin{bmatrix} I \\ K_\infty \end{bmatrix} (I+PK_\infty)^{-1} \begin{bmatrix} I & P \end{bmatrix} \right\|_\infty = \gamma$. The final controller is obtained by W_1, W_2andK_∞, given by $K = W_1K_\infty W_2$. The feedback plant model based on loop shaping design is given in Fig. 3.15.

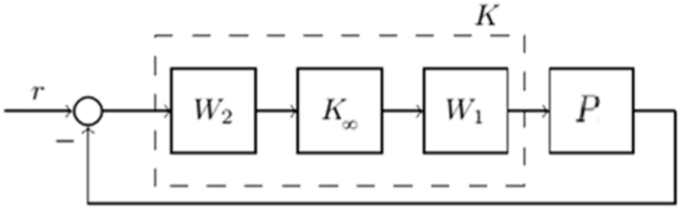

Fig. 3.15. Feedback model for loop shaping design approach

3.7.2 PID controller

One of the most popular conventional controller commonly used in industries are PID (proportional-plus-reset-plus-rate)controllers. It constantly computes the error between desired and measured process variable, thereby giving a control action based on proportional, integral and derivative term. The output of the controller (Stephanopoulos, 1984) is given by:

$$c(t) = K_c e(t) + \frac{K_c}{\tau_I} \int_0^t e(t)\, dt + K_c \tau_D \frac{de}{dt}, \tag{3.35}$$

where K_c is the proportional controller gain, τ_I and τ_D are integral and derivative time constants respectively. The proportional controller gives a control action proportional to the error generated. The controller output is described by the gain given by $K_c = \frac{100}{PB}$, where *PB* is the proportional band. The band is the range of error over which the controller has its full range of action. The presence of integral action changes the output of the controller until the error subsists in the process output. Hence this action can remove small errors. The derivative term in the controller expects the immediate future error and applies a control action against it, thereby producing an anticipatory control over the error. The performance of the controller depends upon the values of the parameters of the controller. Appropriate selection of controller parameter is called tuning of a controller. The two popular methods are processed reaction curve method and the Ziegler-Nichols method.

The process reaction curve method is an empirical tuning method developed by Cohen and Coon. In this method, the system is initially disconnected from the controller and applied a step change input of magnitude *A* to the plant. The response of the plant is recorded which is known as the process reaction curve (Fig. 3.16). The sigmoidal response obtained gives three parameters such as static gain *K*, dead time t_d and time constant τ. The static gain can be calculated as the ratio of output to input at steady states (*B*/*A*). The time constant can be obtained from the ratio of output to the slope of the sigmoidal response (*B*/*S*). Dead time $t_d$gives the time elapsed until the system is responded.

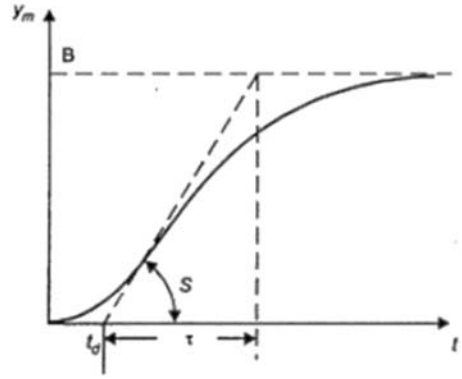

Fig. 3.16 Process reaction curve

Based on these parameters, expressions for controller settings are derived as follows,

$$K_c = \frac{1}{K}\frac{\tau}{t_d}\left(\frac{4}{3}+\frac{t_d}{4\tau}\right),\ \tau_I = t_d\,\frac{32+6\,t_d/\tau}{13+8\,t_d/\tau},\ \tau_D = t_d\,\frac{4}{11+2\,t_d/\tau}$$

The second method of tuning developed by Ziegler and Nichols is based on frequency response analysis, referred as Ziegler-Nichols method. In this method system is initially brought to desired operational condition using proportional control and a set point change is introduced while varying the proportional gain until the system oscillates continuously. If the frequency of oscillation is ω_{CO} and the amplitude of oscillation is M, then two quantities such as ultimate gain and ultimate period is calculated as follows,

Ultimate gain, $K_u = 1/M$

Ultimate period of sustained cycling, $P_u = \dfrac{2\pi}{\omega_{CO}}$ min/cycle

Using these two quantities, the controller settings are derived as follows,

$$K_c = \frac{K_u}{1.7},\ \tau_I = \frac{P_u}{2}\ \text{min},\ \tau_D = \frac{P_u}{8}\ \text{min}$$

3.7.3 The cascade controller

A cooling system involving boiling heat transfer is capable of transferring a larger amount of heat flux from the source and maintains desired safe limit of working temperature of the chip. Flow boiling leads to larger pressure drop during heat transferring process than the single phase systems. Therefore, a single loop control strategy involving the onlytemperature-based control of heat exchanging process in ineffective. Hence the pressure drop across the microchannel array is also estimated and implemented as one of the feedback aspects in a cascade control system.

A cascade controller is used when a system has more than one measurement are available to control a variable. In such a controller, one control loop sets a set point to another control loop forming a cascade configuration (Roffel and Betlem, 2007). It is also called the master-slave controller. The controller output of the master or primary loop (outer loop) forms the set point for the slave controller (inner/secondary loop), as shown in Fig. 3.17. Cascade controller is used when there is a need for increasing the response speed of the main loop or to reduce disturbance. The response of the feedback control is improved by measuring the changes in the inner loop and taking appropriate control action before it is reflected in the main loop.

The present cascade controlsystem has a conventional PID controller as a secondary inner loop which attempts to maintain a minimal pressure drop for proper maintenance of continuous flow through microchannel by regulating the flow rate through the channel. An H_∞ controller based on chip temperature as feedback forms the primary outer loop. Thus the present cascade control system meets both the objectives of reducing the effect of disturbance (changes in heat generation) in the system and maintains an adequate amount of coolant flow so as to avoid flow instabilities as well as the occurrence of CHF.

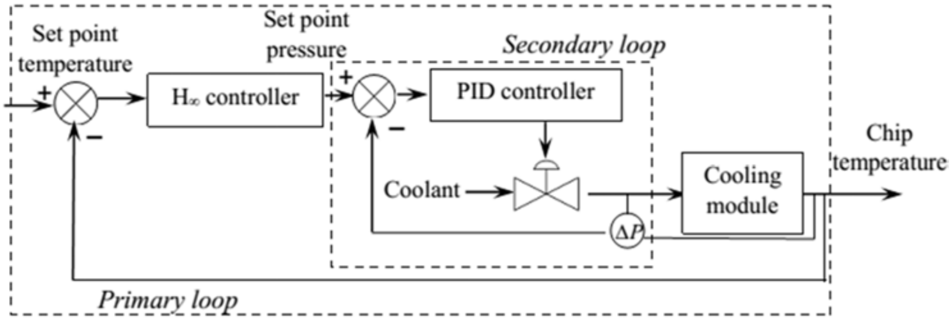

Fig. 3.17 Cascade controller configuration for electronics cooling module

3.8 SUMMARY

Typical thermo-hydraulic physical behaviour in microscalenecessitated specific theoretical models and empirical correlations. A detailed description of fluid flow, heat transfer, and boiling in microchannel were presented. This would enable the development of typical dynamic models for the purpose of simulation and control of heat exchangers used in electronics cooling applications. Empirical correlations are so chosen to have a close resemblance in terms of geometry and other physical conditions to the proposed applications. This ensures the accuracy of the developed dynamic thermal models. Electronic cooling modules have means of heat exchange other than microchannel fluid passages. Theory of natural convection in fin array presents a distinct heat transfer characteristic than its standalone parental single surface. PCM based latent heat storages can offer passive control over heat exchange process, especially in flow boiling. Therefore, the aforementioned theoretical description provides vital input to the development of dynamic heat exchange models for both passive and active control strategies that are described in subsequent chapters.

CHAPTER 4

DYNAMIC THERMAL SYSTEM DESIGN, MODELLING, AND ANALYSIS OF COOLING MODULES

4.1 INTRODUCTION

Mathematical models and correlations for various sub-systems constituting the cooling module were deliberated in the previous chapter. Often heat dissipating systems employed in real application consist of multiple sub-systems for enabling various modes of heat transfer. Natural convection heat sinks, required for managing high heat flux, are often large in size, and need to be supported by high-speed fans to improve convective heat transfer performance. Though single-phase internal convection systems are quite simple to implement, coolant flow rates required for negotiating high heat flux pose challenges in terms of pressure drop, pumping power requirements, and a number of passages. Hence, internal flow and boiling of coolant in microchannels is a promising option for dissipation of high heat flux in electronic cooling applications. With the advents in miniature and microminiature vapour compressor and condensing systems, phase changing coolants in microchannels has become its harmonious cohort in realizing heat dissipation systems in limited spaces. The prime focus of this chapter is to deduce dynamic thermal model for cooling modules that consist of various sub-systems for multi-mode heat transfer. These model make use of established theory and correlations discussed in the preceding chapter. Reconfirmation of the predictability of the developed thermal models is done by comparing the results with appropriate benchmark experimental test cases. Though the flow boiling in the microchannel offer high heat transfer coefficient, operational difficulties associated with rapid bubble growth, flow reversal, and associated instabilities offer challenges for their realization in practical cooling systems. A novel electronics cooling solution based on PCM is presented at the end of this chapter, which is envisaged to overcome the operational difficulties of flow boiling in microchannel employed in an electronics cooling module.

4.2 DESIGN CONSIDERATIONS FOR THE COOLING MODULE

Escalating cooling demands due to high power densities associated with electronics systems used in mission-critical systems call for the development of cooling systems based on liquid convection in microchannels in addition to the conventional air convection heat sinks. A practical approach to the design of natural convection heat sinks and coolant channels has been adopted in this study based on the conventions and empirical relations developed exclusively for these applications. Typical heating rate, area of the electronic chip, and allowable temperature rise have been chosen based on prognoses of the technology roadmaps (Murshed, 2017)) for semiconductor devices. Overall dimensions of the entire cooling system are to be limited to the proportions of the chip to be cooled. Optimum spacing of conventional air convection heat sinks on the exterior can be arrived at based on optimization of natural convection in inter-fin spaces. However, estimation of the dimensions of the coolant channel is quite cumbersome due to various aspects that interfere with one another. Heat transfer in the coolant channel is primarily dependent on its size and the amount of coolant flow. Miniature channels always have the advantage of the high surface area for heat transfer in comparison to its volume. However, the reduction in channel size and an increase in the flow rates lead to excessive pressure drops in channels. This, in turn, demands high-capacity pumping systems. Therefore, an optimum channel size is often arrived at based on allowable pressure drop against which miniature pumping systems can maintain the required flow rate. One can opt for multiple coolant channels to circumvent this limitation imposed by the flow rate of coolant, but it is limited by the available space to accommodate them in the given domain. Adequate space for latent heat storage, provided for negotiating the excessive cooling demands, also needs to be provided based on the aforementioned constraints. The design considerations of the present cooling system is given in Fig. 4.1.

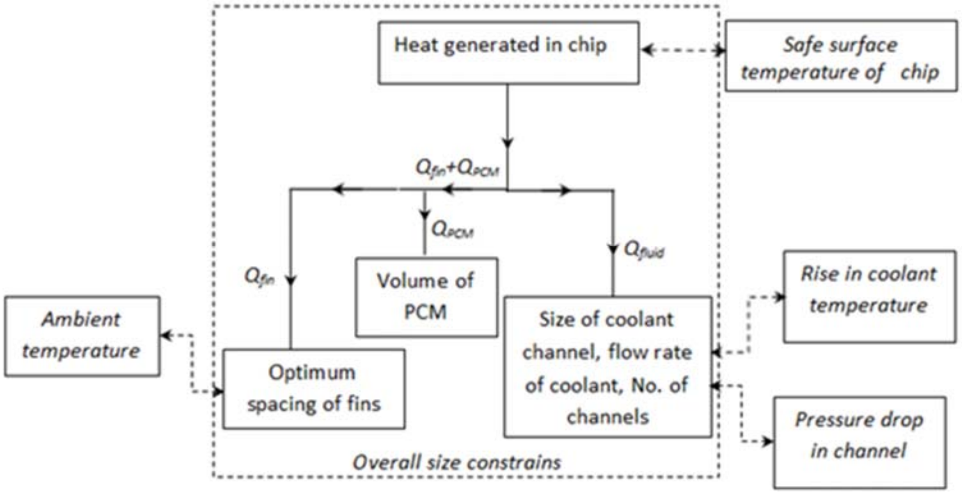

Fig. 4.1. The design considerations of cooling system

The aforementioned design approach is worked out for a simple case by assuming that the heat is dissipated only in two thermal circuits which share the majority of the heat generated in the chip (Q_c). The amount of heat share transferred through fin (Q_1) microchannel (Q_2) depends on respective thermal conductance. The average thermal conductance ($\bar{C}$) and minimum thermal ($C_{\min}$) conductance are often used to quantify the performance of heat transfer system and estimation of peak temperature respectively as follows.

$$\bar{C}_1 = \frac{Q_1}{\bar{T}c - T_\infty} \text{ and } \bar{C}_2 = \frac{Q_2}{\bar{T}c - T_\infty} \tag{4.1}$$

$$C_{1\min} = \frac{Q_1}{Tc_{\max} - T_\infty} \text{ and } C_{2\min} = \frac{Q_2}{Tc_{\max} - T_{fi}} \tag{4.2}$$

Here T_∞ is the ambient temperature, $\bar{T}c$ is the average chip temperature, $Tc_{\max}$ is the maximum chip temperature, and T_{fi} is the temperature of the fluid at the inlet of the microchannel.

Fin array is often arranged on the base plate of a heat sink, which limited to the proportions of the chip to be cooled. An optimum fin spacing (S_{opt}) is that value of spacing, between vertical fins of given height arranged on a horizontal base, for which heat transfer is maximum. Depending on the orientation, viz. horizontal base (Jones and Smith, 1970; Baskaya *et al.* ,2000) or vertical base (Bar-Cohen and Rohsenow, 1984; Yazicioğlu and Yüncü, 2007) optimum fin spacing can be arrived at based on heat transfer analysis. An example of the correlation for optimum fin spacing (Bar-Cohen and Rohsenow, 1984) is

$$S_{opt} = 2.714 \frac{L_c}{Ra_{Lc}^{1/4}} \tag{4.3}$$

Then, the Number of fins on the array will be

$$n = \frac{B}{\left(S_{opt} + t_f\right)} \tag{4.4}$$

where B is the breadth of the base plate and t_f is the thickness of the fin.

Hydrodynamics of microchannel flows have already been discussed in the previous chapter (Section 3.2.1). Frictional pressure drop can be estimated by either assuming it as a fully developed flow (3.1) or by considering the effect of entry length (3.3). In a similar way, based on the theory of heat transfer in microchannel flows (Section 3.2. 2), heat transfer coefficient can also be estimated by either assuming it as a fully developed flow or by considering the effect of entry length depending on the type of wall heating. Therefore, the size of one base element of the electronics cooling module for the design and analysis is limited based on the above estimate of optimum spacing and thickness of fin.

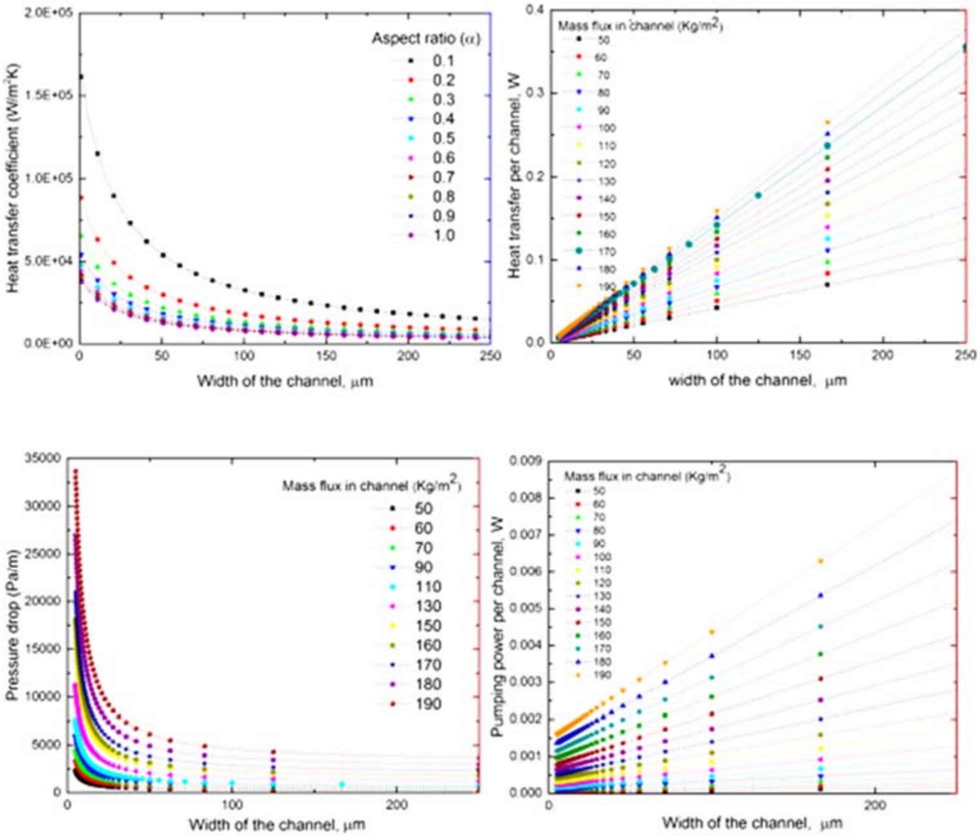

Fig.4.2. Hydraulic and thermal performance parameters for rectangular microchannels of various size.

A number of coolant channels that need to be provided depends on the thermal conductance requirement corresponding to the heat transfer in rectangular microchannel. Though narrower channels can increase the heat transfer coefficient, an optimum value may be chosen based on allowable pressure drop for fluid flow in the channel. Entire spectrum of hydraulic and heat transfer parameter is estimated (per unit length of the channel) based on the aforementioned considerations for demineralized water flow through rectangular microchannels, and is presented in Fig.4.2. Choice of the width of the microchannel, aspect ratio, and number of channels per unit element can be arrived at based on the heat transfer coefficient requirement or the heat transfer demand within allowable pressure loss or pumping power limit.

4.3 ASSUMPTIONS FOR THE SYSTEM MODELLING

Modelling of the actual heat transfer physics involved in multimode heat dissipation in systems analysed in the present work is inherently challenging. Multimode heat dissipation process is simulated based on the dynamic thermal model developed from appropriate heat transfer formulations of its constituent elements. Simplifying assumptions are invoked to enable the mathematical modelling of the dynamic systems using available theory and correlations applicable for individual sub-systems. Following are the major assumptions used the system modelling.

- Heat conduction is one dimensional, i.e. in a direction perpendicular to the coolant flow.
- Axial heat conduction in the microchannel is absent
- There is no heat generation source in the domain of analysis other than the specified source
- The coolant flows inside the microchannel with a steady velocity

There exist other assumptions also, which are applicable to the individual test cases. Modelling of coolant flow for the simple internal forced convection systems assumes it as a single phase flow. The fourth side of the microchannel is assumed as insulated so as to model conjugate heat transfer in microchannel similar to fin array (Eqn. 3.24 and 3.25). PCM encapsulation storages within fins have fixed volume. Whereas, the cross-sectional area of the cavity containing PCM, surrounding the rectangular microchannel, is either constant (4.7.2) varying linearly in the direction of the coolant flow (4.7.3).

4.4 METHODOLOGY FOR MODELLING AND SOLUTION

A broad approach used for modelling and solution adopted in the present work is discussed. Primarily a unit element of the cooling module, which consist of all participating heat dissipating elements, is considered for the analysis. For example, if a cooling module consists of only fin and microchannels, a single fin and an array of microchannels possible within that extent of geometry is considered along with the heat source to form a unit module (Fig. 4.3). This unit element can be again subdivided to finite number of control volumes of length *dx* along the length of the channel.

A thermal circuit representing the one-dimensional heat transfer from the heat generating the chip towards the two heat dissipation branches is given in Fig. 4.3. Since the heat generated in the chip (Q_c) can continuously vary with respect to time in a real scenario, it is chosen here as a time-varying function.

This heat is dissipated through the two branches of the cooling circuits, viz. natural convection to ambient through fin array (Q_1) and the internal forced convection in microchannels (Q_2). The heat Q_1 is dissipated by negotiating the thermal resistance of metallic block and an effective resistance offered by fin due to its conduction and convection resistances while interacting with the ambient.

This is modelled in terms of effective resistance to heat transfer through both finned part (R_{FE}) and unfinned/inter-fin part (R_{UF}) of the external fin array. On the other hand, the heat Q_2 is dissipated negotiating the thermal resistance offered by the internal convection resistance in the microchannel. Assuming that the bottom of the microchannel array is insulated and hence three walls of the microchannel are only participating in heat transfer. Vertical surfaces of each microchannel can be considered equivalent to a fin transferring heat (R_{FC}) from its either surfaces. Remaining part of the heat towards microchannel (R_{HC}) will be transferred by its horizontal surface. In addition to the heat dissipation effect, part of the heat is utilised for increasing the enthalpy of each element. This is modelled as heat capacitance, viz. heat capacitance metallic block with fins (C_M) and heat capacitance of the chip (C_C). The heat balance equation at each node of the control volume is given by the partial differential eqns (4.5) to (4.7).

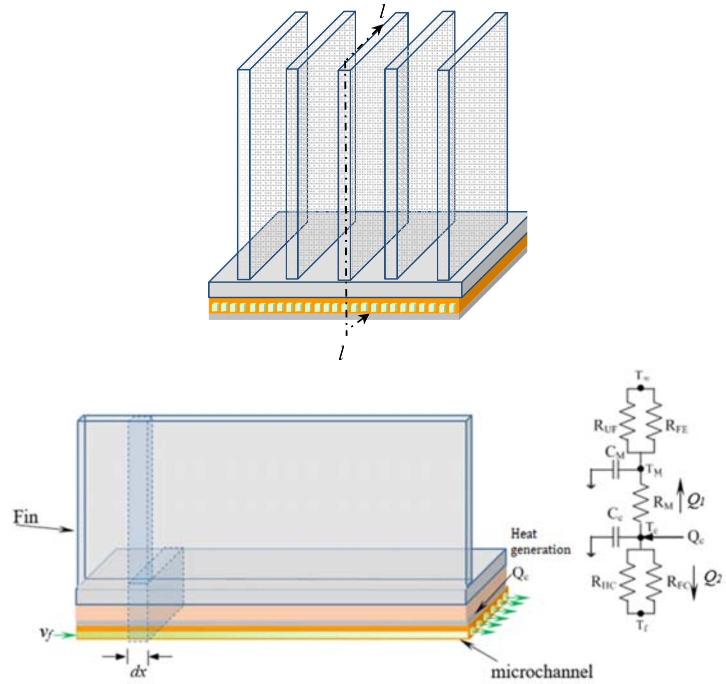

Fig. 4.3. A simple cooling module, unit element and cooling circuit

The rate of change of enthalpy of the coolant at a location in the microchannel is contributed by the heat transferred from the chip and the heat convected to the next location in the microchannel as,

$$C_F \frac{\partial T_F(t,x)}{\partial t} + C_F u \frac{\partial T_F(t,x)}{\partial x} = \frac{T_C(t) - T_F(t,x)}{R_{EQ2}\Delta x} \tag{4.5}$$

where C_F is the heat capacity of the coolant per unit length in the microchannel, given by, $C_F = n_c \rho_F A_F c_F$, n_c is the number of channels in the microchannel. R_{EQ2} is the equivalent thermal resistance between chip and coolant in the microchannel given by, $R_{EQ2} = \left[\frac{1}{R_{HC}} + \frac{1}{R_{FC}}\right]^{-1}$

The rate of change of enthalpy of the chip is contributed by the heat generated inside the chip and heat transferred to adjacent branches of the chip in the network as,

$$C_C \frac{dT_C(t)}{dt} = Q_C - \frac{T_C(t) - T_F(t,x)}{R_{EQ2}} - \frac{T_C(t) - T_M(t)}{R_M} \tag{4.6}$$

where the heat capacity of the chip is given by, $C_C = \rho_C V_C c_C$ and R_M is the resistance between the chip and the metallic fin module.

Correspondingly, the rate of enthalpy of the metallic fin module is determined by the heat transferred to it from the chip and heat transferred to the ambient air as,

$$C_M \frac{dT_M(t)}{dt} = \frac{T_C(t) - T_M(t)}{R_M} - \frac{T_M(t) - T_\infty(t)}{R_{EQ1}} \tag{4.7}$$

where the heat capacity of the fin module is given by, $C_M = \rho_M V_M c_M$ and R_{EQ1} is the equivalent thermal resistance between the metallic fin module and the ambient given by,

$$R_{EQ1} = \left[\frac{1}{R_{UF}} + \frac{1}{R_{FE}}\right]^{-1}$$

The partial differential equations obtained through balancing the energy equations are nonlinear and distributed. Thus the system is an infinite dimensional system. For the purpose of analysis, the system needs to be reduced to finite dimensional form. This done by converting partial differential equation to an ordinary differential equation. A Finite difference method is utilized for this purpose, with a forward difference for time derivative and upwind scheme for the space derivative (Ozisik,, 1994).

To apply this method, the domain is discretized into a finite number of control volumes (*N*) in the direction of coolant flow in the microchannel. The inlet temperature of the coolant is assumed to be equal to the ambient and the entire domain is initialized with this temperature.

Applying a finite difference method for the eqns (4.5) to (4.7), for i^{th} control volume gives,

$$\frac{dT_{F,i}}{dt} = u\left[\frac{T_{F,i} - T_{F,i-1}}{\Delta x}\right] + \frac{T_{C,i} - T_{F,i}}{C_F R_{EQ2} \Delta x} \tag{4.8}$$

$$\frac{dT_{C,i}}{dt} = \frac{Q_C}{C_C} - \frac{T_{C,i} - T_{F,i}}{C_C R_{EQ2}} - \frac{T_{C,i} - T_{M,i}}{C_C R_M} \tag{4.9}$$

$$\frac{dT_{M,i}}{dt} = \frac{T_{C,i} - T_{M,i}}{C_M R_M} - \frac{T_{M,i} - T_\infty}{C_M R_{EQ1}}, \qquad i = 1, \ldots, N \tag{4.10}$$

Rearranging the above equations in the form of state space equation as,

$$\dot{T}_{F,i} = -a_1 T_{F,i} + a_1 T_{C,i} - a_2 T_{F,i-1} \tag{4.11}$$

$$\dot{T}_{C,i} = a_3 T_{F,i} - b_1 T_{C,i} + c_1 T_{M,i} + d_1 Q_C \tag{4.12}$$

$$\dot{T}_{M,i} = b_2 T_{C,i} - c_2 T_{M,i} + d_2 T_\infty \tag{4.13}$$

where $a_1 = \frac{1}{C_F R_{EQ2} \Delta x} + \frac{u}{\Delta x}, a_2 = \frac{u}{\Delta x}, a_3 = \frac{1}{C_C R_{EQ2}}$,

$b_1 = \frac{1}{C_C R_{EQ2}} + \frac{1}{C_C R_M}$, $b_2 = \frac{1}{C_M R_M}, c_1 = \frac{1}{C_C R_M}, c_2 = \frac{1}{C_M R_M} + \frac{1}{C_M R_{EQ1}}$,

$d_1 = \frac{1}{C_C}$, $d_2 = \frac{1}{C_M R_{EQ1}}$

Thus the state space model of the system is given by

$$\dot{\mathbf{T}}(\mathbf{t}) = \mathbf{A}(\mathbf{t})\mathbf{T}(\mathbf{t}) + \mathbf{B}(\mathbf{t})\mathbf{i}(\mathbf{t}) \tag{4.14}$$

where $\dot{\mathbf{T}}$ is the time derivative of nodal temperature; **i** represents the input vector to the system; **A** and **B** represent the state matrix and input matrix respectively which vary along space and time which is given by,

The system T represents the temperature at each node of the network, given by,

$$\mathbf{T} = \begin{pmatrix} T_{F,1} & T_{F,2} & . & T_{F,N} & T_{C,1} & T_{C,2} & . & T_{C,N} & T_{M,1} & T_{M,2} & . & T_{M,N} \end{pmatrix}^T \tag{4.15}$$

The state matrix A is given by,

$$\mathbf{A} = \begin{pmatrix} A_{11} & A_{12} & A_{13} \\ A_{21} & A_{22} & A_{23} \\ A_{31} & A_{32} & A_{33} \end{pmatrix}_{3N \times 3N} \tag{4.16}$$

where all submatrices are $N \times N$ and are given by,

$$A_{11} = \begin{pmatrix} -a_1 & & & \\ -a_2 & -a_1 & & \\ & & & \\ & & -a_2 & -a_1 \end{pmatrix}, \qquad A_{12} = \begin{pmatrix} a_1 & & \\ & a_1 & \\ & & \\ & & a_1 \end{pmatrix},$$

$$A_{21} = \begin{pmatrix} a_3 & & \\ & a_3 & \\ & & \ddots \\ & & & a_3 \end{pmatrix}, \qquad A_{22} = \begin{pmatrix} -b_1 & & \\ & -b_1 & \\ & & \ddots \\ & & & -b_1 \end{pmatrix},$$

$$A_{23} = \begin{pmatrix} c_1 & & \\ & c_1 & \\ & & \ddots \\ & & & c_1 \end{pmatrix}, \qquad A_{32} = \begin{pmatrix} b_2 & & \\ & b_2 & \\ & & \ddots \\ & & & b_2 \end{pmatrix}, \quad \text{and}$$

$$A_{33} = \begin{pmatrix} -c_2 & & \\ & -c_2 & \\ & & \ddots \\ & & & -c_2 \end{pmatrix}$$

The input matrix *B* is given by,

$$\mathbf{B} = \begin{pmatrix} -a_2 & 0 & . & . & & & . & . & & & . & . & 0 \\ 0 & & . & . & 0 & d_1 & d_1 & .. & d_1 & 0 & . & . & 0 \\ 0 & & & . & . & . & . & & 0 & d_2 & d_2 & .. & d_2 \end{pmatrix}^T \tag{4.17}$$

The input vector ***i(t)*** includes the input to the system and the disturbances. The heat generated in the chip (Q_C) forms the input and the input temperature ($T_{F,0}$) and ambient temperature (T_∞) forms the disturbance input. The input vector is given as,

$$\mathbf{i(t)} = \left(T_{F,0} \quad Q_C \quad T_\infty\right)^T \tag{4.18}$$

The output of the system is represented by the output vector given by,

$$\mathbf{y(t) = C(t)T(t) + D(t)i(t)}$$

where ***C(t)*** is the output matrix and ***D(t)*** is the feedthrough the matrix. Since there is no direct feedthrough from input *D(t)* =0 and the output matrix is given by,

$$\mathbf{C(t)} = \begin{pmatrix} 0 & . & . & 0 & \frac{1}{N} & \frac{1}{N} & \cdots & \frac{1}{N} & 0 & . & . & 0 \end{pmatrix}. \tag{4.19}$$

A general solution of the above state space formulation of the system is given by,

$$\mathbf{T(t) = e^{At}T(0) + \int_0^{\tau} e^{A(t-\tau)}B\ i(\tau)d\tau} \tag{4.20}$$

This equation is integrated over space to obtain the solution of the system.

The partial differential equation describing the system can also be solved numerically by selecting an appropriate time step to meet the stability requirement proposed by Courant-Friedrichs-Levy condition $\Delta t \leq \Delta x/u$, along with the boundary condition of inlet coolant temperature and ambient temperature. The solution gives temperature variation of coolant in the microchannel along space and time as well as temporal variation of chip temperature and base of the fin. The numerical procedure followed to implement a computer program is shown in Fig. 4.4.

4.5 VALIDATION TEST CASES

Accuracy and reliability of the present modelling and simulation procedure is ascertained by carrying out simulations of two benchmark validation test cases available in microchannel flows. Single mode heat dissipation validation test cases have been chosen due to the lack of availability of established experimental data for multimode heat transfer situations. Physical and geometrical conditions for these validation cases are resembling the microchannel flows considered in the multimode heat transfer situations dealt with this study. Therefore, the predictability of the modelling procedure can be established for the same range of variables involved in the actual process. Effect of simplifying assumptions such as one-dimensional heat transfer and absence of axial heat conduction is expected to bring substantial effect as they cannot be condoned in experiments.

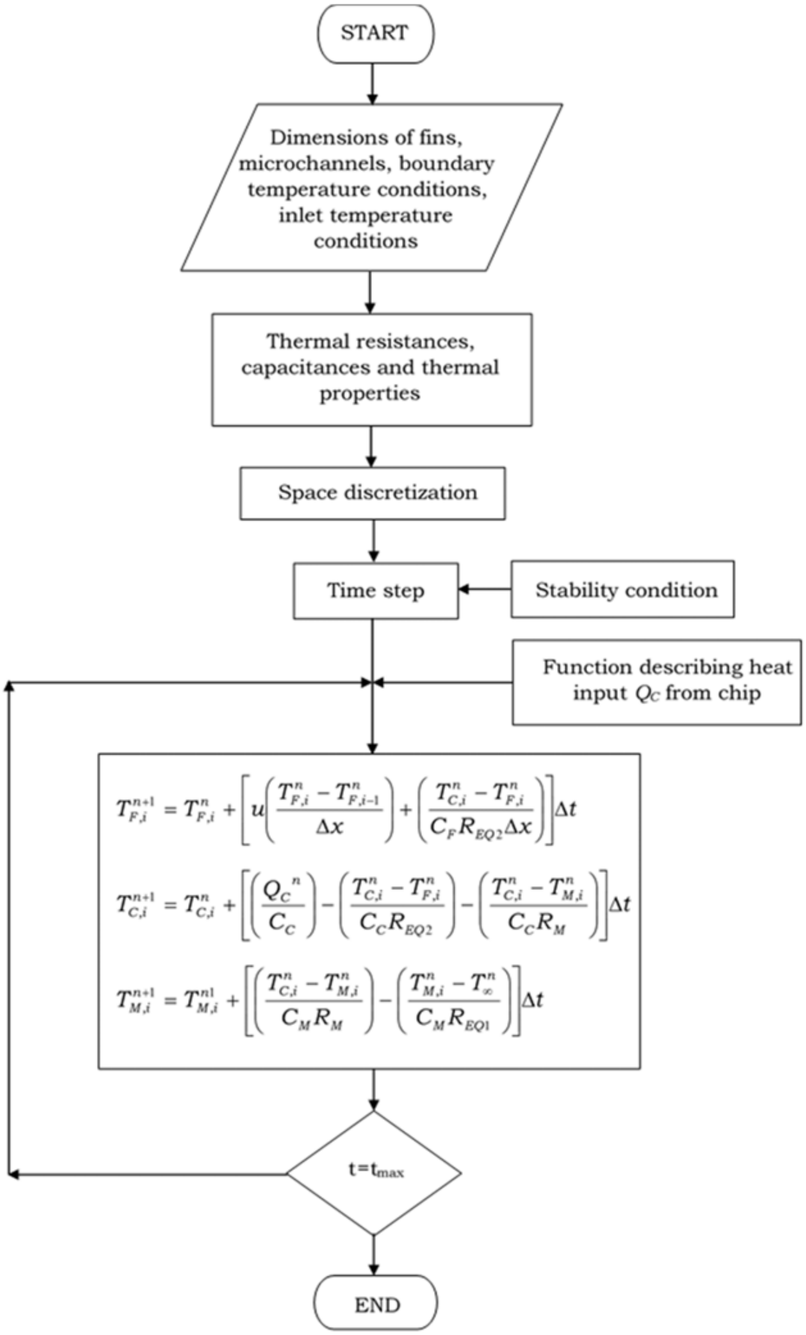

Fig. 4.4. Flowchart for the implementation of the iterative numerical solution procedure

4.5.1 Single phase convection in the microchannel

Experimental results on the thermo-hydraulic characteristics of a single-phase micro-channel heat sink performed by Qu and Mudawar (2002) is used for the first set of validation. The experiment set up consists of an array of rectangular micro-channels with each having a width of 231µm and depth of 713µm as shown in Fig. 4.5 (a). A set of cartridge heaters are used to heat the working fluid (deionised water) at two levels of heat flux; viz. 100W/cm^2 and 200W/cm^2. Present validation trials have been carried using the same geometry and flow conditions for laminar flow ($50<Re<700$) in a single channel (Fig. 4.5 (b)). Theoretical models and correlations available for single-phase internal forced convection in microchannels described in section 3.2 are made use for the simulation with the geometry and flow conditions mentioned above. A comparison of the solution for pressure drop in a microchannel with experiment is shown in Fig. 4.6. Pressure drop increases linearly with flow rate as expected. In general, computed results have a good agreement with the experimental data at lower Reynolds number. Computed values of pressure drop do not match towards higher Reynolds number, as the transitional effects can bring in higher pressure drop in the experiment. Pressure drop declines as heat flux is raised due to drop in viscosity of the liquid. Experimental estimates for Pressure drop in $50<Re<400$ for the heat flux 200W/cm^2 was not available for comparison.

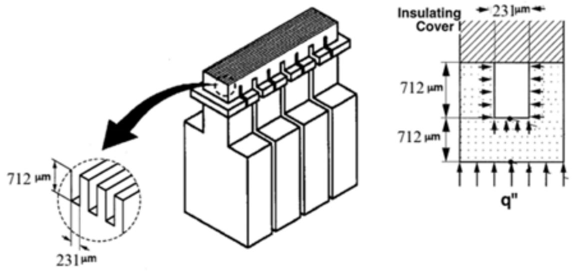

(a) Geometry of microchannel (b) Boundary conditions

Fig. 4.5 Architecture of microchannel

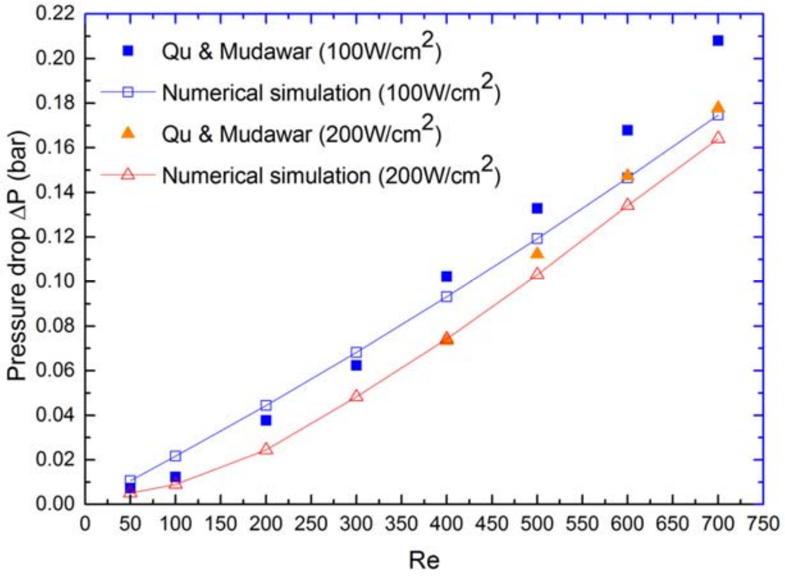

Fig. 4.6. Comparison of the solution for pressure drop in a microchannel with experiment (Qu and Mudawar; 2002)

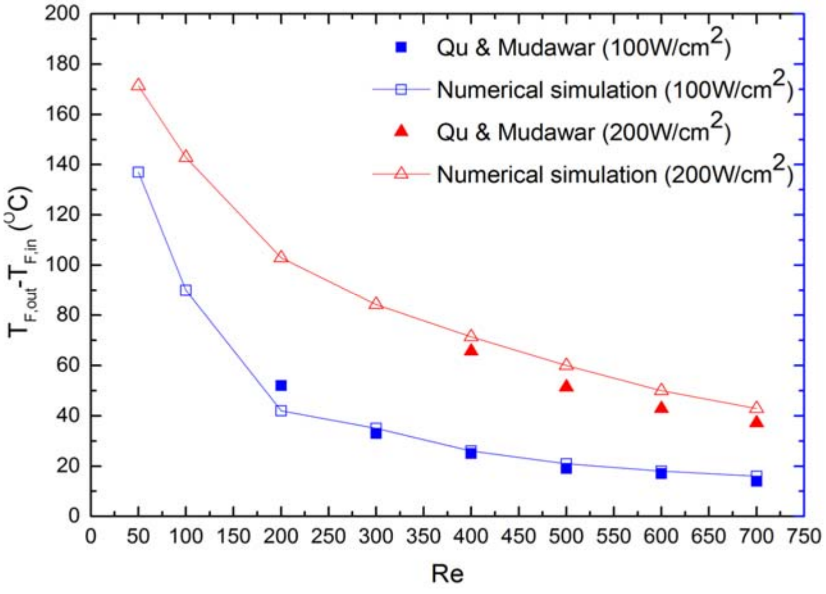

Fig. 4.7. Comparison of the solution temperature build-up in a microchannel with experiment (Qu and Mudawar; 2002)

A comparison of the computed solution for the temperature build-up in a microchannel with that observed in Qu and Mudwar's experiment is given in Fig.4.7. Temperature build-up drops as flow rate is increased as more fluid mass becomes available for carrying away the heat generated. Computed results have a good agreement with the experimental data for the entire range of experimentation. Unlike viscosity, variation of specific heat with respect to temperature is negligible.

4.5.2 Boiling in the microchannel

The experiment set up used by Qu and Mudawar (2004) is similar to that shown in Fig. 4.5 (a).This consists of an array of twenty-one rectangular micro-channels with each having a width of 215μm and depth of 821μm. Water is admitted at 60°C with a mass flux of 225 kg/m^2s. The pressure drop has been estimated for a heat flux range from 30 W/cm^2 to 120 W/cm^2.

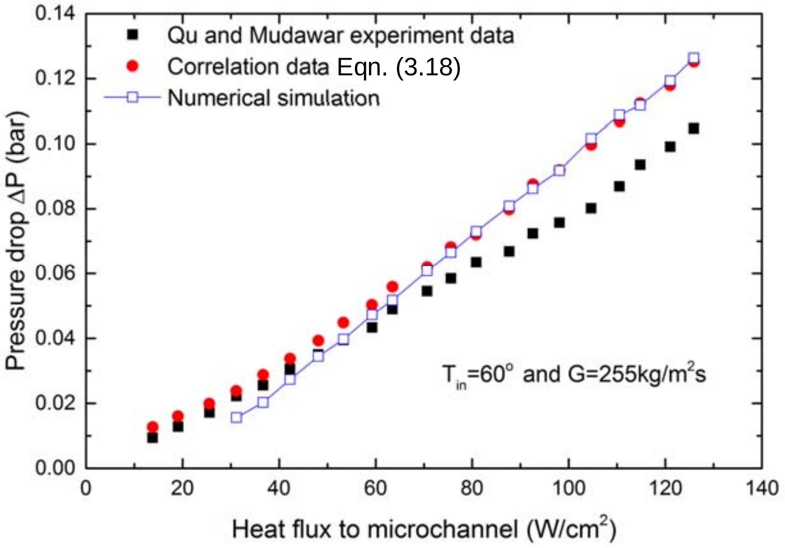

Fig. 4.8. Comparison of the pressure drop estimates for two phase flow in microchannels

A comparison of the computed solution for the pressure drop in a microchannel with that observed in Qu and Mudwar's experiment is given in Fig.4.8. Pressure drop becomes severe as flow rate is increased as more fluid mass evaporates with the heat generated. Computed results have a good agreement with the experimental data for the entire range of experimentation. This establishes predictability of boiling model used in the present dynamic thermal modelling.

4.6 COOLING SYSTEMS WITH INTERNAL FORCED CONVECTION AND NATURAL CONVECTION IN FIN ARRAYS

Modelling and solution procedure for the simulation of a cooling system with internal forced convection in microchannel as well as natural convection in fin arrays was described in section 4.4. The objective of the present attempt is to simulate a cooling system consisting of microchannel and fin array for various type of unsteady heat generation. A chip of dimension 30mm×30mm integrated in a cooling system consisting of fin array and rectangular microchannels. An optimum spacing of 4mm for a fin thickness of 1mm has been arrived at based on the criteria discussed in section 3.5. Therefore, a unit element consisting of twenty-five rectangular microchannels of cross section 100×100μm, with a spacing of 100μm between them, is considered for the present performance analysis. Simulations have been performed for a typical coolant mass flux of 100kg/ m^2.s.

The chip temperature dependency on the velocity of the coolant is given in Fig.4.9. It is observed that the chip temperature drops down drastically for an initial increase of coolant velocity from 0 to 0.4 m/s, but there is no noticeable change is observed for a further increase in velocity. The response of the heat exchanging system has been assessed for two time-varying heat generation model from the chip. Dynamic model could simulate the temperature build up in chip based on the given heat generation pattern. Heat dissipation pattern for an ever increasing heat generation pattern described by $Q = 20\left(1+\tau^{0.15}\right)$ is given in Fig. 4.10. Temperature builds up in the chip quickly as the dissipation from both modes of cooling is feeble.

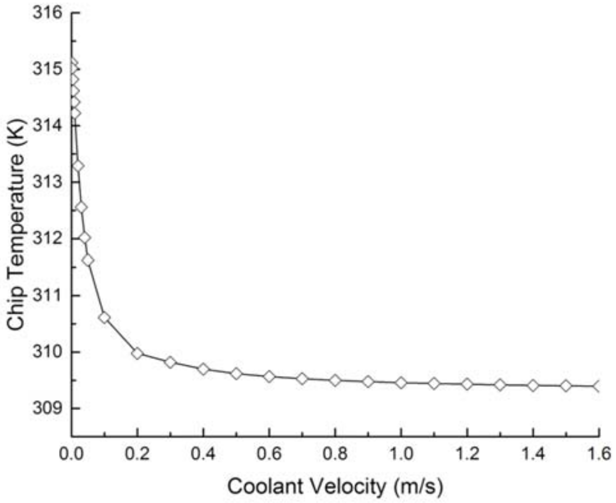

Fig. 4.9 Coolant velocity of the microchannel to maintain safe chip temperature

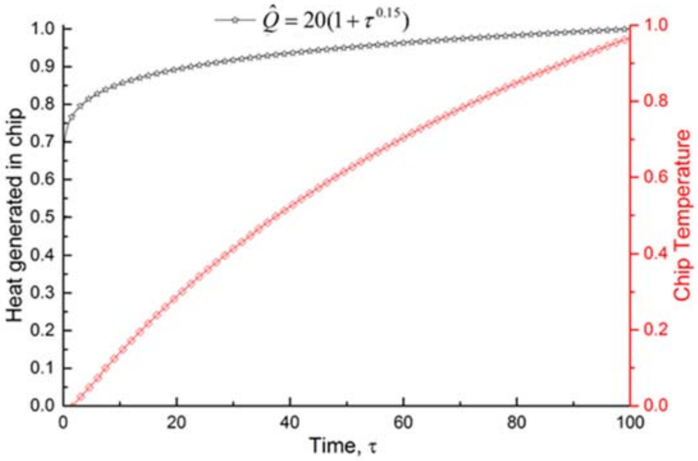

Fig. 4.10. Temperature build-up in the chip for an increasing heat generation pattern

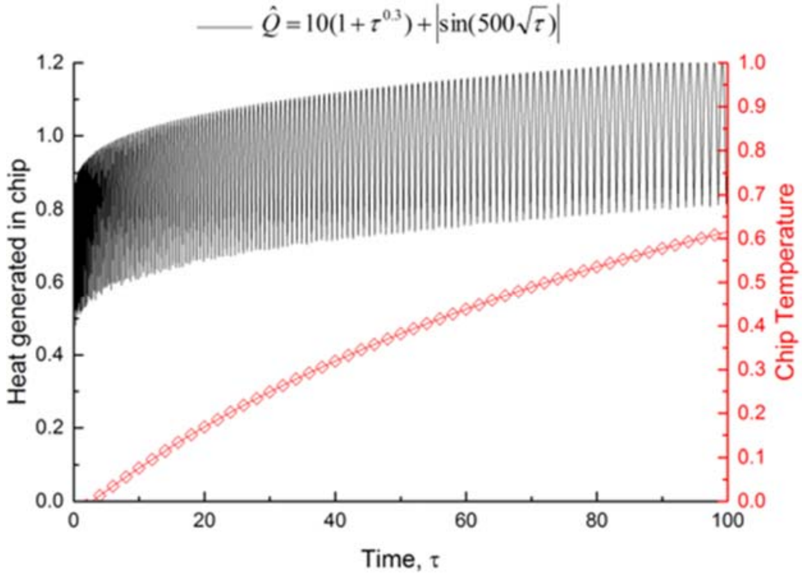

Fig. 4.11. Temperature build-up in the chip for superimposed heat generation pattern.

Fig. 4.11 shows the temperature build-up in the chip for an oscillating heat generation pattern superimposed over another increasing heat generation pattern described by $Q=10\left(1+\tau^{0.3}\right)+\left|\sin\left(500\sqrt{\tau}\right)\right|$. Temperature builds up in the chip quickly due to very low dissipation from both modes of cooling.

Though chip temperature drops down when coolant flow rate is increased, it has a feeble effect after a certain limit. Therefore, the present analysis brings out the necessity of more than one control strategy for efficient thermal management of cooling systems. The data from the present dynamic thermal analysis is quite vital for the design of both active and passive thermal management systems described subsequently in this thesis.

4.7 PASSIVE CONTROL SYSTEM DESIGN EMPLOYING PHASE CHANGE MATERIAL ENCAPSULATION

Microminiaturization together with the processing requirements at higher clock frequencies leads to excessive power densities in electronic chips. This brings multifaceted challenges in the reliable and safe operation of electronic devices used in mission-critical applications. The primary focus of the present attempt is to model the heat transfer in an electronic module, dissipating heat in the liquid flowing through microchannel as well as to ambient by natural convection in presence of a phase changing material embedded in it for the purpose of developing a self-contained and efficient cooling system. Present heat transfer model takes care of the heat stored in phase changing material, heat transferred by natural convection effects in addition to the forced convection heat transfer in microchannel cooling passage. Therefore, the developed model can successfully take account of the effect of the variation in operating atmospheric conditions which are significant in systems employed in harsh thermal environments. Heat generation is formulated as a time-varying function corresponding to typical operating conditions. The developed dynamic thermal models for typical kinds of heat spreaders have been tested for a wide range of operating conditions of the chip.

4.7.1 Effect of phase change material encapsulation in fin arrays

Components of a unit element in the electronics cooling module and its thermal circuit are shown in Fig. 4.12. Coolant inside the microchannel is assumed to flow with a steady velocity v_f and all heat transfer processes are assumed to be one dimensional, taking place perpendicular to this. Heat generated in chip Q_c can be given as a time-varying input function in the present model. Based on the principle of energy balance, Q_c is shared and dissipated in two directions as shown in the thermal circuit; $Q_c = Q_1 + Q_2$.

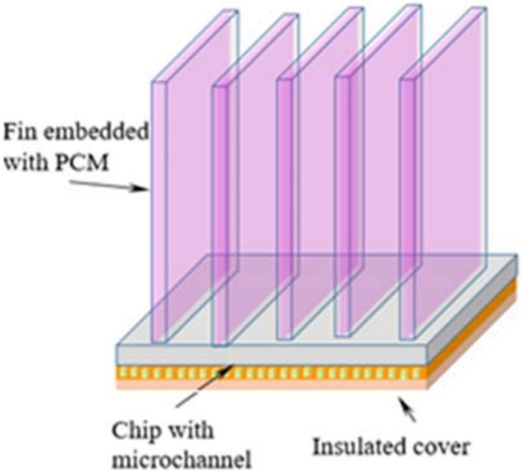

Fig. 4.12. Cooling module with PCM encapsulation in fin array and microchannel cooling passages

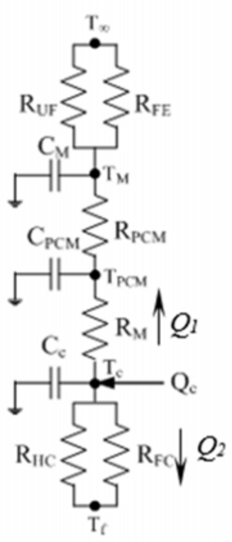

Fig. 4.13. Thermal circuit for the analysis of cooling module with PCM encapsulation in fin array and microchannel

A part of the heat generated in the chip is dissipated through fin array which contains a phase changing material embedded in it. Heat dissipated through this branch has to negotiate thermal resistance offered by a metallic block separating chip surface and fin, conduction as well as convection resistance for heat dissipation through the fin. In addition to this, phase changing material embedded inside the fin array absorbs latent heat when its temperature exceeds its melting point. Otherwise, for all temperatures below the melting point, its conduction resistance also contributes to the heat dissipation through the fin array. This branch of the thermal circuit and resistances/capacitance of various components are shown in Fig. 4.13. The proportion of Q_1 and Q_2 depends on various resistances that come across in the path of heat dissipation and is worked out as per the theoretical models explained in section 3.3 to 3.5.

Dynamic thermal model for the unit element of the cooling module is developed by considering a unit element of the cooling module. This consist of a single fin and an array of microchannels for cooling a part of chip generating heat. This unit element can be again subdivided to a finite number of control volumes along the length of the channel. Application of the energy balance at salient nodes in the thermal circuit such as fluid, chip, phase changing material, and metal body (where fins are attached) gives the following partial differential equations. Governing equations based on nodal energy balance

$$\begin{aligned}
&C_F\frac{\partial T_F(t,x)}{\partial t}+C_F u\frac{\partial T_F(t,x)}{\partial x}=\frac{T_C(t)-T_F(t,x)}{R_{EQ2}\Delta x}\\
&C_C\frac{dT_C(t)}{dt}=Q_C-\frac{T_C(t)-T_F(t,x)}{R_{EQ2}}-\frac{T_C(t)-T_{PCM}(t)}{R_M}\\
&C_{PCM}\frac{dT_{PCM}(t)}{dt}=\frac{T_C(t)-T_{PCM}(t)}{R_M}-\frac{T_{PCM}(t)-T_M(t)}{R_{PCM}}\\
&C_M\frac{dT_M(t)}{dt}=\frac{T_{PCM}(t)-T_M(t)}{R_{PCM}}-\frac{T_M(t)-T_\infty(t)}{R_{EQ1}}
\end{aligned}\tag{4.21}$$

The state equations corresponding to the aforementioned equations are

$$\begin{aligned}
&\dot{T}_{F,i}=-a_1T_{F,i}+a_1T_{C,i}-a_2T_{F,i-1}\\
&\dot{T}_{C,i}=a_3T_{F,i}-b_1T_{C,i}+c_1T_{PCM,i}+e_1Q_C
\end{aligned}\tag{4.22}$$

$$\dot{T}_{PCM,i} = b_2 T_{C,i} - c_2 T_{PCM,i} + d_1 T_M$$

$$\dot{T}_{M,i} = c_3 T_{PCM,i} - d_2 T_{M,i} + e_2 T_\infty$$

where $a_1 = \frac{1}{C_F R_{EQ2} \Delta x} + \frac{u}{\Delta x}$, $a_2 = \frac{u}{\Delta x}$, $a_3 = \frac{1}{C_C R_{EQ2}}$,

$b_1 = \frac{1}{C_C R_{EQ2}} + \frac{1}{C_C R_M}$ $b_2 = \frac{1}{C_{PCM} R_M}$, $c_1 = \frac{1}{C_C R_M}$,

$c_2 = \frac{1}{C_{PCM} R_{PCM}} + \frac{1}{C_{PCM} R_M}$, $c_3 = \frac{1}{C_M R_{PCM}}$, $d_1 = \frac{1}{C_{PCM} R_{PCM}}$,

$d_2 = \frac{1}{C_M R_{PCM}} + \frac{1}{C_M R_{EQ1}}$, $e_1 = \frac{1}{C_C}$, $e_2 = \frac{1}{C_M R_{EQ1}}$

The states are:

$$\begin{aligned} T = (&T_{F,1} \;\; T_{F,2} \;\; .. \;\; T_{F,N} \\ &T_{C,1} \;\; T_{C,2} \;\; .. \;\; T_{C,N} \\ &T_{PCM,1} \;\; T_{PCM,2} \;\; .. \;\; T_{PCM,N} \\ &T_{M,1} \;\; T_{M,2} \;\; .. \;\; T_{M,N}) \end{aligned} \tag{4.23}$$

The state matrix A:

$$A = \begin{pmatrix} A_{11} & A_{12} & A_{13} & A_{14} \\ A_{21} & A_{22} & A_{23} & A_{24} \\ A_{31} & A_{32} & A_{33} & A_{34} \\ A_{41} & A_{42} & A_{43} & A_{44} \end{pmatrix}_{4N \times 4N}$$

$$A_{11} = \begin{pmatrix} -a_1 & & & \\ -a_2 & -a_1 & & \\ & & & \\ & & -a_2 & -a_1 \end{pmatrix}, \qquad A_{12} = \begin{pmatrix} a_1 & & \\ & a_1 & \\ & & \\ & & a_1 \end{pmatrix},$$

$$A_{21} = \begin{pmatrix} a_3 & & \\ & a_3 & \\ & & \\ & & a_3 \end{pmatrix}, \qquad A_{22} = \begin{pmatrix} -b_1 & & \\ & -b_1 & \\ & & \\ & & -b_1 \end{pmatrix},$$

$$A_{23} = \begin{pmatrix} c_1 & & \\ & c_1 & \\ & & \\ & & c_1 \end{pmatrix}, \qquad A_{32} = \begin{pmatrix} b_2 & & \\ & b_2 & \\ & & \\ & & b_2 \end{pmatrix},$$

$$A_{33} = \begin{pmatrix} -c_2 & & \\ & -c_2 & \\ & & \\ & & -c_2 \end{pmatrix}, \qquad A_{34} = \begin{pmatrix} d_1 & & \\ & d_1 & \\ & & \\ & & d_1 \end{pmatrix},$$

$$A_{43} = \begin{pmatrix} c_3 & & \\ & c_3 & \\ & & \\ & & c_3 \end{pmatrix}, \qquad A_{44} = \begin{pmatrix} -d_2 & & \\ & -d_2 & \\ & & \\ & & -d_2 \end{pmatrix}$$

The input matrix *B*,

$$B = \begin{pmatrix} -a_2 & 0 & . & . & & & . & . & . & & & . & . & . & & 0 \\ 0 & . & . & 0 & e_1 & e_1 & .. & e_1 & 0 & & & . & . & . & & 0 \\ 0 & . & . & & . & . & . & & & . & . & 0 & e_2 & e_2 & .. & e_2 \end{pmatrix}^T \qquad (4.24)$$

The output matrix is,

$$C(t) = \begin{pmatrix} 0 & . & . & 0 & \frac{1}{N} & \frac{1}{N} & \cdots & \frac{1}{N} & 0 & . & . & & . & . & 0 \end{pmatrix} \qquad (4.25)$$

Simulations for the electronics cooling module have been performed, based on the developed dynamic system model of the cooling system, for various time-varying heat generation in the chip. A chip of dimension 30mm×30mm integrated into a cooling system consisting of fin array and rectangular microchannels. This is a modification of the cooling module discussed in section 4.6 by adding PCM encapsulation within the external fins. An optimum spacing of 4mm for a fin thickness of 1mm has been arrived at based on criteria discussed in section 3.5. Therefore, a unit element consisting of twenty-five rectangular microchannels of cross section 100×100μm, with a spacing of 100μm between them, is considered for the present performance analysis. Simulations have been performed for a typical coolant mass flux of $100kg/m^2.s$.

The response of the two branches of the cooling circuits available in the module, viz. fin array with phase changing material storage and microchannel heat exchanger, have been assessed for various modes of heat generation from the chip. Heat dissipation pattern for various modes of heat generation from the chip is shown in Fig. 4.14. Heat dissipation in a cooling circuit containing fin array with phase changing material storage is responding well for sudden cooling demands without dumping considerable heat to the microchannel. Therefore, the phase changing material storage is a suitable option to combine with microchannel heat exchanger intended for single-phase convection heat transfer to avoid the possibility of boiling. Coolant temperature build-up along the length of the microchannel for various type of heat generation in the chip is shown in Fig. 4.15. This has been compared with the performance of a similar cooling module, without the presence of phase changing material, dissipating a steady heat generation from the chip (20W). Cooling module with phase changing material storage is giving rise only very less temperature build-up in coolant microchannel for various type of heat generation in the chip. Phase changing material absorbs latent heat of fusion and helps to negotiate escalating cooling demand, so that the heat dissipation through coolant in microchannel is effective due to the available temperature potential.

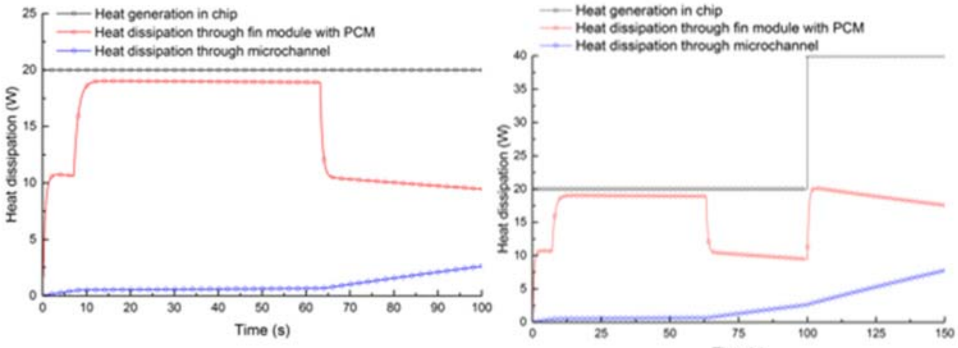

(a) Q_c=20W *for all t*

(b) $Q_C = \begin{cases} 20\text{ W}; t \le 100s \\ 40\text{W}: t \ge 100s \end{cases}$

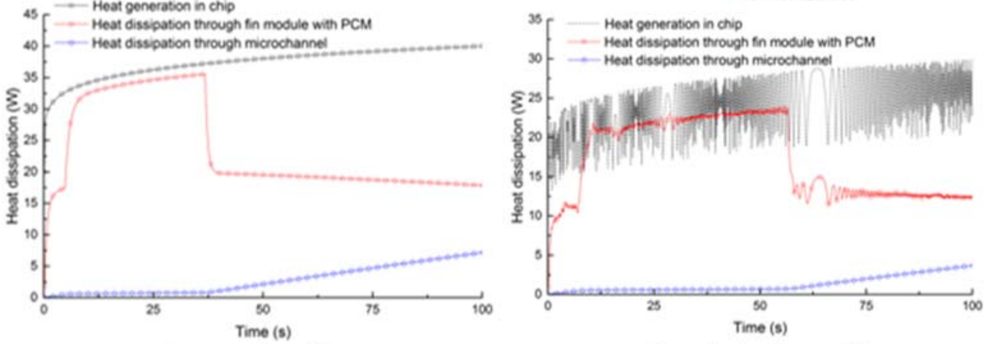

(c) $Q_c = 20(1+\sqrt{t})$W

(d) $Q_c = 10(1+t^{0.3}) + |\sin(10000\sqrt{t})|$W

Fig. 4.14 Heat dissipation pattern for various modes of heat generation

Temperature response for the chip surface as well as the coolant in the microchannel for various time-varying heat generation rates has been obtained for test cases with and without the presence of the phase changing material (Fig. 4.16). Temporal variation of fluid temperature along the length of the rectangular microchannel is also given to indicate heat transfer to the fluid for time-varying heat generation rate. The present study shows that the fin array (embedded with phase changing material) part of the thermal circuit can successfully negotiate sudden cooling demands by the optimal sharing of the heat dissipation among various components in cooling circuit. Temperature build-up for the coolant, during its flow through the microchannel, can be controlled with the use of fin array embedded with the phase changing material. This aspect has been verified for various modes of heat generation in chip. It can also be observed that the fin array embedded with the phase changing material can maintain its safe working temperature for various modes of heat generation in the chip.

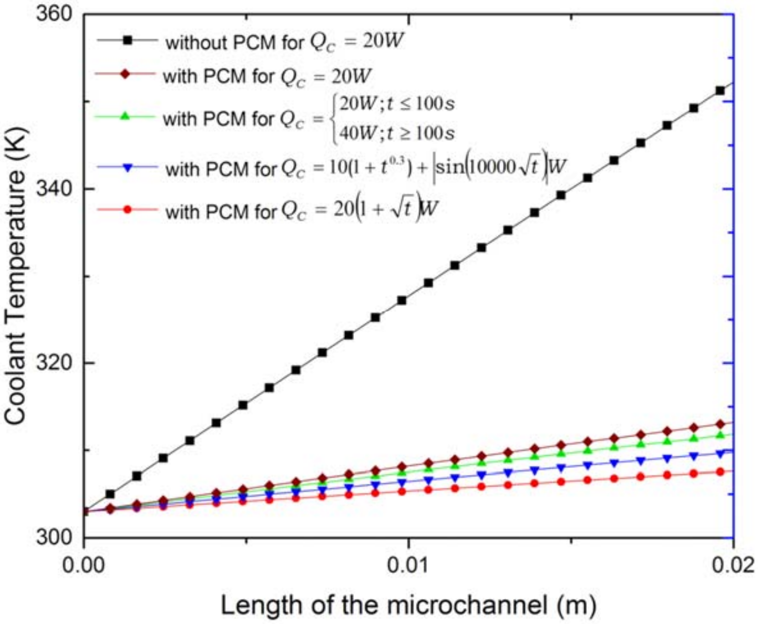

Fig. 4.15 Coolant temperature build-up along the length of the microchannel for various type of heat generation

Negotiation of peak heat dissipation in limited space has been a challenging task in the development of electronics cooling solutions. Coolants introduced through microfluidic passages integrated in the electronic processors can dissipate high heat fluxes and has already emerged as a solution for escalating needs for thermal management. Though phase changing fluids used in microchannels can dissipate the higher amount of heat for a given mass flow rate of the coolant, the system faces various operational difficulties such as flow reversal, instability, excessive pressure drop, vapour cutback near Critical Heat Flux (CHF) conditions.

Therefore, effective self-contained cooling methods are being developed for high heat flux removal in limited space due to the difficulties associated with support systems for cooling. Therefore, the focus of research in boiling inside microchannel has also shifted toward efforts to improve the flow boiling stability.

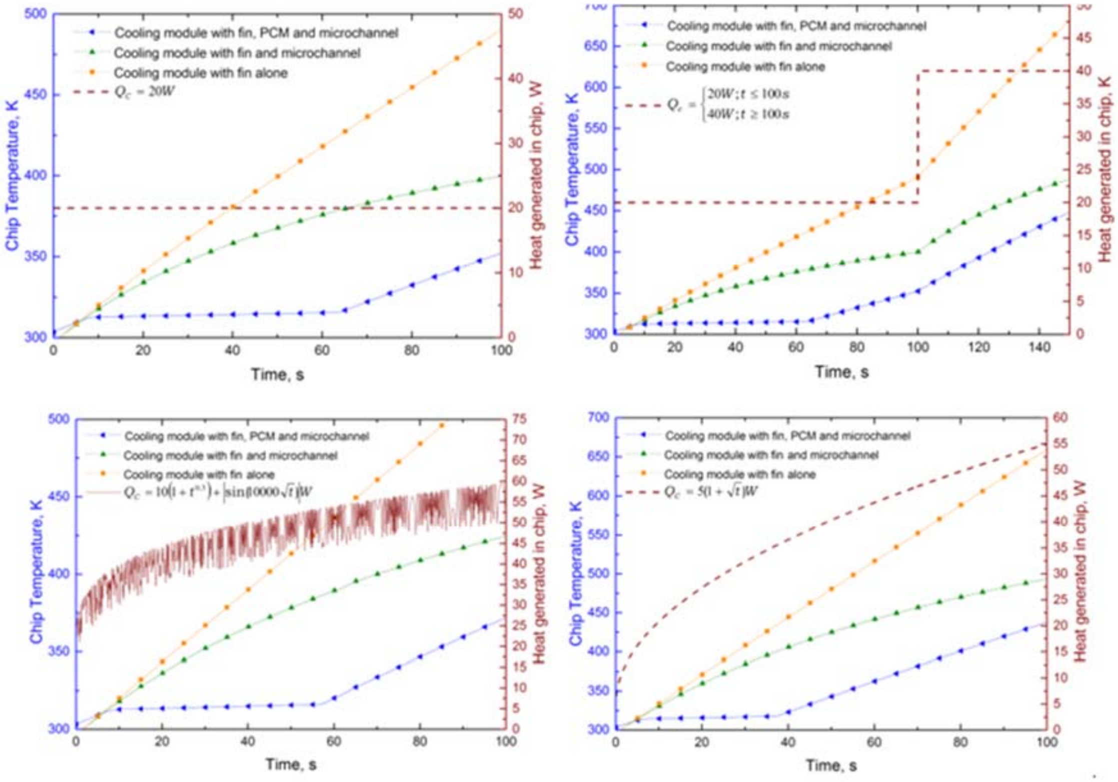

Fig. 4.16 Comparison of cooling system performance with various options and heat generation

4.7.2 Effect of phase change material encapsulation surrounding the microchannels

A novel heat sink design to make use of higher heat transfer coefficients associated with subcooled flow boiling in presence of a Phase Changing Material (PCM) is envisaged here. Subcooled liquid entry to the microchannel heat exchanging system is an attractive option and have been investigated by many researchers in recent past. Subcooled liquid entry with controlled wall superheat helps to set in stable boiling in miniature passages. Nucleation in flow boiling depends on wall superheat and local thermal conditions of the fluid. Latent heat absorbed beyond the melting point temperature of the PCM, stored in electronics cooling module, helps to prevent the rapid growth of vapour bubbles inside microchannels under excessive cooling demand.

A novel self-contained electronics cooling system based on encapsulated phase changing material assisted microchannel flow boiling is proposed here. A schematic of the cooling system is given in Fig. 4.17. Phase changing material is contained in base part of the fin array absorbs heat from coolant while it flows in the microchannel. A dynamic thermal model is developed based on the energy balance of an elemental control volume in a unit element of the cooling module which dissipates heat from a chip with multiple cooling methods. The motivation for the development of a dynamic thermal model is to couple multiple heat transfer elements and analyse their behaviour when the cooling system is subjected to rapid changes in load or operating parameters. A passive control strategy for wall superheat based on local thermal conditions of the fluid and overall cooling demand can be implemented based on such dynamic thermal models.

Consider a unit element of the cooling module consisting of a single fin and its variable area base volume containing the PCM and set of rectangular microchannels that can be accommodated within it. A control volume of length dl is considered in this unit element for the analysis. A thermal circuit representing the one-dimensional heat transfer from the heat generating the chip towards the two heat dissipation branches is given in Fig. 4.18 (a).

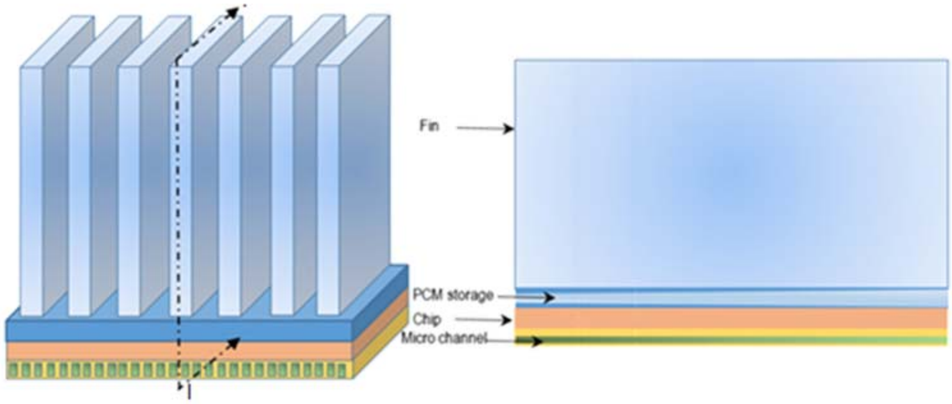

Fig. 4.17 Schematic of the cooling system based on encapsulated PCM assisted microchannel flow boiling

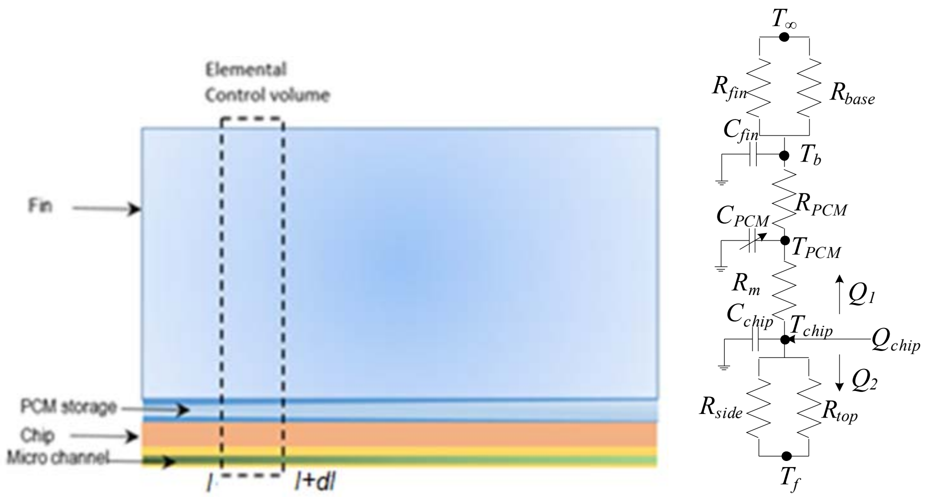

(a) Control volume chosen for modelling (b) Thermal circuit

Fig. 4.18. Model of an encapsulated PCM assisted microchannel

Heat generated in the chip can continuously vary with respect to time in a real scenario, therefore Q_{chip} is chosen here as a time-varying function. This heat is dissipated through the two branches of the cooling circuits, viz, natural convection to ambient through PCM encapsulated fin (Q_1) and the internal forced convection and flow boiling in microchannels (Q_2). The heat Q_1 is dissipated by negotiating the thermal resistance of metallic block and variable area PCM storage, (shown as R_m and R_{pcm} respectively in Fig. 4.18 (b)) and an effective resistance offered by fin due to its conduction and convection (R_{fin} and R_{base}) resistances while interacting with the ambient. On the other hand, the heat Q_2 is dissipated negotiating the thermal resistance offered by the internal convection resistance in the microchannel (R_{side} and R_{top}). PCM contained in the cooling module near to the microchannel absorbs latent heat when its temperature exceeds its melting point

A unit element of the cooling module consists of a single fin and an array of microchannels for cooling a part of chip generating heat. The temperature distribution of the cooling module is obtained by applying energy balance at salient nodes in the thermal circuit for an incremental element dl is given by following partial differential equations.

$$
\begin{aligned}
& C_f \frac{\partial T_f(t,l)}{\partial t} + C_f u \frac{\partial T_f(t,l)}{\partial l} = \frac{\eta_{och} h_{ch} A_{ch} \left(T_{chip} - T_f\right)}{\Delta l} \\
& C_{chip} \frac{dT_{chip}}{dt} = Q_{chip} - \eta_{och} h_{ch} A_{ch} \left(T_{chip} - T_f(t,l)\right) - \frac{\left(T_c - T_{pcm}\right)}{R_m} \\
& C_{pcm} \frac{dT_{pcm}}{dt} = \frac{\left(T_{chip} - T_{pcm}\right)}{R_m} - \frac{\left(T_{pcm} - T_b\right)}{R_{pcm}} \\
& C_{fin} \frac{dT_b}{dt} = \frac{\left(T_{pcm} - T_b\right)}{R_{pcm}} - \eta_{ob} h_\infty A_b \left(T_b - T_\infty\right)
\end{aligned}
\qquad (4.26)
$$

A state space model of the cooling module is created based on governing equations given above. In the present analysis, the unit element of the cooling module is subdivided into a finite number of control volumes with a length *dx* along the length of the channel. Let the element be divided into *N* control volumes. The system state *T* represents the temperature at each node such as fluid, chip, PCM, and the base of the fin in the thermal circuit for every control volume as.

$$\begin{aligned} T = [&T_{f_1}\ T_{f_2}\ ..T_{fN} \\ &T_{c_1}\ T_{c_2}\ ..T_{cN} \\ &T_{PCM_1}\ T_{PCM_2}\ ..T_{PCMN} \\ &T_{b_1}\ T_{b_2}\ ..T_{bN}]^T \end{aligned} \tag{4.27}$$

The system order is 4*N*. The state equations by approximating the spatial deviation for entire length of the system, based on energy conservation on each node, gives

$$\begin{aligned} \dot{T}_{f_j} &= -\left(\frac{\eta_{och} h_{ch} A_{ch}}{C_f} + \frac{u}{\Delta l}\right) T_{f_j} + \frac{\eta_{och} h_{ch} A_{ch}}{C_f} T_{chip_j} + \left(\frac{u}{\Delta l}\right) T_{f_{j-1}} \\ \dot{T}_{chip_j} &= \frac{\eta_{och} h_{ch} A_{ch}}{C_{chip}} T_{f_j} - \left(\frac{\eta_{och} h_{ch} A_{ch}}{C_{chip}} + \frac{1}{C_{chip} R_m}\right) T_{chip_j} + \frac{T_{pcm_j}}{C_{chip} R_m} + \frac{Q_{chip}}{C_{chip}} \\ \dot{T}_{pcm_j} &= \frac{T_{chip_j}}{C_{pcm} R_b} - \left(\frac{1}{C_{pcm} R_b} + \frac{1}{C_{pcm} R_{pcm}}\right) T_{pcm_j} + \frac{T_{b_j}}{C_{pcm} R_{pcm}} \\ \dot{T}_{b_j} &= \frac{T_{pcm_j}}{C_b R_{pcm}} - \left(\frac{1}{C_b R_{pcm}} + \frac{\eta_{ob} h_\infty A_b}{C_b}\right) T_{b_j} + \frac{\eta_{ob} h_\infty A_b}{C_b} T_\infty \end{aligned} \tag{4.28}$$

where *j (j=1, 2, ..., N)* indicates the spatial variation of the system.

The general state space model of the system is given by

$$\dot{\mathbf{T}}(t) = \mathbf{A}(t)\mathbf{T}(t) + \mathbf{B}(t)\mathbf{i}(t) \qquad (4.29)$$

where $\dot{\mathbf{T}}$ is the time derivative of nodal temperature; **i** represents the input vector to the system; **A** and **B** represent the state matrix and input matrix respectively which vary along space and time which is given by,

$$\mathbf{A} = \begin{bmatrix}
-(b+c) & 0 & . & . & b & 0 & . & . & . & . & . & . & . & . & . & 0 \\
0 & -(b+c) & . & . & 0 & b & . & . & . & . & . & . & . & . & . & . \\
. & 0 & . & . & . & 0 & . & . & . & . & . & . & . & . & . & . \\
. & . & . & -(b+c) & . & . & . & b & . & . & . & . & . & . & . & . \\
e & . & . & 0 & -(e+f) & . & . & 0 & f & . & . & . & . & . & . & . \\
0 & e & . & . & 0 & -(e+f) & . & . & 0 & f & . & . & . & . & . & . \\
. & 0 & . & . & . & 0 & .. & . & . & 0 & . & . & . & . & . & . \\
. & . & . & e & . & . & . & -(e+f) & . & . & . & f & . & . & . & . \\
. & . & . & 0 & k & . & . & 0 & -(k+l) & . & . & 0 & l & . & . & . \\
. & . & . & . & 0 & k & . & . & 0 & -(k+l) & . & . & 0 & l & . & . \\
. & . & . & . & . & 0 & . & . & . & 0 & . & . & . & 0 & . & . \\
. & . & . & . & . & . & . & k & . & . & . & -(k+l) & . & . & 0 & l \\
. & . & . & . & . & . & . & 0 & m & . & . & 0 & -(m+n) & . & . & 0 \\
. & . & . & . & . & . & . & . & 0 & m & . & . & 0 & -(m+n) & . & . \\
. & . & . & . & . & . & . & . & . & . & . & . & . & 0 & . & . \\
0 & . & . & . & . & . & . & . & . & . & . & m & . & . & 0 & -(m+n)
\end{bmatrix}$$

$$\mathbf{B} = \begin{bmatrix}
c & 0 & 0 \\
0 & . & . \\
. & . & . \\
. & . & . \\
. & d & . \\
. & d & . \\
. & . & . \\
. & d & . \\
. & 0 & . \\
. & . & . \\
. & . & . \\
. & . & . \\
. & . & n \\
. & . & n \\
. & . & . \\
0 & . & n
\end{bmatrix}$$

$$b = \frac{\eta_{och} h_{ch} A_{ch}}{C_f}, c = \frac{u}{\Delta x}, e = \frac{\eta_{och} h_{ch} A_{ch}}{C_{chip}},$$

where, $d = \dfrac{1}{C_{chip}}, f = \dfrac{1}{C_{chip} R_m} k = \dfrac{1}{C_{pcm} R_b},$

$$l = \frac{1}{C_{pcm} R_{pcm}}, m = \frac{1}{C_b R_{pcm}}, n = \frac{\eta_{ob} h_{\infty} A_b}{C_b}$$

The input vector considered for the system includes input to the system as well as a disturbance. Heat generated in the chip (Q_c) is given as a time-varying the input to the system. Coolant inlet temperature (T_{f0}) and ambient temperature (T_∞) forms the disturbance input to the system. The input vector is given by

$$\mathbf{i}(\boldsymbol{t}) = \begin{bmatrix} T_{f0} & Q_{chip} & T_\infty \end{bmatrix}^T . \tag{4.30}$$

The output of the system is represented by the output vector

$$\mathbf{y}(\boldsymbol{t}) = \mathbf{C}(\boldsymbol{t})\mathbf{T}(\boldsymbol{t}) + \mathbf{D}(\boldsymbol{t})\mathbf{i}(\boldsymbol{t}) \tag{4.31}$$

where **C(*t*)** is the output matrix and **D(*t*)** is the feed-through matrix.

Since there is no direct feedthrough (or feedforward) from input to output

$$\mathbf{D}(\boldsymbol{t}) = [0].$$

The output matrix **C(*t*)** is given by

$$\mathbf{C} = \begin{bmatrix} 0 & . & . & 0 & \frac{1}{N} & \frac{1}{N} & . & . & \frac{1}{N} & 0 & . & . & . & . & . & 0 \end{bmatrix}. \tag{4.32}$$

The variation of the heat transfer coefficient of fluid with respect to the vapour quality of the fluid is computed using two-phase relations given in section 3.3. This when applied for the present microchannel flow boiling problem, exhibits the typical heat transfer coefficient profile as given in Fig.4.19. The negative vapour quality indicates single-phase heat transfer, while positive vapour quality indicates two-phase heat transfer. The heat transfer coefficient is found to be maximum of the order of 10^5 W/m^{2}K at $x = 0$ and decreases with the increase of vapour quality. The decreasing trend of heat transfer coefficient indicates the dominance of nucleate boiling as predicted by Steinke and Kandlikar, (2004 b). The vapour quality along the length of the microchannel is found to be different for various heat fluxes applied on microchannel wall as given in Figure 4. 20 As the heat flux to the microchannel increases, boiling initiation occurs as soon as the fluid enters the microchannel resulting in the dominance of saturated boiling for the entire length of the channel.

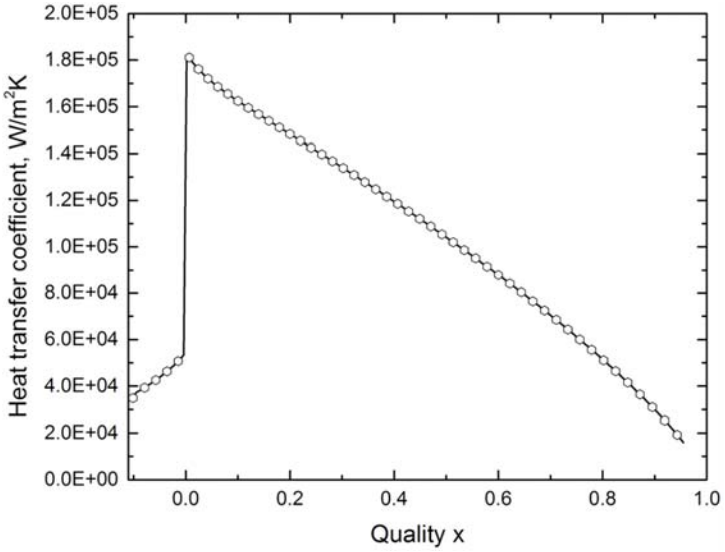

Fig.4.19. Variation of heat transfer coefficient with vapour quality

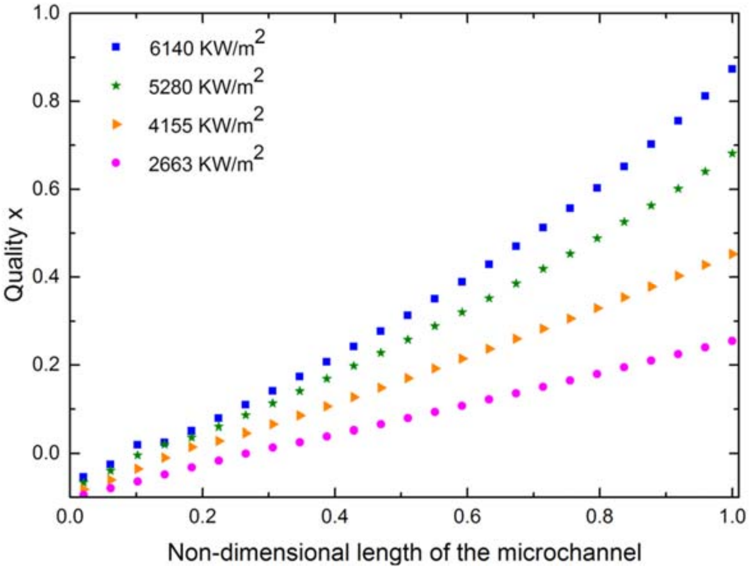

Fig. 4. 20 Thermodynamic vapour quality along the length of the microchannel

A unit element of an electronics cooling module consisting of an array of 20 identical microchannels with a cross-section of 250µm×250µm and length of 20mm has been chosen for the simulation. PCM is encapsulated in a constant cross-sectional area cavity above the microchannel array, with a cross-section of 500µm×500µm at the inlet of the microchannel. External fin is having a thickness of 1.2mm and is assumed to be spaced identically on the surface of the cooling module. Coolant temperature in the microchannel is initialized with its inlet temperature and integrated in time with time-varying heat flux.

Heat developed in the electronic chip is dissipated in two branches of the thermal circuit. This heat share depends on the available thermal conductance in each branch. Heat dissipation through the microchannel and PCM encapsulated fin for a time varying heat input is shown in Fig 4.21. Heat dissipation to coolant is affected after the completion of melting of the PCM. Hence for a given time interval, the heat flux to the microchannel is lower compared to the cooling module without PCM (Fig.4.22).

The critical heat flux calculated using correlations is approximately of the order of 10^6 for the microchannel of given dimensions. The cooling module with PCM storage delays the occurrence of CHF, thereby prolonging the occurrence of dry out condition. The reduction of heat flux to microchannel in the cooling modules with PCM storage suppresses the boiling phenomenon. This is evident from the nature of vapor generation profile in the microchannel given in Fig. 4.23.

The effect of PCM reflected in the vapor quality at the exit of the rectangular microchannel as well (Fig. 4.24). PCM could control the boiling for the sufficiently longer duration of time so that sudden shift of boiling phase to CHF conditions will not occur. Advantages of higher heat transfer coefficients associated with nucleate boiling can be prolonged for a longer duration with the presence of PCM

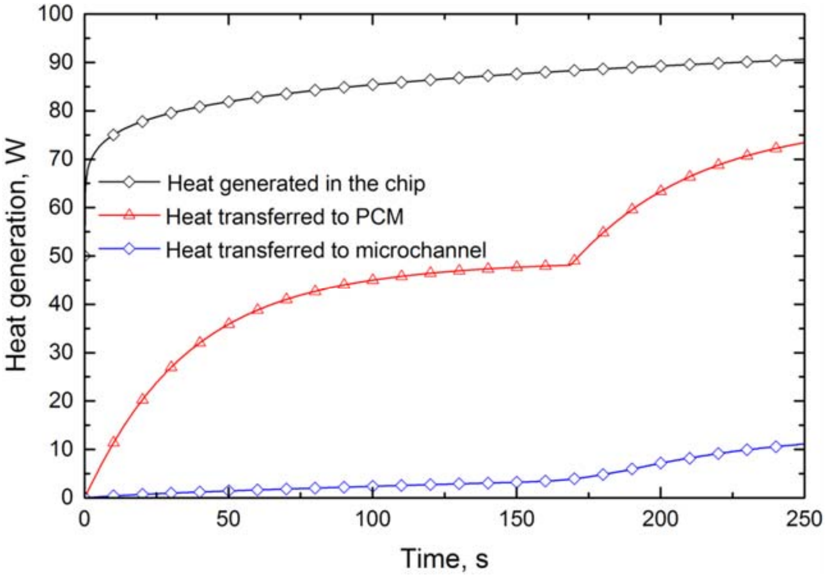

Fig. 4.21. Heat dissipation through the microchannel and PCM encapsulated fin for a time varying heat input

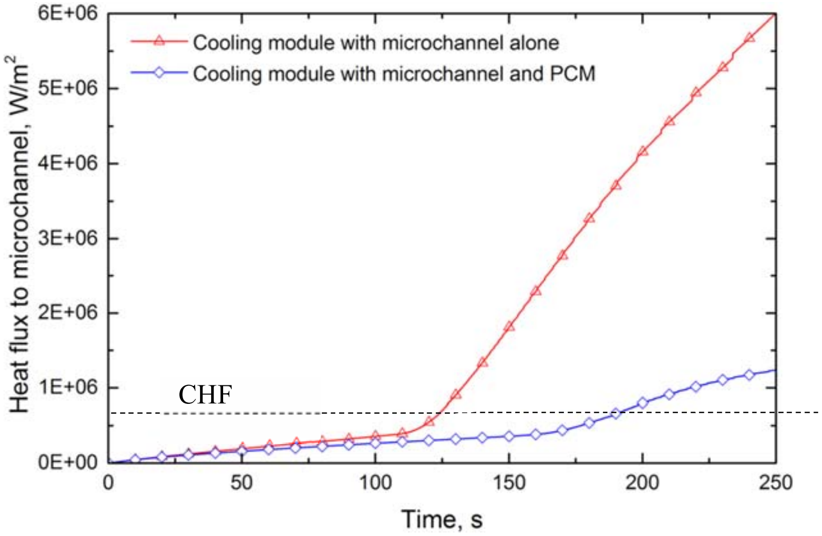

Fig. 4.22. Comparison of heat flux to microchannel in cooling modules with and without PCM storage

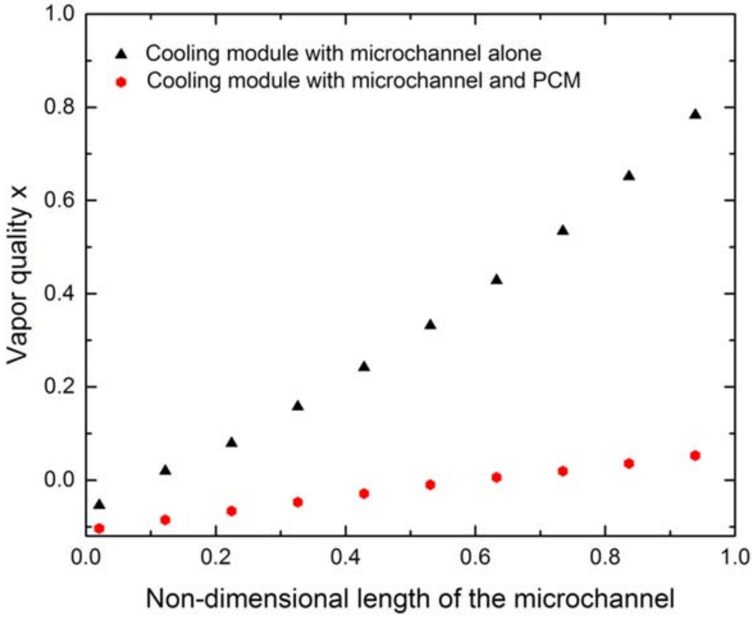

Fig. 4.23. Vapour quality along the length of the microchannel in cooling modules with and without PCM storage

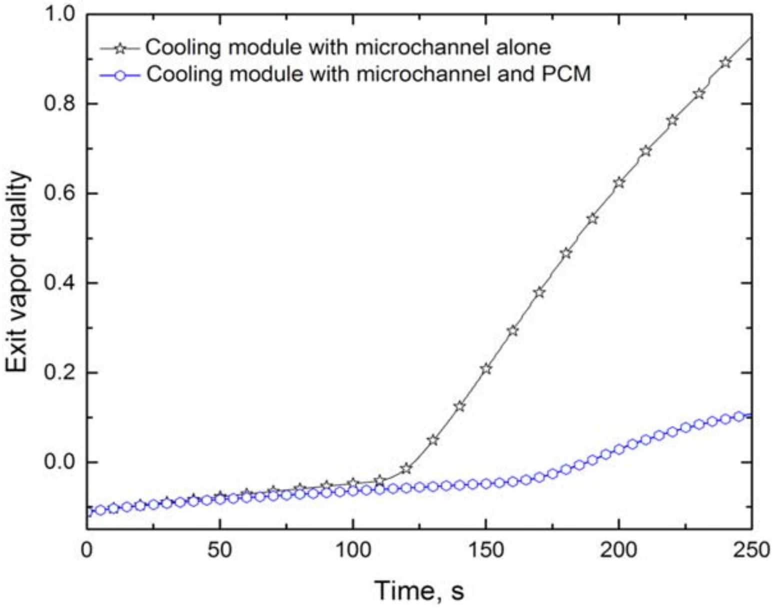

Fig. 4.24. Exit vapour quality in cooling modules with and without PCM

Temporal development of chip surface and local fluid temperature are available from the solution of simultaneous equations governing the dynamics of the system. Wall superheat at two axial locations has been worked out from the solution for the given time-varying heat input (Fig.4.25). PCM is found to effectively control the wall superheat during its melting. The differing slope of temperature response at different locations is attributed by the additional heat capacity offered by the PCM storage. The effect of PCM on wall superheat is evident in Fig.4.26, where the wall superheat of the cooling module with and without PCM storage is compared.

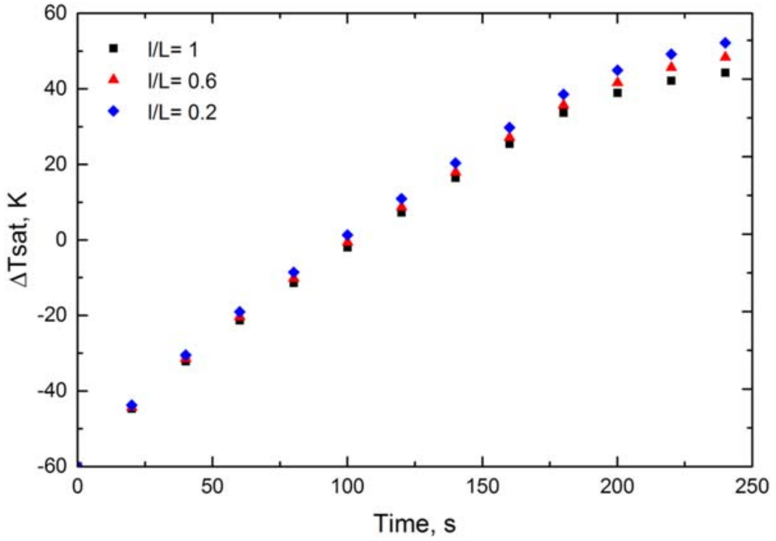

Fig. 4.25 Wall superheat at two axial locations in the microchannel

Simulations have also been performed by varying the mass flux of the coolant for a given time-varying heat flux generated in the chip (Fig.427). Noticeable change in chip temperature was not observed beyond a coolant mass flux of 400kg/m^{2}s. This is due to the limitation in heat flow towards the coolant in a microchannel, as heat dissipation is divided among both cooling circuits based on available thermal conductance.

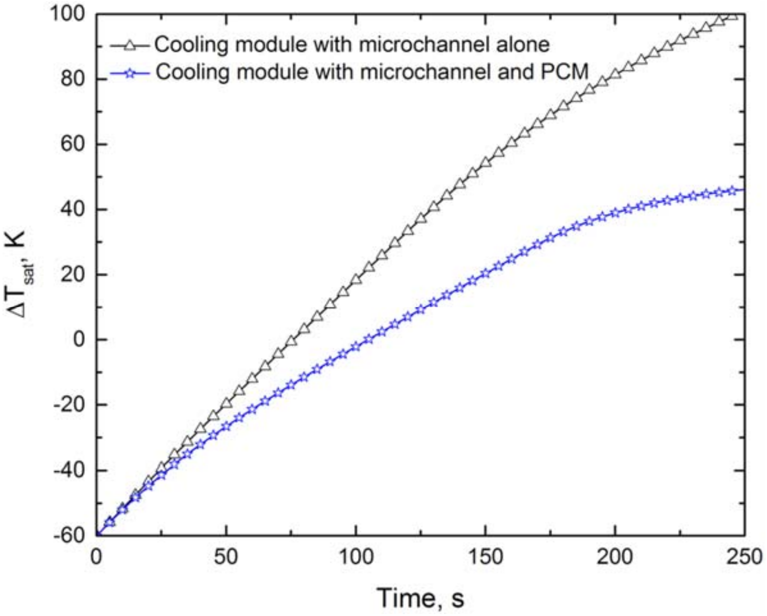

Fig. 4.26. Comparison of wall superheat in cooling modules with and without PCM storage

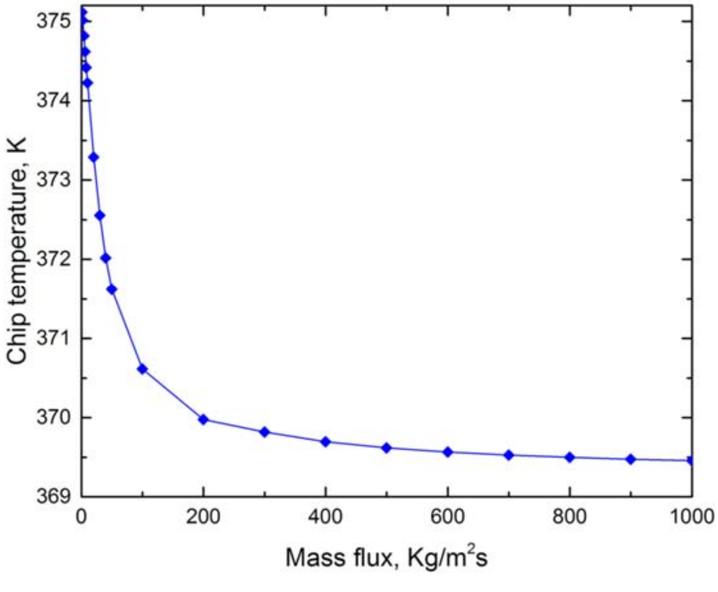

Fig. 4.27. Chip temperature corresponding to various fluid mass flux

4.7.3 Effect of variable area phase change material encapsulation surrounding the microchannels

Now the previous configuration has been modified by adding a variable cross-sectional area PCM storage embedded near the base of the heat sink which contains PCM with higher melting temperature and another storage in inter-fin spaces with lower melting temperature. A schematic of the cooling module is given in Fig. 4.28. PCM with lower melting temperature absorbs heat during the normal operation of the chip and the latter storage in which PCM with higher melting temperature prevents the possibilities of unstable bubble dynamics in restricted fluid passage period during the peak heat dissipation demand.

System dynamics modelling and simulation of a miniature electronics cooling module employing PCM assisted flow boiling of coolant in rectangular microchannel has been carried out. A state space model for the simultaneous solution of conjugate heat transfer in solid, PCM and liquid domain is formulated based on the energy balance of the differential control volume considered in cooling module. Each component of this unit cooling element is modelled based on the appropriate heat transfer models and are assembled to analyze the multimode heat dissipation from the chip. This system of equations is integrated in space by updating coefficient matrices and input vector to take care of the spatial variation in thermal capacities of constitutive components and heating up of coolant in microchannel along the length of the unit element.

An element of the cooling module consisting of a single fin embedded with PCM (of type 1) and another PCM (of type 2) inside variable area storage surrounding the rectangular microchannels. A schematic of the control volume considered in unit element of the cooling module and extent of PCM storages are shown in Fig.29 (a).

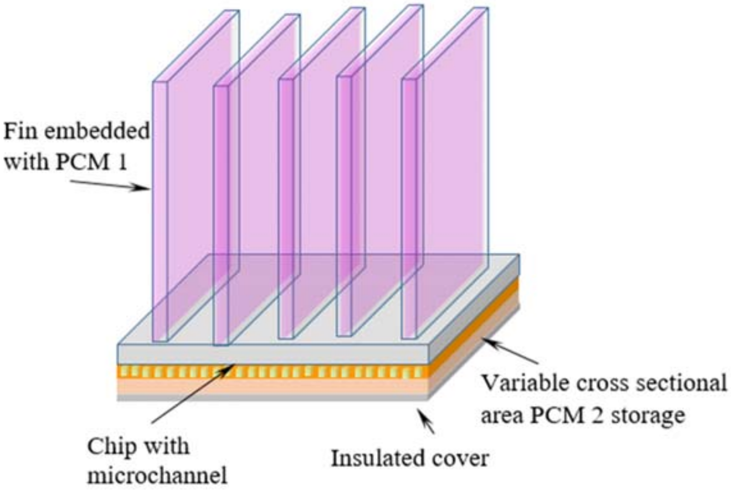

Fig. 4.28. Schematic of the cooling system based on variable area encapsulated PCM assisted microchannel flow boiling

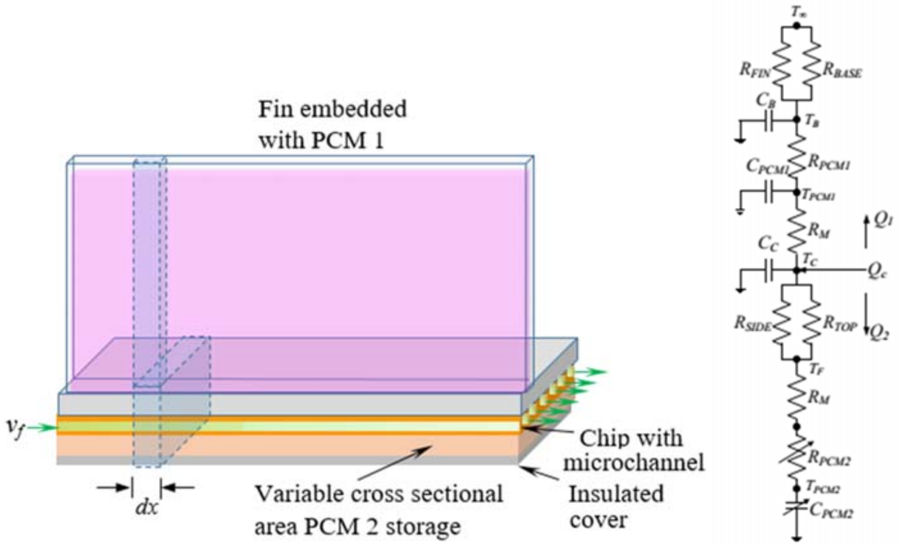

(a) Control volume chosen for modelling (b) Thermal circuit

Fig 4.29. Model of a variable area encapsulated PCM assisted microchannel

Consider a control volume in this base element of length dx in the direction of coolant flow. An equivalent thermal circuit representing heat dissipation through various components of the cooling module is shown in Fig. 4.29 (b)

Governing equations developed based on nodal energy balance are

$$
\begin{aligned}
&C_F \frac{\partial T_F(t,x)}{\partial t} + C_F u \frac{\partial T_F(t,x)}{\partial x} = \frac{T_C(t) - T_F(t,x)}{R_{EQ2}\Delta x} - \frac{T_F(t) - T_{PCM2}(t)}{R_M + R_{PCM2}} \\
&C_C \frac{dT_C(t)}{dt} = Q_C - \frac{T_C(t) - T_F(t,x)}{R_{EQ2}} - \frac{T_C(t) - T_{PCM1}(t)}{R_M} \\
&C_{PCM1} \frac{dT_{PCM1}(t)}{dt} = \frac{T_C(t) - T_{PCM1}(t)}{R_M} - \frac{T_{PCM1}(t) - T_M(t)}{R_{PCM1}} \\
&C_M \frac{dT_M(t)}{dt} = \frac{T_{PCM1}(t) - T_M(t)}{R_{PCM1}} - \frac{T_M(t) - T_\infty(t)}{R_{EQ1}} \\
&C_{PCM2} \frac{dT_{PCM2}(t)}{dt} = \frac{T_F(t) - T_{PCM2}(t)}{R_M + R_{PCM2}},
\end{aligned}
\tag{4.33}
$$

where C_{PCM2} varies with the length of the microchannel

The state equations are:

$$
\begin{aligned}
\dot{T}_{F,i} &= -a_1 T_{F,i} + b_1 T_{C,i} - a_2 T_{F,i-1} + e_1 T_{PCM\,2,i} \\
\dot{T}_{C,i} &= a_3 T_{F,i} - b_2 T_{C,i} + c_1 T_{PCM\,1,i} + f_1 Q_C \\
\dot{T}_{PCM\,1,i} &= b_3 T_{C,i} - c_2 T_{PCM\,1,i} + d_1 T_M \\
\dot{T}_{M,i} &= c_3 T_{PCM\,1,i} - d_2 T_{M,i} + f_2 T_\infty \\
\dot{T}_{PCM\,2,i} &= a_4 T_{F,i} - e_2 T_{PCM\,2,i}
\end{aligned}
\tag{4.34}
$$

where $a_1 = \dfrac{1}{C_F R_{EQ2} \Delta x} + \dfrac{u}{\Delta x} + \dfrac{1}{C_F (R_M + R_{PCM2})}$, $a_2 = \dfrac{u}{\Delta x}$, $a_3 = \dfrac{1}{C_C R_{EQ2}}$,

$$a_4 = \frac{1}{C_{PCM2}(R_M + R_{PCM2})},\ b_1 = \frac{1}{C_F R_{EQ2}\Delta x} + \frac{u}{\Delta x},\ b_2 = \frac{1}{C_C R_{EQ2}} + \frac{1}{C_C R_M},$$

$$b_3 = \frac{1}{C_{PCM1} R_M},\ c_1 = \frac{1}{C_C R_M},\ c_2 = \frac{1}{C_{PCM1} R_{PCM1}} + \frac{1}{C_{PCM1} R_{M1}},$$

$$c_3 = \frac{1}{C_M R_{PCM1}},\ d_1 = \frac{1}{C_{PCM1} R_{PCM1}},\ d_2 = \frac{1}{C_M R_{PCM1}} + \frac{1}{C_M R_{EQ1}},$$

$$e_1 = \frac{1}{C_F(R_M + R_{PCM2})}, e_2 = \frac{1}{C_{PCM2}(R_M + R_{PCM2})}$$

The states are:

$$T = \begin{bmatrix} T_{F,1} \\ .. \\ T_{F,N1} \\ T_{C,1} \\ .. \\ T_{C,N} \\ T_{PCM1,1} \\ .. \\ T_{PCM1,N} \\ T_{M,1} \\ .. \\ T_{M,N} \\ T_{PCM2,1} \\ .. \\ T_{PCM2,N} \end{bmatrix}$$

The state matrix A:

$$A = \begin{pmatrix} A_{11} & A_{12} & A_{13} & A_{14} & A_{15} \\ A_{21} & A_{22} & A_{23} & A_{24} & A_{25} \\ A_{31} & A_{32} & A_{33} & A_{34} & A_{35} \\ A_{41} & A_{42} & A_{43} & A_{44} & A_{45} \\ A_{51} & A_{52} & A_{53} & A_{54} & A_{55} \end{pmatrix}_{5N\times 5N}$$

$$A_{11}=\begin{pmatrix} -a_1 & & & \\ -a_2 & -a_1 & & \\ & & & \\ & & -a_2 & -a_1 \end{pmatrix}, \qquad A_{12}=\begin{pmatrix} b_1 & & & \\ & b_1 & & \\ & & & \\ & & & b_1 \end{pmatrix},$$

$$A_{15}=\begin{pmatrix} e_1 & & & \\ & e_1 & & \\ & & & \\ & & & e_1 \end{pmatrix}, \qquad A_{21}=\begin{pmatrix} a_3 & & & \\ & a_3 & & \\ & & & \\ & & & a_3 \end{pmatrix},$$

$$A_{22}=\begin{pmatrix} -b_2 & & & \\ & -b_2 & & \\ & & & \\ & & & -b_2 \end{pmatrix}, \qquad A_{23}=\begin{pmatrix} c_1 & & & \\ & c_1 & & \\ & & & \\ & & & c_1 \end{pmatrix},$$

$$A_{32}=\begin{pmatrix} b_3 & & & \\ & b_3 & & \\ & & & \\ & & & b_3 \end{pmatrix}, \qquad A_{33}=\begin{pmatrix} -c_2 & & & \\ & -c_2 & & \\ & & & \\ & & & -c_2 \end{pmatrix},$$

$$A_{34}=\begin{pmatrix} d_1 & & & \\ & d_1 & & \\ & & & \\ & & & d_1 \end{pmatrix}, \qquad A_{43}=\begin{pmatrix} c_3 & & & \\ & c_3 & & \\ & & & \\ & & & c_3 \end{pmatrix},$$

$$A_{44}=\begin{pmatrix} -d_2 & & & \\ & -d_2 & & \\ & & & \\ & & & -d_2 \end{pmatrix}, \qquad A_{51}=\begin{pmatrix} a_4 & & & \\ & a_4 & & \\ & & & \\ & & & a_4 \end{pmatrix},$$

$$A_{55}=\begin{pmatrix} -e_2 & & & \\ & -e_2 & & \\ & & & \\ & & & -e_2 \end{pmatrix}$$

The input matrix *B*,

$$B=\begin{pmatrix} -a_2 & 0 & . & . & & & . & . & . & & & . & . & . & & 0 \\ 0 & . & . & 0 & f_1 & f_1 & .. & f_1 & 0 & & & . & . & . & & 0 \\ 0 & . & . & & . & . & . & & & . & . & 0 & f_2 & f_2 & .. & f_2 \end{pmatrix}^T \qquad (4.35)$$

This system of equations is integrated in space by updating coefficient matrices and input vector to take care of the spatial variation in thermal capacities of constitutive components and heating up of coolant in microchannel along the length of the unit element.

Multimode heat dissipation process occurring in an electronics cooling module is simulated based on the dynamic thermal model developed from appropriate heat transfer formulations of its constituent elements. A unit element in an electronics cooling module (as shown in Fig. 4.29) has been simulated. This unit model has an external fin of thickness 1mm. The thickness of the metallic cover given for the PCM encapsulated in it is negligible. An array of 25 microchannels with each channel having a length of 0.02m and hydraulic diameter of 100μm is chosen. They are separated by a wall thickness of 0.1mm. Water has chosen as the working fluid for the present study and is flowing inside the channel with a constant velocity of 0.01m/s. A transient heat generation $\hat{Q}=20\left(1+\tau^{0.15}\right)$ is introduced in the chip. The heat generated in the chip is dissipated through two branches of the cooling circuit as discussed before. Temporal variation of the temperature of the chip and coolant (temperature averaged for the entire length) in microchannel are shown in Fig. 4.30 Sudden rise of the heat in chip during the initial transient raises the chip temperature. The higher amount of heat dissipation towards ambient (Q_1) through the external fin array containing PCM 1 is observed during this period of operation (Fig. 4.31). This due to relatively lesser resistance in this branch of the cooling system during this period. This leads to the quick melting of PCM1 and in-turn control the temperature level of the chip in the desired range.

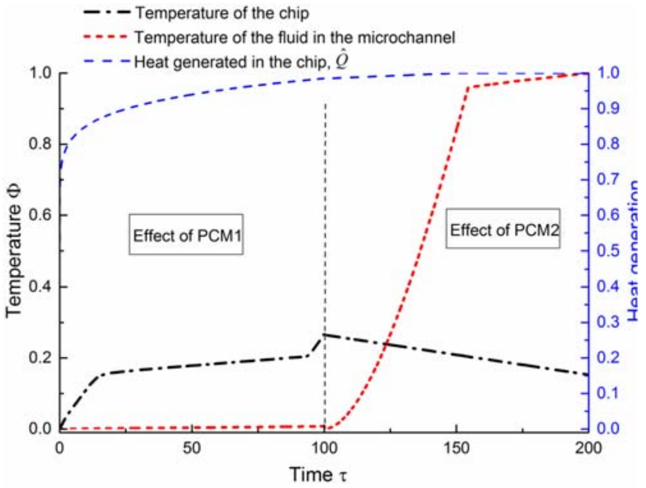

Fig. 4.30 Effect of PCM1 and PCM2 in controlling the chip temperature for the entire operation of cooling module

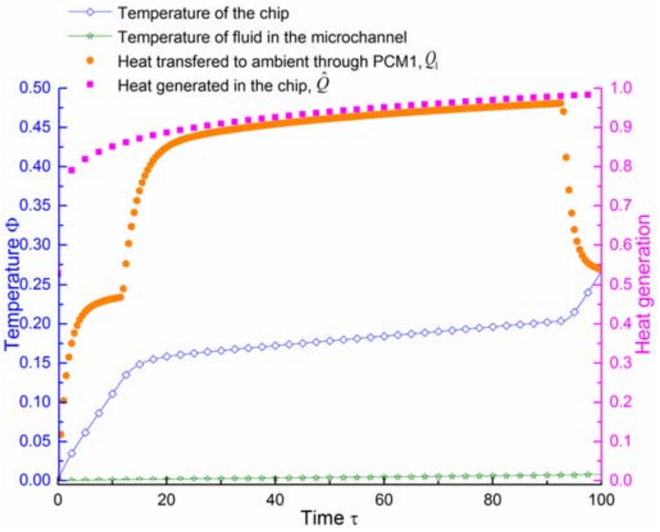

Fig. 4.31 Variation of heat transfer to the ambient (Q1) through the PCM encapsulated in fin during the initial transient heat generation in chip

The trend of heat dissipation discussed above continues till the completion of melting process in PCM1 encapsulation. Subsequently, the majority of the heat dissipation happens through the coolant inside the microchannel (*Q_2*) due to the favourable conditions arising due to the relative change in resistance. This increases in temperature of the coolant in microchannel till the incipience of boiling. Further heat absorption leads to formation of vapor inside the channel. Variation of quality of coolant along the length of the channel at two instances of time are shown in Fig. 4.32. Initiation of melting of PCM2 controls the evaporation in microchannel.

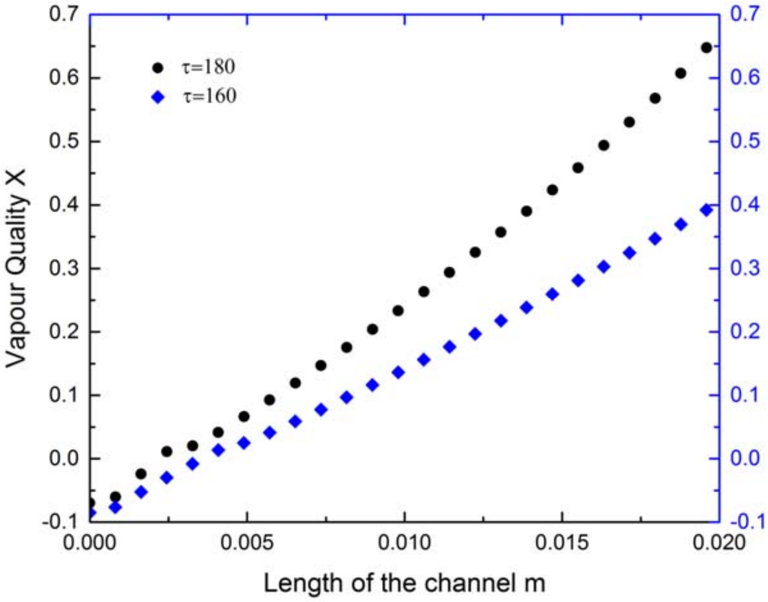

Fig. 4.32 Profile of the quality of working fluid

Microchannel wall surrounds variable area PCM storage whose cross-section varies linearly along its length. PCM storage surrounding the microchannel starts absorbing latent heat for its melting when the surrounding temperature approaches its melting point. Overall heat capacity in latent heat storages increases along the flow direction. This controls the further rise of coolant temperature inside the channel as shown in Fig. 4.33. Chip temperature remains within safer limits due to the high heat flux removal by boiling in the microchannel.

The actual amount of heat flux carried into the fluid inside the microchannel is calculated from the solution of the dynamic thermal model. Variation in heat flux transferred to the microchannel (averaged along the length of the channel) during flow boiling period alone is shown in Fig.4.34. Effect of the latent heat stored by PCM2 in controlling the heat flux to the fluid inside the microchannel is evident.

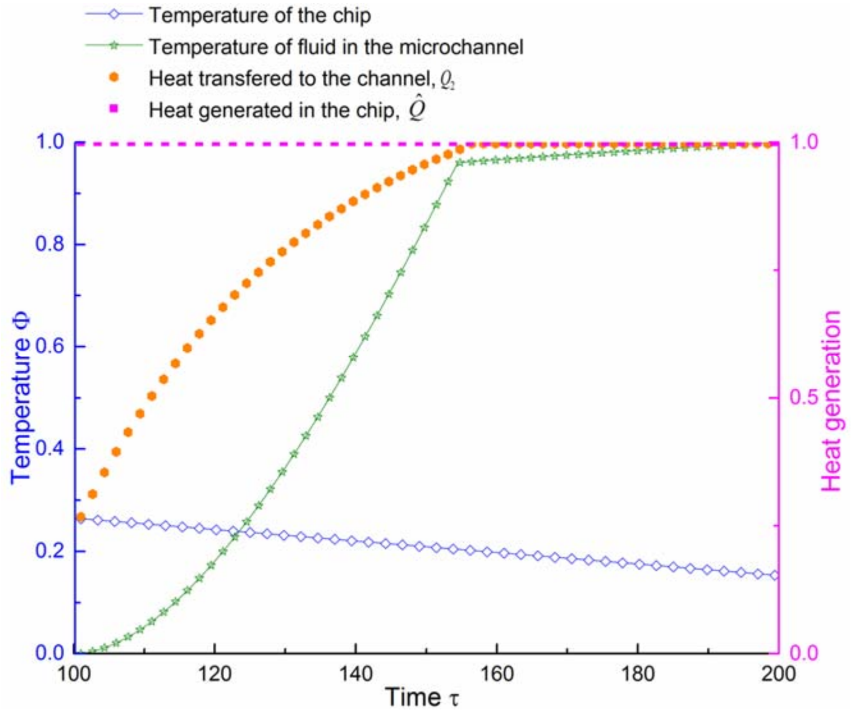

Fig. 4.33 Variation of heat transfer to the fluid in a microchannel (Q2) during the steady heat generation in chip

Two-phase heat transfer coefficient worked out using the correlation proposed by Steinke and Kandlikar (2004 b) was used in the present modelling. This helps to update internal convection heat transfer coefficient based on the quality of working fluid, available wall heat flux and mass flux of the coolant. Fig. 4.35 shows the variation of the local two phase heat transfer coefficient with respect to length of the channel. The evaluation of the local two phase heat transfer coefficient is crucial in determining the actual amount of heat carried in to the fluid inside the microchannel at each location.

The phase changing material embedded in external fin array is effective during the initial phase of operation where the resistance of heat flow in that path is minimum. Later the PCM storage surrounding the microchannel wall controls the heat dissipation in that path and effectively limits the temperature build-up of the chip. Variation in the capacity volume of the latent heat storage helps to prolong the favourable heat transfer conditions offered by flow boiling.

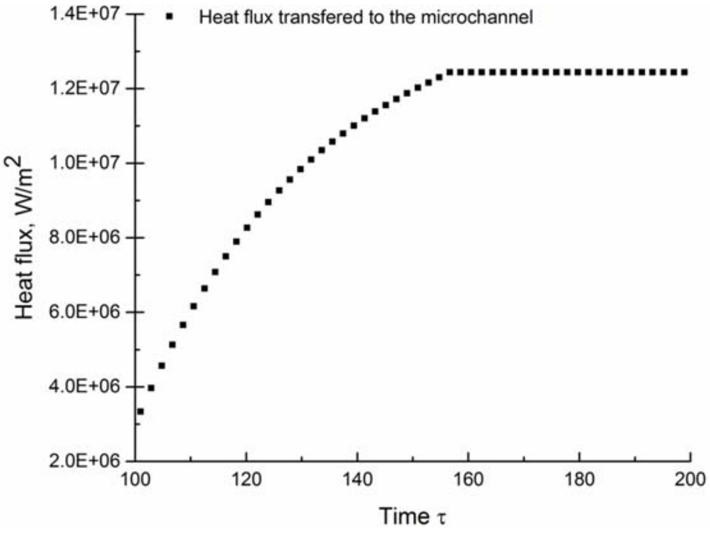

Fig. 4.34. Variation in heat flux transferred to the microchannel during flow boiling period

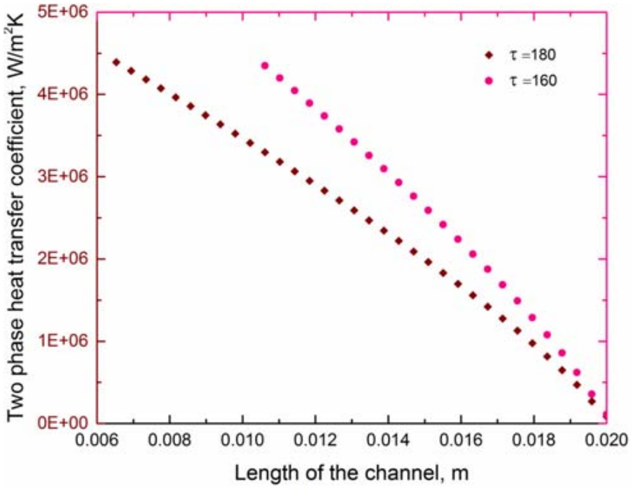

Fig. 4.35 Estimated local two-phase heat transfer coefficient for two instances during flow boiling

4.8 SUMMARY

Dynamic thermal system design, modelling, and analysis of cooling modules involving more than one heat dissipation modes were discussed. A detailed deliberation of system modelling based on the mathematical models and correlations for various sub-systems constituting the cooling module has been carried out. Predictability of the developed thermal models is established by comparing the results with widely acceptable benchmark experimental test cases. Effect of PCM in damping chip temperature during peak heat dissipation in single phase convection systems is established. Analysis has been extended to two-phase systems and the role of variable area PCM storages in controlling boiling is also affirmed. This has been established through detailed parametric studies involved in flow boiling based on the solution of the state space model developed for the dynamic system model. Few active control strategies have also been attempted based on the developed dynamic thermal models for the cooling module. These active control system design and simulation studies are presented in the next chapter.

CHAPTER 5

ACTIVE CONTROL SYSTEM DESIGN, MODELLING, AND SIMULATION

5.1 INTRODUCTION

Active control system design and simulation of a microchannel based electronics cooling system are presented. Control of chip surface temperature is vital in maintaining the performance of the processor. Therefore, the chip temperature is chosen as the controlled variable. It is already established in the preceding sections that flow rate of coolants hasan insignificant effect in maintaining chip temperature for single-phase internal forced convection. The temperature of coolant at the inlet of the microchannel is selected as manipulating variable. The objective of the active control design is to stabilize the chip temperature for a given transient heat generation by manipulating inlet coolant temperature. Control system design and simulation of the heat exchanging process involving single-phase forced convection are carried out using H_∞ control as well as PID control, and their performance aspects are compared. Flow boiling in microchannel results in excessive pressure drop and oscillations during the heat exchanging process which in turn leads to system instability. Therefore, a cascade controller involving control loops for both pressure and temperature are designed and simulated. Dynamics of the heat exchanging system in response to the various heat generation pattern (major disturbance in the system) are assessed in detail. Electronics cooling module also may have heat dissipation by natural convection through fin array. Therefore, ambient temperature is also considered as a minor disturbance in the system.

5.2 SYSTEM MODELLING FOR CONTROL

A unit element of the cooling module, consisting of a microchannel array and a fin (Fig. 5.1), is considered for the development of a system model for control.

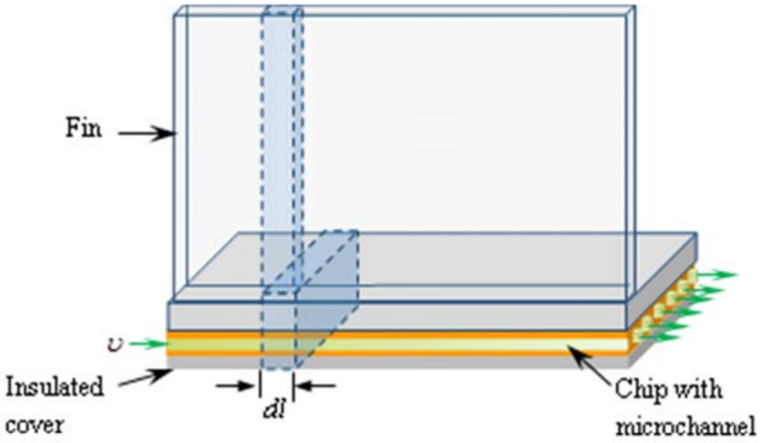

Fig. 5.1Unit element considered for developing a system model

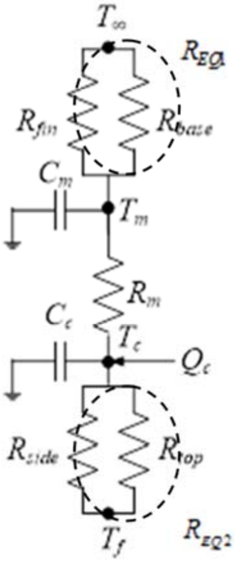

Fig. 5.2 Thermal circuit for the system model

Applying energy balance on the nodes considered at fluid, chip and base of the fin gives the following equations

$$
\begin{aligned}
&C_F \frac{\partial T_F(t,x)}{\partial t} + C_F u \frac{\partial T_F(t,x)}{\partial x} = \frac{T_C(t) - T_F(t,x)}{R_{EQ2}\Delta x} \\
&C_C \frac{dT_C(t)}{dt} = Q_C - \frac{T_C(t) - T_F(t,x)}{R_{EQ2}} - \frac{T_C(t) - T_M(t)}{R_M} \\
&C_M \frac{dT_M(t)}{dt} = \frac{T_C(t) - T_M(t)}{R_M} - \frac{T_M(t) - T_\infty(t)}{R_{EQ1}}
\end{aligned}
\qquad (5.1)
$$

Physical parameters involved in the present problem are similar to those described in section 4.4 and are further transformed to the following dimensionless terms,

Temperature expressed in terms of reference temperature T_r is $\Theta_i = \frac{T_i - T_r}{\Delta T_r}$, $i = F, C, M$, the length along microchannel $\xi = \frac{C_F}{C_c} x$, time $\tau = \frac{t}{C_C R_M}$, heat input $\hat{Q}_c = \frac{Q_c}{Q_{\max}}$, and the velocity $\hat{U} = \frac{C_c R_M}{\Delta x} u$

Heat transfer resistance ratios are $R_1 = \frac{R_M}{R_{EQ2}}$ and $R_2 = \frac{R_M}{R_{EQ1}}$ Heat capacity ratios are $C_1 = \frac{C_F}{C_C} \Delta x$ and $C_2 = \frac{C_M}{C_C}$. Partial differential equations based on energy balance (5.1) can be rewritten in terms of aforementioned dimensionless parameters as,

$$
\begin{aligned}
&\frac{\partial \Theta}{\partial \tau} = -\frac{\hat{U}}{C_1} \frac{\partial \Theta}{\partial \xi} + \frac{R_1}{C_1}\left(\Theta_C - \Theta_F\right) \\
&\frac{d\Theta_C}{d\tau} = \hat{Q}_C - R_1\left(\Theta_C - \Theta_F\right) - \left(\Theta_C - \Theta_M\right) \\
&\frac{d\Theta_M}{d\tau} = \frac{\Theta_C - \Theta_M}{C_2} - \frac{R_2}{C_2}\left(\Theta_M - \Theta_\infty\right)
\end{aligned}
\qquad (5.2)
$$

The finite difference expressions for the above equations can be formulated for any control volume *i* as,

$$\begin{aligned}
\frac{d\Theta_{F,i}}{d\tau} &= -\frac{1}{C_1}\frac{\hat{U}}{\Delta\xi}\left(\Theta_{F,i}-\Theta_{F,i-1}\right)+\frac{R_1}{C_1}\left(\Theta_{C,i}-\Theta_{F,i}\right)\\
\frac{d\Theta_{C,i}}{d\tau} &= \hat{Q}_C - R_1\left(\Theta_{C,i}-\Theta_{F,i}\right)-\left(\Theta_{C,i}-\Theta_{M,i}\right)\\
\frac{d\Theta_{M,i}}{d\tau} &= \frac{\Theta_{C,i}-\Theta_{M,i}}{C_2}-\frac{R_2}{C_2}\left(\Theta_{M,i}-\Theta_{\infty}\right), \qquad i=1,\ldots,N
\end{aligned} \tag{5.3}$$

The first one among the above set of equations is nonlinear as the velocity term is getting multiplied by the states. Hence it is to be linearized by eliminating the time derivative terms. Hence the steady-state form of this equation can be deduced as

$$-\frac{\overline{\hat{U}}}{C_1\Delta\xi}\left(\overline{\Theta}_{F,i}-\overline{\Theta}_{F,i-1}\right)+\frac{R_1}{C_1}\left(\overline{\Theta}_{C,i}-\overline{\Theta}_{F,i}\right)=0$$

Let $a_1 = -\frac{1}{C_1}\left[\frac{\overline{\hat{U}}}{\Delta\xi}+R_1\right]$, $a_2 = -\frac{1}{C_1}\frac{\overline{\hat{U}}}{\Delta\xi}$ and $b_1 = \frac{R_1}{C_1}$

Then, $a_1\overline{\Theta}_{F,i}+a_2\overline{\Theta}_{F,i-1}+b_1\overline{\Theta}_{C,i}=0$

The steady state matrix (A_S) and steady input matrix (B_S) are as follows

$A_s = \begin{pmatrix} A_1 & A_2 \end{pmatrix}_{N\times 2N}$ and $B_s = \begin{pmatrix} a_2\overline{\Theta}_{F,0} & 0 & \cdots & 0 \end{pmatrix}^T$

where $A_1 = \begin{pmatrix} a_1 & & & \\ a_2 & a_1 & & \\ & \ddots & \ddots & \\ & & a_2 & a_1 \end{pmatrix}$, $A_2 = \begin{pmatrix} b_1 & & & \\ & b_1 & & \\ & & \ddots & \\ & & & b_1 \end{pmatrix}$

Dimensionlesstemperature at microchannel and chip nodes of the network is

$$\overline{\Theta}_s = \begin{pmatrix} \overline{\Theta}_{F,1} & \overline{\Theta}_{F,2} & \cdots & \overline{\Theta}_{F,N} & \overline{\Theta}_{C,1} & \overline{\Theta}_{C,2} & \cdots & \overline{\Theta}_{C,N} \end{pmatrix}^T$$

The above set of equations is in the form $A_S X_S = B_S$, where X_S is the temperature in steady state and can be solved as $X_S = A_S^{-1} B_S$. In order to linearize the firstone among the above set of equations (5.3), replacing the variables by the sum of steady state value and deviation about the steady state.

$\hat{U} = \overline{\hat{U}} + \delta\hat{U}$, $\Theta_{F,i} = \overline{\Theta}_{F,i} + \delta\Theta_{F,i}$ and $\Theta_{C,i} = \overline{\Theta}_{C,i} + \delta\Theta_{C,i}$

On substitution and by neglecting the higher order terms

$$\frac{d\left(\delta\Theta_{F,i}\right)}{d\tau} = -\frac{\overline{\hat{U}}}{C_1 \Delta\xi}\left(\delta\Theta_{F,i} - \delta\Theta_{F,i-1}\right) + \frac{R_1}{C_1}\left(\delta\Theta_{C,i} - \delta\Theta_{F,i}\right) - \frac{\overline{\Theta}_{F,i} - \overline{\Theta}_{F,i-1}}{C_1 \Delta\xi}\delta\hat{U}$$

Renaming $\delta\Theta_{F,i} = \Theta_{F,i}$, $\delta\Theta_{F,i-1} = \Theta_{F,i-1}$ and $\delta\Theta_{C,i} = \Theta_{C,i}$

$$\frac{d\Theta_{F,i}}{d\tau} = -\frac{\overline{\hat{U}}}{C_1 \Delta\xi}\left(\Theta_{F,i} - \Theta_{F,i-1}\right) + \frac{R_1}{C_1}\left(\Theta_{C,i} - \Theta_{F,i}\right) - \frac{\overline{\Theta}_{F,i} - \overline{\Theta}_{F,i-1}}{C_1 \Delta\xi}\hat{U}$$

Now the resulting linear finite difference equationscan be written as

$$\begin{aligned}
\frac{d\Theta_{F,i}}{d\tau} &= -\frac{\overline{\hat{U}}}{C_1 \Delta\xi}\left(\Theta_{F,i} - \Theta_{F,i-1}\right) + \frac{R_1}{C_1}\left(\Theta_{C,i} - \Theta_{F,i}\right) - \frac{\overline{\Theta}_{F,i} - \overline{\Theta}_{F,i-1}}{C_1 \Delta\xi}\hat{U} \\
\frac{d\Theta_{C,i}}{d\tau} &= \hat{Q}_C - R_1\left(\Theta_{C,i} - \Theta_{F,i}\right) - \left(\Theta_{C,i} - \Theta_{M,i}\right) \qquad (5.4) \\
\frac{d\Theta_{M,i}}{d\tau} &= \frac{1}{C_2}\left(\Theta_{C,i} - \Theta_{M,i}\right) - \frac{R_2}{C_2}\left(\Theta_{M,i} - \Theta_{\infty}\right) \qquad i=1\ldots N
\end{aligned}$$

Rearranging the above equations in the form of state space equation as,

$$\begin{aligned}
\dot{\Theta}_{F,i} &= a_1\Theta_{F,i} + b_1\Theta_{C,i} + a_2\Theta_{F,i-1} + e\hat{U} \\
\dot{\Theta}_{C,i} &= a_3\Theta_{F,i} + b_2\Theta_{C,i} + c_1\Theta_{M,i} + d_1\hat{Q}_C \qquad (5.5) \\
\dot{\Theta}_{M,i} &= b_3\Theta_{C,i} + c_2\Theta_{M,i} + d_2\Theta_{\infty}
\end{aligned}$$

where $a_1 = -\frac{1}{C_1}\left[\frac{\overline{\hat{U}}}{\Delta\xi} + R_1\right]$, $a_2 = -\frac{1}{C_1}\frac{\overline{\hat{U}}}{\Delta\xi}$, $a_3 = R_1$, $b_1 = \frac{R_1}{C_1}$,

$$b_2 = -[R_1 + 1], \quad b_3 = \frac{1}{C_2}, \quad c_2 = -\frac{1}{C_2}[1 + R_2], \quad d_2 = \frac{R_2}{C_2}, \quad c_1 = d_1 = 1,$$

$$e = -\frac{1}{C_1}\frac{\overline{\Theta}_{F,i} - \overline{\Theta}_{F,i-1}}{\Delta\xi}$$

The state space model of the system is given by

$$\dot{\Theta}(\tau) = \mathbf{A}(\tau)\Theta(\tau) + \mathbf{B}(\tau)\mathbf{i}(\tau) \tag{5.6}$$

where the states are given by

$$\Theta = \begin{pmatrix}\Theta_{F,1} & \Theta_{F,2} & .. & \Theta_{F,N} & \Theta_{C,1} & \Theta_{C,2} & .. & \Theta_{C,N} & \Theta_{M,1} & \Theta_{M,2} & .. & \Theta_{M,N}\end{pmatrix}^T$$

The state matrix A is given by,

$$\mathbf{A} = \begin{pmatrix} A_{11} & A_{12} & A_{13} \\ A_{21} & A_{22} & A_{23} \\ A_{31} & A_{32} & A_{33} \end{pmatrix}_{3N \times 3N}$$

The input matrix for each inputsare given by:

$$\mathrm{B}_{\hat{U}} = \begin{pmatrix} e_{1\times N} & 0_{1\times 2N} \end{pmatrix}^T \qquad \mathrm{B}_{\Theta_{\mathrm{F},0}} = \begin{pmatrix} a_2 & 0_{1\times(3N-1)} \end{pmatrix}^T$$

$$\mathrm{B}_{\hat{\mathrm{Q}}_{\mathrm{C}}} = \begin{pmatrix} 0_{1\times N} & d_{1_{1\times N}} & 0_{1\times N} \end{pmatrix}^T \qquad \mathrm{B}_{\Theta_\infty} = \begin{pmatrix} 0_{1\times 2N} & d_{2_{1\times N}} \end{pmatrix}^T$$

The state equation can be rewritten as,

$$\frac{d\Theta}{d\tau} = \mathrm{A}\Theta + \mathrm{B}_{\Theta_{\mathrm{F},0}}\Theta_{F,0} + \mathrm{B}_{\hat{U}}\hat{U} + \mathrm{B}_{\hat{\mathrm{Q}}_{\mathrm{C}}}\hat{Q}_C + \mathrm{B}_{\Theta_\infty}\Theta_\infty \tag{5.7}$$

The relevant outputs, that characterise the behaviour of the system, among the solution of system variables are, the outlet temperature of the channel ($\Theta_{F,N}$), the average, chip temperature (Θ_C) and the metal temperature of the fin base (Θ_M), along the length of the cooling module.

$$\Theta_{F,N} = \mathrm{C}_{\Theta_{\mathrm{F,N}}}\Theta, \; \Theta_C = \mathrm{C}_{\Theta_{\mathrm{C}}}\Theta, \; \Theta_M = \mathrm{C}_{\Theta_{\mathrm{M}}}\Theta \tag{5.8}$$

where, $\mathrm{C}_{\Theta_{\mathrm{F,N}}} = \begin{pmatrix} 0_{1\times(3N-1)} & 1 \end{pmatrix}$, $\mathrm{C}_{\Theta_{\mathrm{C}}} = \begin{pmatrix} 0_{1\times N} & \left(1/N\right)_{1\times N} & 0_{1\times N} \end{pmatrix}$,

$$\mathrm{C}_{\Theta_\mathrm{C}} = \begin{pmatrix} 0_{1\times 2N} & \left(1/N\right)_{1\times N} \end{pmatrix}$$

The input-output relationship can be obtained from their transfer functions given below

$$G_{\Theta_{F,0},\Theta_{F,N}} = \frac{\Theta_{F,N}(s)}{\Theta_{F,0}(s)} = \mathrm{C}_{\Theta_\mathrm{F,N}}\left(sI-\mathrm{A}\right)^{-1}\mathrm{B}_{\Theta_\mathrm{F,0}}$$

$$G_{\hat{Q}_C,\Theta_{F,N}} = \frac{\Theta_{F,N}(s)}{\hat{Q}_C(s)} = \mathrm{C}_{\Theta_\mathrm{F,N}}\left(sI-\mathrm{A}\right)^{-1}\mathrm{B}_{\hat{\mathrm{Q}}_\mathrm{C}}$$

$$G_{\Theta_\infty,\Theta_{F,N}} = \frac{\Theta_{F,N}(s)}{\Theta_\infty(s)} = \mathrm{C}_{\Theta_\mathrm{F,N}}\left(sI-\mathrm{A}\right)^{-1}\mathrm{B}_{\Theta_\infty}$$

$$G_{\hat{U},\Theta_{F,N}} = \frac{\Theta_{F,N}(s)}{\Theta_{\hat{U}}(s)} = C_{\Theta_{F,N}}\left(sI-A\right)^{-1}B_{\hat{U}}$$

$$G_{\Theta_{F,0},\Theta_C} = \frac{\Theta_C(s)}{\Theta_{F,0}(s)} = C_{\Theta_C}\left(sI-A\right)^{-1}B_{\Theta_{F,0}}$$

$$G_{\hat{Q}_C,\Theta_C} = \frac{\Theta_C(s)}{\hat{Q}_C(s)} = C_{\hat{Q}_C}\left(sI-A\right)^{-1}B_{\Theta_{F,0}}$$

$$G_{\Theta_\infty,\Theta_C} = \frac{\Theta_C(s)}{\Theta_\infty(s)} = C_{\Theta_C}\left(sI-A\right)^{-1}B_{\Theta_\infty}$$

$$G_{\hat{U},\Theta_C} = \frac{\Theta_C(s)}{\Theta_{\hat{U}}(s)} = C_{\Theta_C}\left(sI-A\right)^{-1}B_{\hat{U}}$$

$$G_{\Theta_{F,0},\Theta_M} = \frac{\Theta_M(s)}{\Theta_{F,0}(s)} = C_{\Theta_M}\left(sI-A\right)^{-1}B_{\Theta_{F,0}}$$

$$G_{\hat{Q}_C,\Theta_M} = \frac{\Theta_M(s)}{\hat{Q}_C(s)} = C_{\Theta_M}\left(sI-A\right)^{-1}B_{\hat{Q}_C}$$

$$G_{\Theta_\infty,\Theta_M} = \frac{\Theta_M(s)}{\Theta_\infty(s)} = C_{\Theta_M}\left(sI-A\right)^{-1}B_{\Theta_\infty}$$

$$G_{\hat{U},\Theta_M} = \frac{\Theta_M(s)}{\Theta_{\hat{U}}(s)} = \mathrm{C}_{\Theta_\mathrm{M}}\left(sI-\mathrm{A}\right)^{-1}\mathrm{B}_{\hat{U}}$$

The transfer function matrix of the system model is

$$\begin{bmatrix}\Theta_{F,N}\\ \Theta_{C}\\ \Theta_{M}\end{bmatrix}=\begin{bmatrix} G_{\hat{U},\Theta_{F,N}} & G_{\Theta_{F,0},\Theta_{F,N}} & G_{\hat{Q}_C,\Theta_{F,N}} & G_{\Theta_M,\Theta_{F,N}}\\ G_{\hat{U},\Theta_{C}} & G_{\Theta_{F,0},\Theta_{C}} & G_{\hat{Q}_C,\Theta_{C}} & G_{\Theta_M,\Theta_{C}}\\ G_{\hat{U},\Theta_{M}} & G_{\Theta_{F,0},\Theta_{M}} & G_{\hat{Q}_C,\Theta_{M}} & G_{\Theta_M,\Theta_{M}}\end{bmatrix}\begin{bmatrix}\hat{U}\\ \Theta_{F,0}\\ \hat{Q}_C\\ \Theta_M\end{bmatrix} \tag{5.9}$$

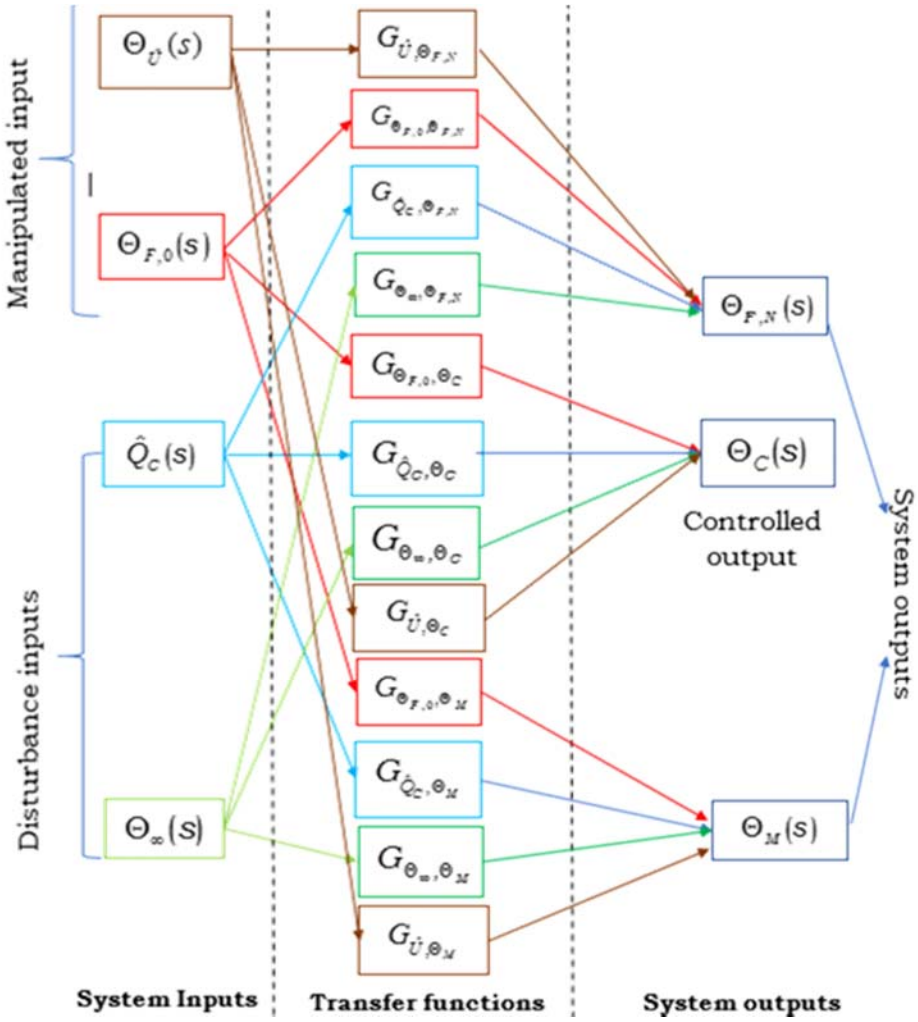

Fig. 5.3. Control system architecture

The overall architecture of the cooling module plant containing the entire possible input and output is shown in Fig. 5.3. Two types of inputs considered for studying the control dynamics of the present system are the manipulated input and the disturbance input. Coolant inlet temperature ($\Theta_{F,0}$) and coolant velocity ($\Theta_{\hat{U}}$)are the manipulated input identified for the present study.Coolant flowrate has not provided any significant effect in heat transfer control for the single-phase internal forced convection. Transient heat generation in chip ($\hat{Q}_C$) as well as the ambient temperature (Θ_∞) are chosen as the possible disturbance input of the present system. The block diagram representation of the entire input-output model of the whole cooling module excluding the effect of coolant velocity for the single-phase internal forced convectionis shown in Fig. 5.4.

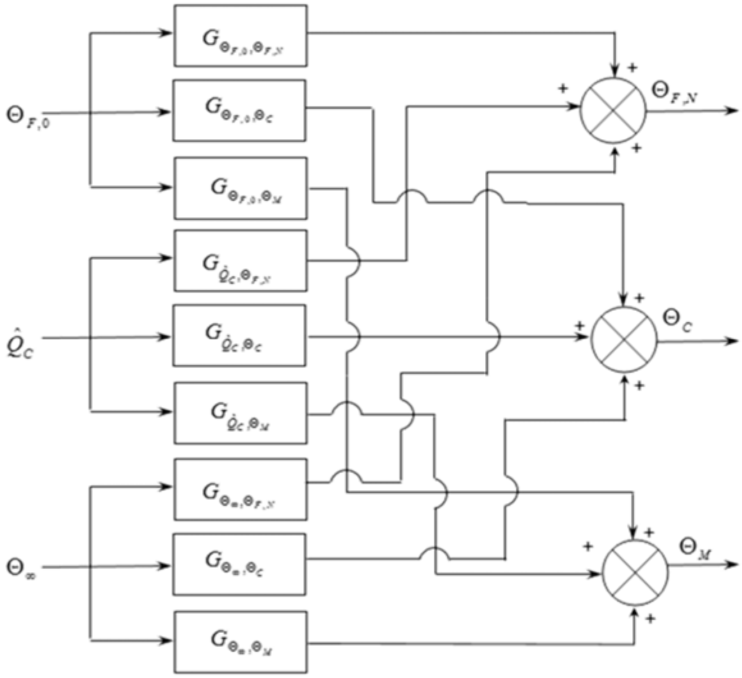

Fig. 5.4 Block diagram for the entire input-output model of the cooling module

Though there are several input and output available for the given dynamic system, the specific objective of the present control design is to maintain the chip temperature at a specified safe level. Therefore, a simplified system representing the single desired output and input that are necessarily affecting the same. A simplified block diagram showing the single output and required input is shown in Fig. 5.5.

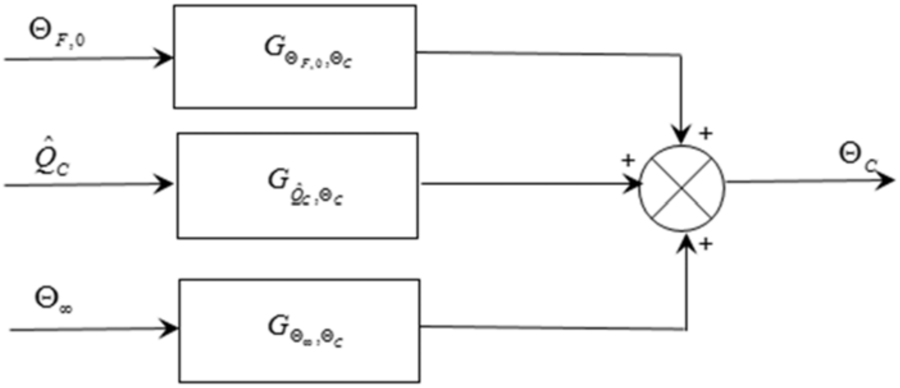

Fig. 5.5 Simplified block diagramshowing the single output and required input

Salient dimensions of elements of the electronics cooling module (Fig. 5.1) and thermal conditions are identical to that described in section 4.6.This configuration does not contain PCM storages and its operation is supported by the respective type of active control system.

Open loop response for the heat transfer characteristics for the cooling module are assessed for two types of transient heat generation in the chip ($\hat{Q}_C$). Open loop response of heat transfer characteristic for the heat generation pattern described by $Q = 20\left(1+\tau^{0.15}\right)$ is shown in Fig. 5.6. Chip temperature rises steadily because of the insufficient heat dissipation in two branches of the cooling circuit.

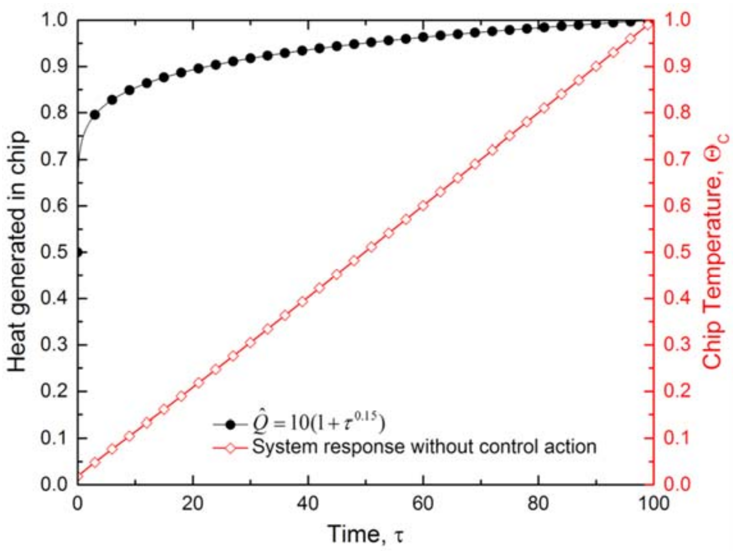

Fig. 5.6 Open loop response of heat transfer for a steady rise heat generation

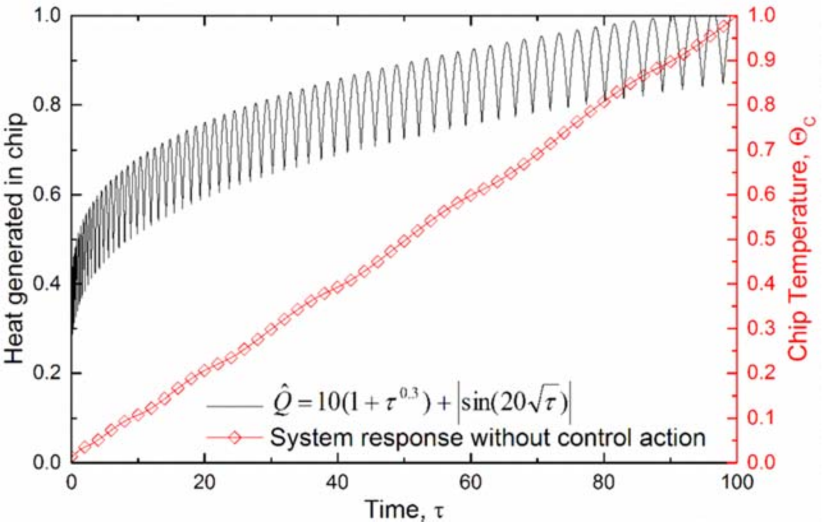

Fig. 5.7 Open loop response of heat transfer for a sinusoidal heat generation

Fig. 5.7 shows the temperature build-up in the chip for an oscillating heat generation pattern superimposed over another increasing heat generation pattern described by $Q=10\left(1+\tau^{0.3}\right)+\left|\sin\left(500\sqrt{\tau}\right)\right|$. Here also the temperature builds up quickly in the chip due to very low dissipation through both modes of cooling. These open loop responses for the heat transfer characteristics for the cooling module obviously indicate the need of active control of the heat transfer process for maintaining safe working temperature of the electronic chip.

5.3 CONTROL DESIGN AND SIMULATIONS OF COOLING SYSTEMS WITH INTERNAL FORCED CONVECTION

Active control system design and simulation based on H_∞ and PID strategies for a microchannel based electronics cooling system involving only internal forced convection are presented. The controlled variable is the chip temperature and is to be regulated by modifying the inlet fluid temperature. Feedback controllers are designed by properly selecting the weighing function which improves dissipation of heat to a coolant in the microchannel. The dynamics of the heat exchanging process in the cooling module by incorporating these feedback control systems are assessed by monitoring the chip temperature for different transient heat generation imposed on chip. A comparison of H_∞ and PID control strategies are evaluated by analyzing overshoots and settling time while achieving the desired set value of chip temperature.

5.3.1 H_∞ control

The state space representation of the generalized cooling module model (Fig. 5.8) with feedback for the application of H_∞ control is

$$\dot{\Theta}(\tau) = \mathrm{A}\Theta(\tau) + \begin{bmatrix} \mathrm{B}_{\hat{\mathrm{Q}}_\mathrm{C}} \\ \mathrm{B}_{\Theta_\infty} \end{bmatrix} w(\tau) + \mathrm{B}_{\Theta_{\mathrm{T}_{\mathrm{F},0}}}(\xi)\Theta_{F,0}(\tau) \tag{5.10}$$

$$\begin{bmatrix} \mathrm{z}_1 \\ \mathrm{z}_2 \\ \mathrm{z}_3 \end{bmatrix} = \begin{bmatrix} 0 \\ W_1 \\ 0 \end{bmatrix} e(\tau) + \begin{bmatrix} 0 \\ 0 \\ W_2 \end{bmatrix} \Theta_{F,0}(\tau) + \begin{bmatrix} W_3 \\ 0 \\ 0 \end{bmatrix} \Theta_C(\tau) \tag{5.11}$$

$$y(\tau) = C_{\Theta_C}\Theta(\tau) \tag{5.12}$$

where,z is the performance output to evaluate the performance of the system. W_1, W_2, and W_3 are the dependent weights used to obtain the controller function.

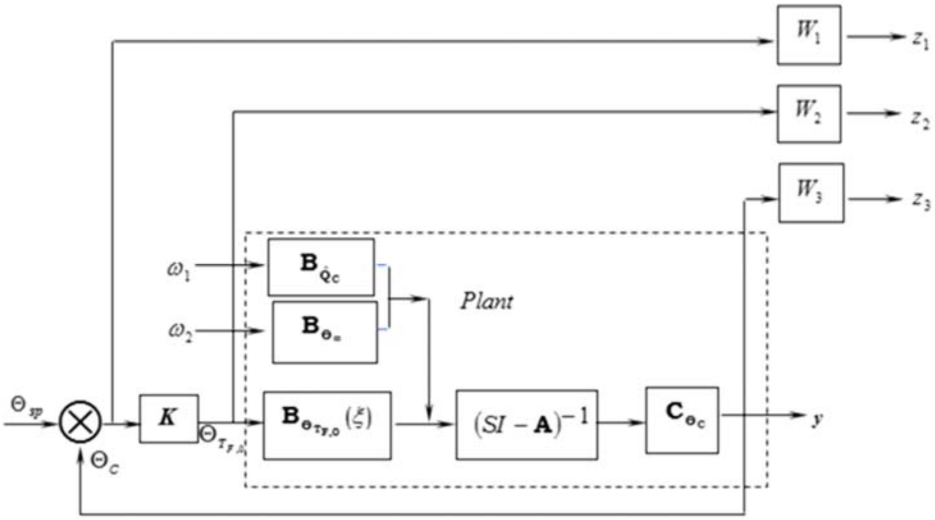

Fig. 5.8 Generalised cooling module model with feedback

The input uncertainty weight Wu is selected by satisfying the stability condition,

$$\left|W_2(j\omega)\right| \geq e(j\omega), \forall\omega \tag{5.13}$$

where, $e(j\omega)$ is the relative error of the transfer function.

The error due to time delay and gain uncertainty is estimated. The first order pade approximation of time delay is given by,

$$t_d = \frac{2\frac{\theta}{2}s}{\left(1+\frac{\theta}{2}s\right)} \tag{5.14}$$

where θ is the delayed time.

The overall multiplicative uncertainty weight W_2 is obtained by adding the gain error (ε) to the approximated time delay. Thus, the weight transfer function W_2, for $\theta = 0.5s$ and $\varepsilon = 0.2$ is given by,

$$W_2 = \frac{0.5s + 0.2}{0.25s + 1}$$

The bode plot of relative error of plant transfer function and weight W_2 is shown in Fig.5.9. W_2 is selected such that weight transfer function lies above the relative error of the plant. The weights W_1 and W_3 are appropriately estimated to reject the noise and disturbances respectively. As noise is a high-frequency signal, the W_1 should be small in higher frequency band. Whereas, the disturbance signal has lower frequency components, the weight W_3 should be small in low-frequency band. Thus the weights are estimated as,

$$W_1 = \frac{s+10}{100s+1} \text{ and } W_3 = \frac{0.1s + 0.01}{0.01s+1}$$

The Bode plot representing the weights W_1 and W_3 is shown in Fig. 5.10. Using the weights W_1, W_2 and W_3 the controller function K is calculated such that it satisfies the sensitivity, control effort and complementary sensitivity inequalities, as given below,

$$\left.\begin{aligned} \bar{\sigma}S(j\omega) &< \gamma\, \underline{\sigma}W_1^{-1}(j\omega) \\ \bar{\sigma}R(j\omega) &< \gamma\, \underline{\sigma}W_2^{-1}(j\omega) \\ \bar{\sigma}T(j\omega) &< \gamma\, \underline{\sigma}W_3^{-1}(j\omega) \end{aligned}\right\}, \forall\, \omega$$

The Singular Value (SV) plot indicating the aforementioned inequality is shown in Fig. 5.11. It can be observed that the sensitivity (S), control effort (R), and complementary sensitivity (T) of the closed-loop transfer function are less than γW_1^{-1}, γW_2^{-1}, and γW_3^{-1} respectively.

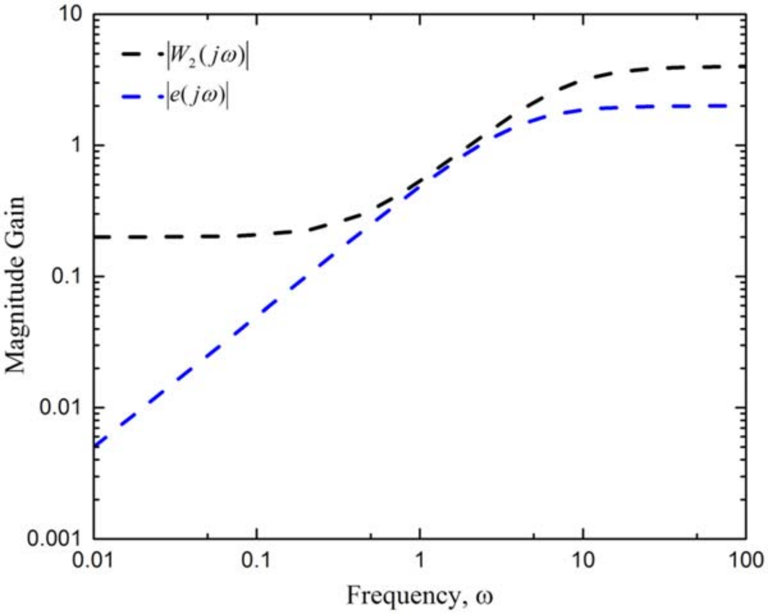

Fig. 5. 9 Criteria for estimating weight W_2

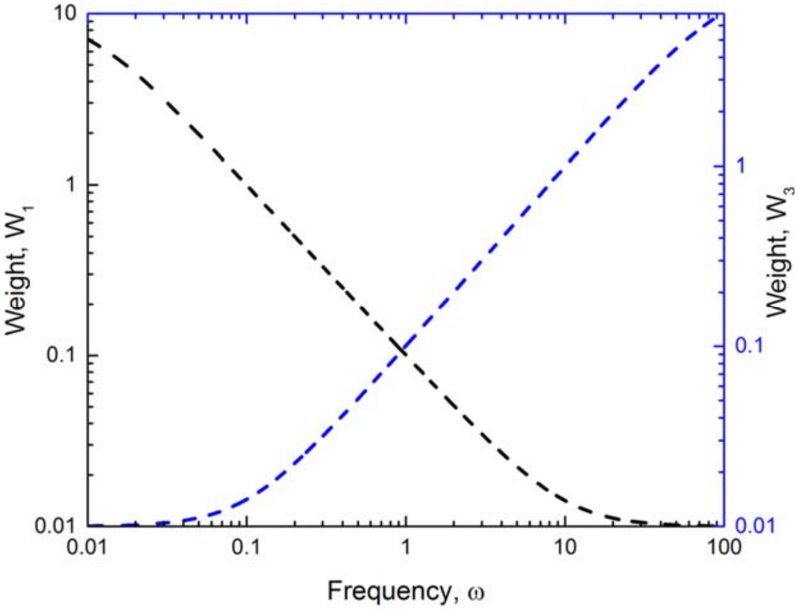

Fig. 5.10 Strategy for frequency dependent weight selection

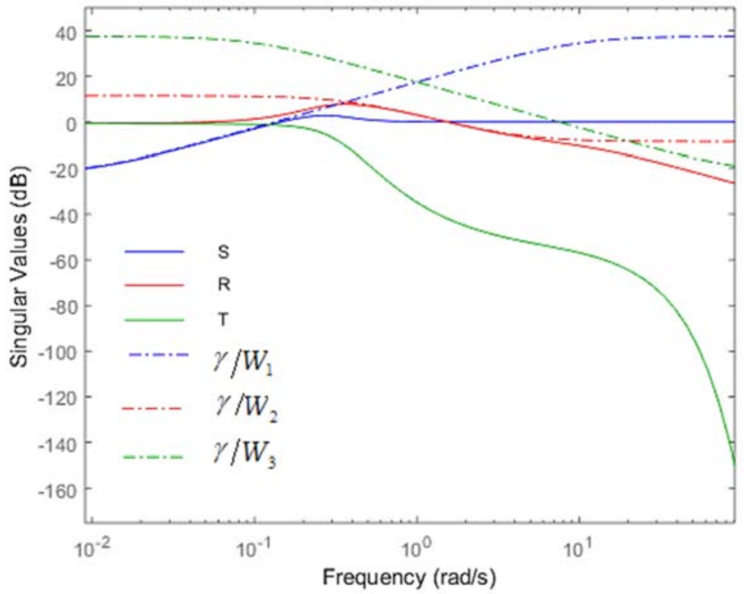

Fig. 5. 11The SV plot for the frequency response of inequalities

Heat transfer response after the implementation of H_∞ control for the single phase microchannel cooling process for the various transient heat generations is shown in Fig. 5.12 and 5.13.Here the dimensionless temperature (Θ_C), which is expressed in terms of the reference temperature, is evaluated based on the maximum temperature (473K) obtained from their respective open-loop response. These results show that the developed H_∞ control strategy is effective in achieving as well as maintaining the desired target of set temperature value (353K) of the chip. It can be observed from the Fig. 5.12 that the controller could bring the chip temperature value without oscillations for a steadily rising heat generation described by $\hat{Q} = 20\left(1+\tau^{0.15}\right)$. Whereas, the response of H_∞ control system for sinusoidal heat generation superimposed over increasing heat generation patterndescribed by $\hat{Q} = 10\left(1+\tau^{0.3}\right)+\left|\sin\left(20\sqrt{\tau}\right)\right|$ shows that (Fig. 5.13)more time is elapsed in achieving the desired target of set temperature value. Note that Θ_C is evaluated for this case is based on the maximum temperature (520K) obtained from its respective open-loop response.

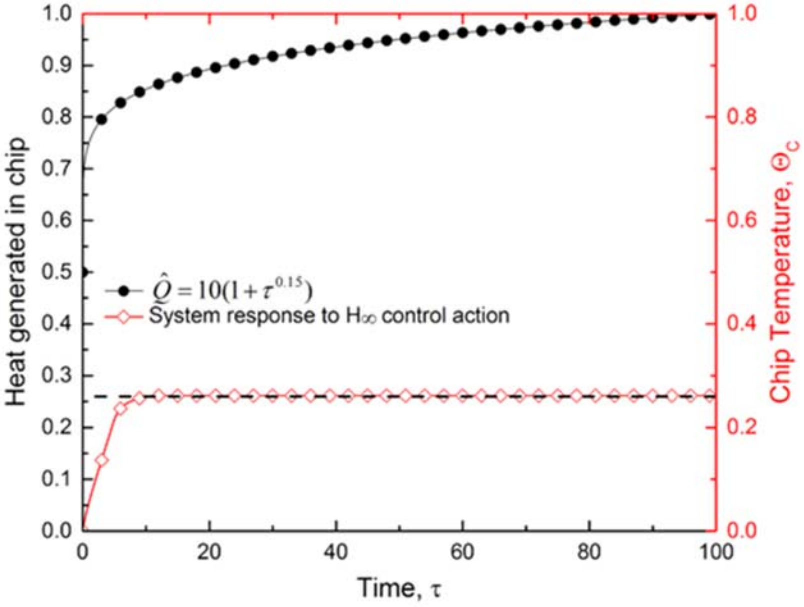

Fig. 5. 12 Heat transfer response with H∞ control for a steady rise heat generation

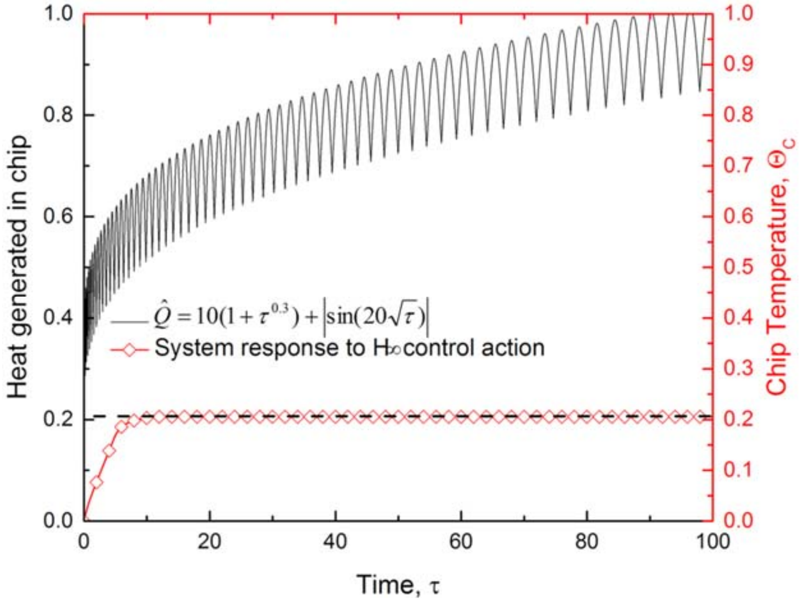

Fig. 5. 13 Heat transfer response with H∞ control for a sinusoidal heat generation

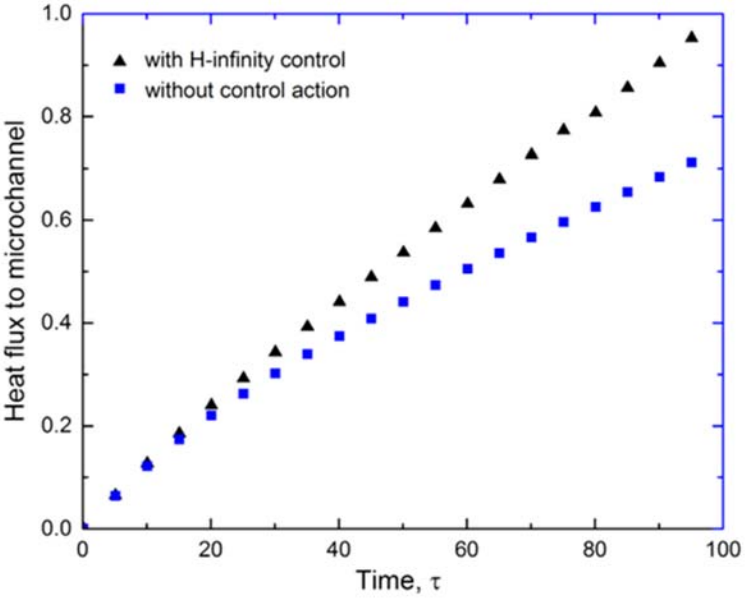

Fig. 5.14 Effect of H_∞ control on heat transfer to fluid in the microchannel

Now the effect of H_∞ control is assessed in detail to explore other consequences of control action than maintenance of required level of chip temperature. Fig. 5.14 shows the extent of heat transfer to the fluid in microchannel after the implementation of H_∞ control for the steady increase in heat generation in chip described by $\hat{Q} = 20\left(1 + \tau^{0.15}\right)$. Heat transfer towards the fluid in microchannel is found to increase as more heat is generated in the chip when control action is in force, in comparison with another situation when no control action is applied. This is due to the increase in available temperature potential to transfer the heat towards the coolant in microchannel as the H_∞ controller attempts to provide cooler fluid at the inlet of the heat exchanger.

5.3.2 PID control

The generalized transfer function of PID controller is

$$C(s) = Kc\left(1 + \frac{1}{\tau_I s} + \tau_D s\right) \tag{5.15}$$

where Kc is the proportional gain, τ_I and τ_D are integral and derivative time constants respectively. The controller parameters are evaluated using the Ziegler-Nichols method and the procedure of evaluation have already deliberated in Chapter 3. The sustained oscillation response of the system to a proportional controller with a proportional gain of $K_u = 1$ is shown in Fig. 5.15, where the frequency of oscillation $P_u = 40s / cycle$. The gain values for the PID controller estimated based on these K_u and P_u are K_C = 0.588, τ_I = 20.04s, τ_D = 5.004s. The resulting transfer function of PID controller output is

$$C(s) = \frac{(0.05s + 0.3)^2}{s}$$

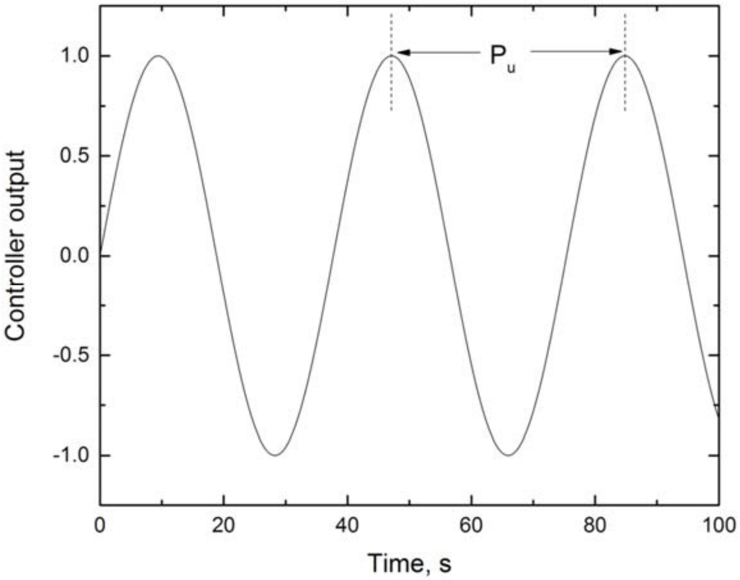

Fig. 5.15 Evaluation of period of oscillation for the tuning of PID controller

PID control logic is implemented to maintain the chip temperature within a desired value by regulating inlet coolant temperature. This regulation is effective till the error becomes a minimum value or the chip temperature attains the set value of 353K. Heat transfer response after the implementation of PID control for the single phase microchannel cooling process for the various transient heat generations is shown in Fig. 5.16 and 5.17.The dimensionless temperature values are evaluated based on the maximum temperature obtained in the respective open-loop performance. It is evident from these results that PID control with present design values is effective in achieving as well as maintaining the desired target of set temperature value (353K) of the chip.PID control exhibit underdamped response for both types of heat generation pattern. Though the steady increase in heat generation leads to a slightly higher amount of overshoot quickly, it leads to settling early to the desired set point.

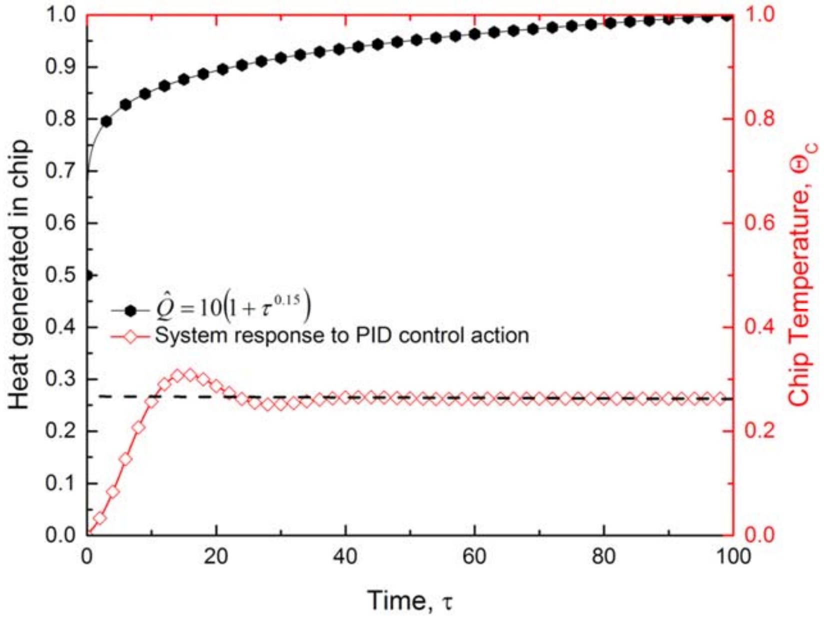

Fig. 5.16 Heat transfer response with PID control for a steady rise heat generation

A comparison of performance aspects of the PID control action for the heat generation patterns imposed for the microchannel-based cooling module is summarized and given in Table 5.1.

Table 5.1. Performance aspects of the PID control

Heat generation pattern	Peak time (s)	Rise time (s)	Settling time (s)	Delay time (s)	% overshoot
$\hat{Q} = 20\left(1 + \tau^{0.15}\right)$	15.51	10.41	37.26	5.6	17.86
$\hat{Q} = 10\left(1 + \tau^{0.3}\right) + \left\|\sin\left(20\sqrt{\tau}\right)\right\|$	16.56	12.79	41.06	6.74	11.95

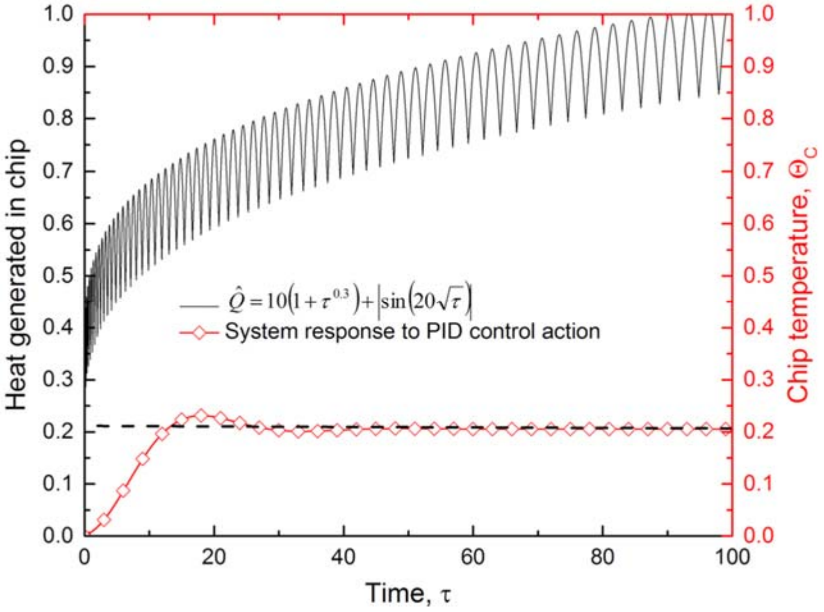

Fig. 5. 17 Heat transfer response with PID control for a sinusoidal heat generation

5.3.3 Comparison of controllers

Heat exchange system has been independently controlled using PID and H_∞ control systems and their performance aspects are compared. Responses of the control actions imposed on microchannel based cooling module for the two types of heat generation pattern are compared in Fig. 5.18 and Fig. 5.19. H_∞ control exhibit critical damping to the system for both type of heat generation input.The response shows that it approaches the set value of chip temperature faster than PID control.

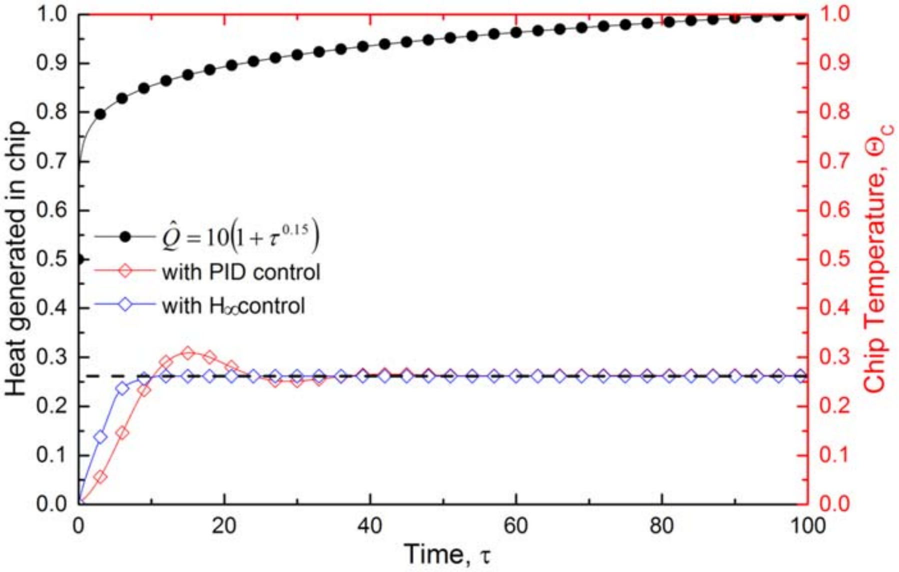

Fig. 5.18 Comparison of temperature control offered for a steady rise heat generation

The performance of the controllers is evaluated based on time integral performance criteria viz., Integral of the Square Error (ISE), Integral of the Absolute value of the Error (IAE) and Integral of the Time-weighted Absolute Error (ITAE). A comparison of time integral performance criteria are given in Table 5.2.

ISE and IAE values obtained for H_∞ control scheme is lower than PID. Hence H_∞ control is ideal for the disturbances leading to a larger error at the set point for the present system. Whereas, ITAE value is found smaller for PID control scheme. This indicates that the PID controller maintains lower error values for a persisting disturbance in the system.

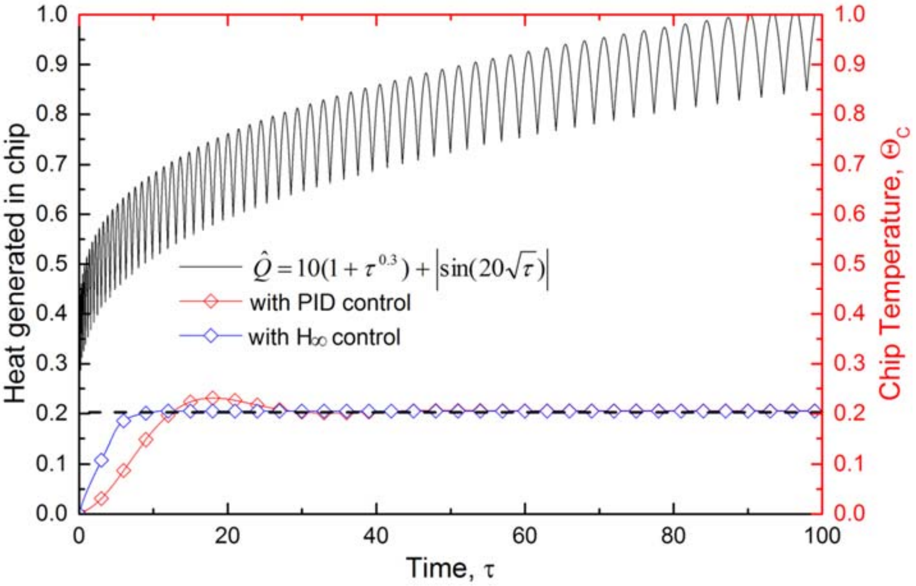

Fig. 5.19 Comparison of temperature control offered for a sinusoidal heat generation

Table 5.2. Comparison based on the time integral performance criteria

Controller	**Heat generation pattern**	**ISE**	**IAE**	**ITAE**
H_∞	$\hat{Q} = 20\left(1+\tau^{0.15}\right)$	12.6	80.9	191
	$\hat{Q} = 10\left(1+\tau^{0..3}\right) + \left\|\sin\left(20\sqrt{\tau}\right)\right\|$	7.78	63.4	150
PID	$\hat{Q} = 20\left(1+\tau^{0.15}\right)$	28.4	194	153
	$\hat{Q} = 10\left(1+\tau^{0..3}\right) + \left\|\sin\left(20\sqrt{\tau}\right)\right\|$	21	167	122

5.4 CONTROL DESIGN AND SIMULATIONS OF COOLING SYSTEMS WITH FLOW BOILING

A cascade controller design and simulation, with a PID controller as a secondary controller and H_∞ controller as the primary controller, for a microchannel based cooling system with flow boiling option, is presented.

Two-phase flow boiling process in microchannels has the disadvantage of flow instabilities leading to excessive pressure drop and early CHF occurrence. This adversely affects the thermal condition of the chip resulting to burnt out due to a shortage of coolant flow. Hence it is important to control the pressure drop along with the chip temperature for its efficient operation. A cascade controller is introduced to overcome the operational difficulty by controlling the pressure drop in the microchannel along with the feedback of the chiptemperature. An inner PID controller regulates the pressure drop by manipulating the valve, which regulates the flow rate of the coolant. This change in flow rate keeps the pressure drop inside the microchannel within a desired range, leading to an optimal control of flow boiling process.

5.4.1 Cascade control design

The simple open loop block diagram considered for the cascade control option is shown in Fig 5.20. The transfer function $G_{\hat{U},\Theta_C}$ relates chip temperature to flow rate of the coolant in the microchannel, which is the manipulating variable of the system. The transfer function $G_{\hat{Q}_C,\Theta_C}$ relates the chip temperature to heat generated in the chip, which is the disturbance of the system. Open loop operation of microchannel heat exchanger in the electronics cooling system lead to undesirable operating conditions when it is given with a steady heat generation. The sudden transition from nucleate boiling leads to excessive pressure drop as shown in Fig. 5.21 and 5.22. Sudden formation of vapor slugs offer resistance to flow and can lead to local dry-out. Admission of more coolant can circumvent this rapid shift in the boiling pattern. Therefore, a cascade controller based on the pressure drop feedback is an ideal option for maintaining the operational efficiency of heat exchanging system.

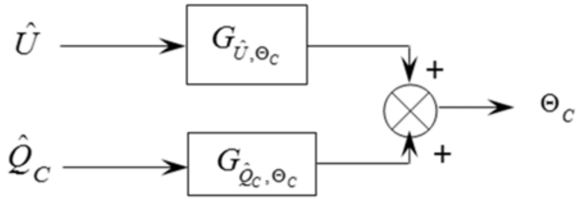

Fig. 5. 20 Simple open loop block diagram of a cooling module with single output and required inputs

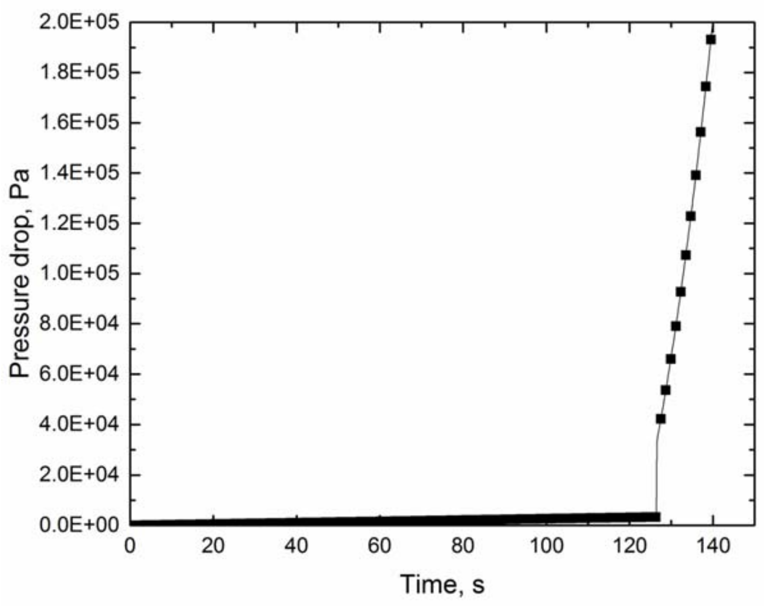

Fig. 5. 21 Pressure drop characteristic during flow boiling

The block diagram of cascade feedback control system is shown in Fig. 5.23. Here the inner controller G_{PID} and a valve transfer function G_V with feedback signal of pressure drop forms the inner or secondary loop. While the transfer functions representing the cooling module such as $G_{\hat{U},\Theta_C}$ and $G_{\hat{Q}_C,\Theta_C}$, and the outer controller G_{H_∞} with feedback signal of chip temperature forms the outer or primary loop. The master loop or the primary loop measures the temperature of the chip and uses an external set point for the control purpose, whereas the slave or secondary loop uses the output of the primary controller as its set point.

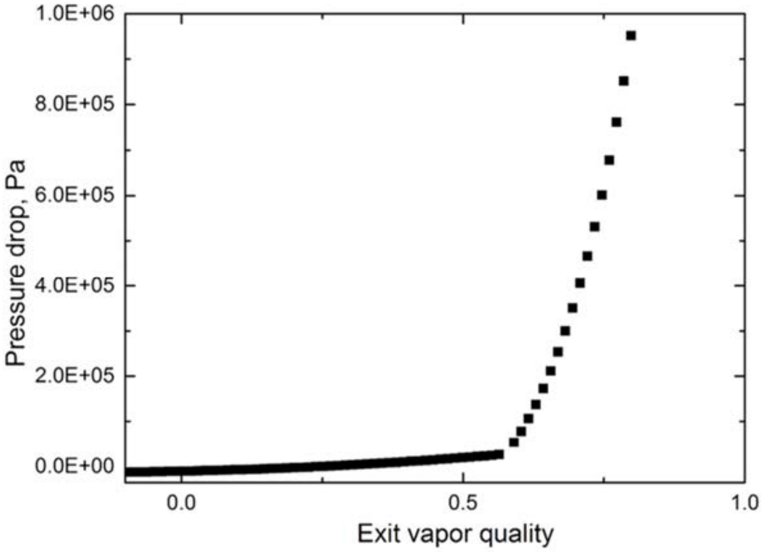

Fig. 5.22 Pressure drop corresponding to various regimes of flow boiling in a microchannel

The individual H∞ and PID control design used in cascade control follow the same procedure used in sections 5.3.1 and 5.3.2 respectively. The weights W_1, W_2, and $W_3$are designed satisfying the design criteria are also the same as discussed in section5.3 . The designed weights are:

$$W_1 = \frac{4s+10}{50s+1},\ W_2 = \frac{0.2s+0.1}{0.5s+1},\ \text{and}\ W_3 = \frac{0.7s+1}{0.01s+1}$$

For the PID controller, the controller parameters are tuned using the Ziegler-Nichols method with a proportional gain of $K_u = 1.5$. A sustained oscillation response of the system is obtained with a frequency of oscillation of $P_u = 20s/cycle$. The gain values estimated are K_C= 0.882, τ_I= 20s, τ_D=

2.5*s*. The resulting PID controller transfer function is $C(s)=\dfrac{(0.0375s+0.113)^2}{s}$.

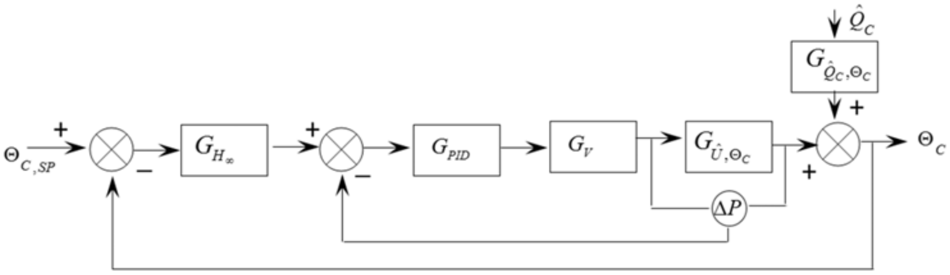

Fig. 5. 23 Block diagram representation of cascade control of microchannel heat exchanger

5.4.2 Simulation results

A cascade control system designed as per the criteria discussed in the previous section is now simulated for a steady rising heat input generated in the chip. Excessive pressure drop initiated during nucleate boiling regime triggers the linear valve which admits additional coolant. Single phase forced convection has not shown any significant control of heat transfer by the increase in coolant flow rate. But the introduction of liquid coolant prolongs the phase transition in the nucleate boiling regime. Fig. 5.24 shows the variation of two-phase pressure drop with liquid coolant admission. The pressure drop across the channel is getting reduced as more coolant is admitted. Fig. 5.25 shows the variation of quality of coolant with the fresh coolant admission. This trend has been predicted based on the present cascade control action with the flow boiling heat transfer models described in section 3.3. Extend of formation of vapor is found to get control for the given linearly increasing heat input during the time period of simulation. Comparison of heat flux towards the microchannel fluid with and without control action is shown in Fig. 5.26. The time period here is so chosen that the activity beyond nucleate boiling regime in the uncontrolled event can be compared with that of cascade control. This shows that the introduction of cascade control can prolong the occurrence of CHF in microchannel heat exchanger.

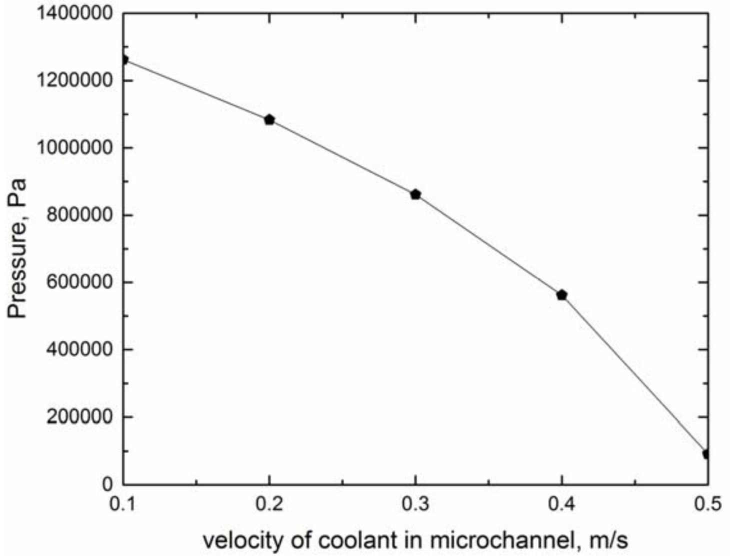

Fig. 5.24 Variation of two-phase pressure drop with liquid coolant admission

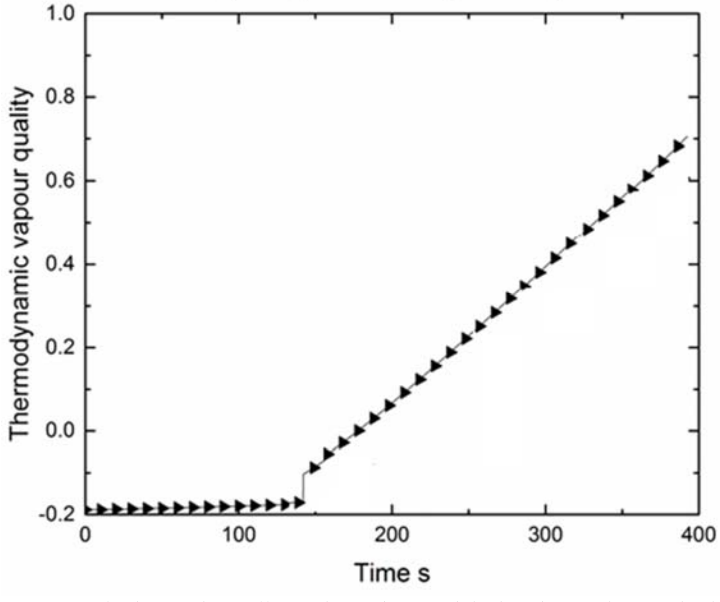

Fig. 5.25 Variation of quality of coolant with fresh coolant admission

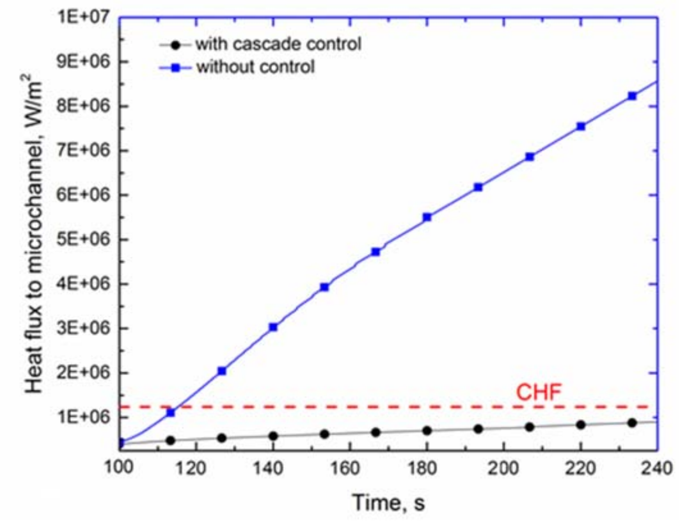

Fig. 5.26 Comparison of heat flux towards the microchannel fluid

5.5 SUMMARY

Control system design and simulation for heat transfer process in a microchannel-based electronics cooling module based on the developed dynamic thermal models are deliberated. Heat transfer involving single-phase forced convection is controlled using H_∞ as well as PID control, whereas a cascade control system is designed and simulated for the flow boiling in the microchannel. Control systems are found to be effective in maintaining the chip at the desired temperature level. Performance aspects of H_∞ and PID control schemes are compared for two different heat generation disturbance patterns. H_∞ control exhibit critical damping characteristic for both type of heat generation input and the set value of chip is attained faster than PID control. A cascade control system based on the feedback of pressure as well as chip temperature is found to be robust in alleviating the flow instabilities during flow boiling. This could maintain the chip temperature at the desired level even during high heat dissipation demand. Major findings based on the passive and active control modelling and simulations are outlined in the next chapter.

CHAPTER 6

CONCLUSIONS

6.1 INFERRING REMARKS

Requirements to dissipate a large amount of heat from limited space has become a challenge today due to the recent advents in microminiaturization and ever-growing processing capability of electronic devices. Though the microchannel-based heat exchangers have been emerged as a solution to circumvent excessive cooling requirement, negotiation of peak heat flux and fluctuating heat dissipation demand may lead to several operational difficulties and inefficiency. Boiling in microchannels can offer higher cooling rate for a given mass flow rate of the fluid. However, the various operational difficulties such as flow reversal, instability, excessive pressure drop, vapor cutback near CHF conditions, etc. impose challenges in implementing it as a reliable cooling method in standalone electronic systems. Various passive and active control methods are proposed and simulated in the present work. These methods effectively control the multi-mode heat dissipation process in microchannel based heat exchangers used in electronic cooling devices.

Dynamic thermal models that take in to account the multi-mode heat dissipation process in microchannel based heat exchangers, as well as latent heat storages facilitated by PCM for the passive control of heat transfer, have been developed. Extensive simulations based on these models could reveal the heat transfer characteristics for the various type of possible heat generation. Active control systems are also developed based on these dynamic thermal models. These are found to be effective in maintaining safe working temperature of the chip and offer stable heat transferring process.

6.2 CONCLUSIONS

Salient scientific contributions in the current study are summarized as follows

- Theory of single phase and two-phase heat transfer in the microchannel is compiled for the purpose of developing dynamic thermal models for electronic cooling modules. A comprehensive literature review focusing on the latest developments in this active research area has been presented.

- A design procedure for cooling modules with multimode heat dissipation process has been framed. The data for thermos-hydraulic performance aspects form the basic guidelines for selection of geometry and operational parameters of the heat exchanging system.

- Dynamic thermal models for electronic cooling packages involving multi-mode heat dissipation have been developed, validated with suitable experimental data, and simulated for various kind of transient heat generation patterns.

- All heat transfer models developed in this work takes care of the ambient temperature in one of the heat dissipation path. Therefore, the effectiveness of heat exchanging process in electronics cooling modules for various ambient conditions can be assessed based on these models. This is helpful in ascertaining the performance aspects of electronic packages used in mission-critical applications which are subjected to harsh thermal environments.

- Heat transfer from the chip cannot be controlled alone by increasing the coolant velocity for single-phase convection in microchannels. This study shows that there exists a limit for heat transfer towards the coolant for a given geometry of the microchannel and thermal properties of the coolant used.

- The fin array embedded with phase changing material can successfully negotiate sudden cooling demands as the optimal sharing of the heat dissipation take place among various components in the cooling circuit. This aspect has been verified for various types of time-varying heat inputs.
- PCM assisted flow boiling offers excellent control of heat transfer for wide range of time-varying heat input. Wall superheat response are analyzed for two axial locations for atypical ramping up of cooling load on the system. Analysis of the response shows that the heat absorbed in variable area PCM storage helps to damp the wall superheat within the nucleate boiling regime till the completion of its melting. This is helpful in maintaining high heat transfer coefficient for longer extent of operation.
- Dynamic thermal models for the microchannel-based electronics cooling modules have also been used to design and simulate active control systems. $H_\infty$and PID control schemes are found to be effective in single-phase forced convection in microchannel based heat exchanger. The effectiveness of these control schemes are ascertained by extensive control simulations with differing heat generation patterns and their performance aspects are compared.
- Cascade control system could take care of the inherent instability of flow boiling in microchannels by providing a secondary PID based control loop based on the feedback of pressure drop across the channel.

6.3 SCOPE FOR THE FUTURE STUDIES

Dynamic thermal models presented in this study are based on the assumptions stated in section 4.3 of this thesis. There can be minor variations in all these aspects in a real scenario. Surface feature based heat transfer enhancement methods are widely used in microchannel applications. Present models cannot take care of any passive or active heat transfer enhancement method effects. The present study does not take care of the real operating characteristics of various system components such as valves and flow regulators. The study can be extended by including the real operating characteristics of such components to mimic real conditions. Active control strategies deliberated in the present work can be initially simulated using virtual instrument engineering platforms and thereafter implemented in real systems using programmable logic controllers. In short, an experimental research is essential to complement, compare, and contrast the results presented in this thesis.

BIBLIOGRAPHY

1. **Abbasov, N.M., R. I. Zeinalov, O. M. Azizova,** and **S. N. Imranova,** (2006). Dynamic models of heat exchangers. *Chemistry and Technology of Fuels and Oils,* **42**, 25-29.
2. **Abhat, A.**, (1983) Low temperature latent heat thermal energy storage: heat storage materials. *Solar Energy,* **30**,313-332.
3. **Ahn, H.S**. and **M. H. Kim,** (2012) A review on critical heat flux enhancement with nanofluids and surface modification. *Journal of Heat Transfer,* **134**, 024001.
4. **Al-Neama, A. F., N. Kapur, J. Summers,** and **H. M. Thompson,** (2017) An experimental and numerical investigation of the use of liquid flow in serpentine microchannels for microelectronics cooling. *Applied Thermal Engineering*, **116**, 709-723.
5. **Alotaibi, S., M. Sen, B. Goodwine,** and **K. T. Yang,** (2002) Numerical simulation of the thermal control of heat exchangers. *Numerical Heat Transfer: Part A: Applications,***41**, 229-244.
6. **Azar, K.** *Thermal measurements in electronics cooling*. CRC press, 1997.
7. **Azar, K.**, (2000) Power consumption and generation in the electronics industry. A perspective. *Semiconductor Thermal Measurement and Management Symposium, 2000. Sixteenth Annual IEEE.*
8. **Baby, R.** and **C. Balaji,** (2012) Thermal management of electronics using phase change material based pin fin heat sinks.*Journal of Physics: Conference Series***395**, 012134.

9. **Bahiraei, M.** and **S. Heshmatian**, (2017) Application of a novel biological nanofluid in a liquid block heat sink for cooling of an electronic processor: Thermal performance and irreversibility considerations. *Energy Conversion and Management,***149**, 155-167.

10. **Bakošová, M.** and **J. Oravec,** (2012) Robust model predictive control of heat exchangers. *Chemical Engineering Transactions,* **29**, 1465-1470.

11. **Bang, I. C., S. H. Chang,** and **W. P. Baek,** (2005) Visualization of a principle mechanism of critical heat flux in pool boiling. *International Journal of Heat and Mass Transfer,* **48**, 5371-5385.

12. **Bar-Cohen, A.** and **W.M. Rohsenow,** (1984) Thermally optimum spacing of vertical, natural convection cooled, parallel plates. *Journal of Heat Transfer,* **106**, 116-123.

13. **Baskaya, S., M. Sivrioglu,** and **M. Ozek,** (2000) Parametric study of natural convection heat transfer from horizontal rectangular fin arrays. *International Journal of Thermal Sciences,* **39**, 797-805.

14. **Bar-Cohen, A.,** (1993) Thermal management of electronic components with dielectric liquids. *JSME International Journal Series B Fluids and Thermal Engineering*, **36**, 1-25.

15. **Bergles, A. E.,** (2002) ExHFT for fourth generation heat transfer technology. *Experimental Thermal and Fluid Science*, **26**, 335-344.

16. **Bergles, A. E.** and **S. G. Kandlikar, (**2005) On the nature of critical heat flux in microchannels. *Transactions of the ASME-C-Journal of Heat Transfer*, **127**, 101-107.

17. **Bergles, A. E.** and **W. M. Rohsenow, (**1964) The determination of forced-convection surface-boiling heat transfer. *Journal of Heat Transfer*, **86**, 365-372.

18. **Bilir, S.,** (2002) Transient conjugated heat transfers in pipes involving two-dimensional wall and axial fluid conduction. *International Journal of Heat and Mass Transfer*, **45**, 1781-1788.

19. **Bowers, M. B.** and **I. Mudawar, (**1994) High flux boiling in low flow rate, low pressure drop mini-channel and micro-channel heat sinks. *International Journal of Heat and Mass Transfer*, **37**, 321-332.

20. **Brandner, J. J., W. Benzinger, U. Schygulla, S.Zimmermann,** and **K. Schubert, (**2007) *Metallic Micro Heat Exchangers: Properties, Applications and Long Term Stability*, **383**.

21. **Burns, J. A.** and **E. M. Cliff, (**2014) Numerical methods for optimal control of heat exchangers. In *American Control Conference (ACC),*June, 1649-1654.

22. **Chein, R.** and **G. Huang, (**2004) Thermoelectric cooler application in electronic cooling. *Applied Thermal Engineering*, **24**, 2207-2217.

23. **Chintakrinda, K., R. J. Warzoha, R. D. Weinstein,** and **A. S. Fleischer,** **(**2012) Quantification of the impact of embedded graphite nanofibers on the transient thermal response of paraffin phase change material exposed to high heat fluxes. *Journal of Heat Transfer*, **134**, 071901.

24. **Chintakrinda, K., R. D. Weinstein,** and **A. S. Fleischer, (**2011) A direct comparison of three different material enhancement methods on the transient thermal response of paraffin phase change material exposed to high heat fluxes. *International Journal of Thermal Sciences*, **50**, 1639-1647.

25. **Chisholm, D.,** (1983) Two-phase flow in pipelines and heat exchangers. *G. Godwin in association with Institution of Chemical Engineers.*

26. **Chiu, H.C., J.H. Jang, H.W. Yeh,** and **M. S. Wu, (**2011) The heat transfer characteristics of liquid cooling heatsink containing microchannels. *International Journal of Heat and Mass Transfer,* **54**, 34-42.

27. **Choi, S. U.,** (2009) Nanofluids: from vision to reality through research. *Journal of Heat Transfer,* **131**, 033106.

28. **Chowdhury, I., R. Prasher, K. Lofgreen, G. Chrysler, S. Narasimhan, R. Mahajan, D. Koester, R. Alley,** and **R. Venkatasubramanian, (**2009) On-chip cooling by superlattice-based thin-film thermoelectrics. *Nature Nanotechnology,* 4, 235-238.

29. **Chu, R. C., R.E. Simons,** and **G. M. Chrysler,** (1999) Experimental investigation of an enhanced thermosyphon heat loop for cooling of a high performance electronics module. *In Semiconductor Thermal Measurement and Management Symposium,* Fifteenth Annual IEEE, March, 1-9.

30. **Colgan, E. G., B. Furman, M. Gaynes, W. S. Graham, N. C. LaBianca, J. H. Magerlein, R.J. Polastre, M. B. Rothwell, R. J. Bezama, R. Choudhary,** and **K. C. Marston,** (2007) A practical implementation of silicon microchannel coolers for high power chips. *IEEE Transactions on Components and Packaging Technologies,* **30**, 218-225.

31. **Cornwell, K.** and **P.A. Kew,** (1993) Boiling in small parallel channels. *In Energy Efficiency in Process Technology,*624-638.

32. **Cotter, T.P.,** (1984) Principles and prospects for micro heat pipes *(No. LA-UR-84-120; CONF-840578-1).* Los Alamos National Lab., NM (USA), January.

33. **Dharaiya, V. V.** and **S. G. Kandlikar,** (2012) Numerical investigation of heat transfer in rectangular microchannels under H2 boundary condition during developing and fully developed laminar flow. *Journal of Heat Transfer*, **134**, 020911.

34. **Ebadian, M.A.** and **C. X. Lin, (**2011) A review of high-heat-flux heat removal technologies. *Journal of Heat Transfer*, **133**, 110801.

35. **Fan, L.** and **J.M. Khodadadi,** (2011) Thermal conductivity enhancement of phase change materials for thermal energy storage: a review. *Renewable and Sustainable Energy Reviews,* **15**, 24-46.

36. **Farid, M.M., A.M. Khudhair, S. A. K. Razack,** and **S. Al-Hallaj,** **(**2004) A review on phase change energy storage: materials and applications. *Energy Conversion and Management*, **45**, 1597-1615.

37. **Fu, Y., N. Nabiollahi, T. Wang, S. Wang, Z. Hu, B. Carlberg, Y. Zhang, X. Wang,** and **J. Liu,** (2012) A complete carbon-nanotube-based on-chip cooling solution with very high heat dissipation capacity. *Nanotechnology,***23**, 045304.

38. **Ge, H., H. Li, S. Mei,** and **J. Liu,** (2013) Low melting point liquid metal as a new class of phase change material: An emerging frontier in energy area. *Renewable and Sustainable Energy Reviews,* **21**,331-346.

39. **Gunnasegaran, P., H.A. Mohammed, N. H. Shuaib,** and **R. Saidur,** (2010) The effect of geometrical parameters on heat transfer characteristics of microchannels heat sink with different shapes. *International Communications in Heat and Mass Transfer*, **37**, 1078-1086.

40. **Hall, D.D.** and **I. Mudawar, (**2000) Critical heat flux (CHF) for water flow in tubes—II.: Subcooled CHF correlations. *International Journal of Heat and Mass Transfer,* **43**, 2605-2640.

41. **Hannemann, R.J.,** (2003)*Thermal control of electronics: Perspectives and prospects.*

42. **Harahap, F.** and **H. N. McManus, (**1967) Natural convection heat transfer from horizontal rectangular fin arrays. *Journal of Heat Transfer,* 89, 32-38.

43. **Heo, S., S.S. Jogwar,** and **P. Daoutidis, (**2011) Dynamics and control of high duty counter-current heat exchangers. In *Control & Automation (MED) 19th Mediterranean Conference, IEEE,* June, 034-1039.

44. **Hetsroni, G., A. Mosyak, E. Pogrebnyak,** and **L.P. Yarin,** (2005) Heat transfer in micro-channels: Comparison of experiments with theory and numerical results. *International Journal of Heat and Mass Transfer,* **48**, 5580-5601.

45. **Ho, J. Y., Wong, K. K., Leong, K. C.,** and **Wong, T. N.,** (2017) Convective heat transfer performance of airfoil heat sinks fabricated by selective laser melting, *International Journal of Thermal Sciences,*114, 213-228.

46. **Hosseinizadeh, S. F., F. L. Tan,** and **S. M. Moosania,** (2011) Experimental and numerical studies on performance of PCM-based heat sink with different configurations of internal fins. *Applied Thermal Engineering,* **31**, 3827-3838.

47. **Howard, A. H.** and **G. P. Peterson,** (1995) Investigation of a heat pipe array for convective cooling. *Transactions of the ASME-P-Journal of Electronic Packaging,* **117**, 208-214.

48. **Hsu, Y. Y.,** (1962) On the size range of active nucleation cavities on a heating surface. *Journal of Heat Transfer,* **84**, 207-213.

49. **Huh, C., J. Kim,** and **M. H. Kim,** (2007) Flow pattern transition instability during flow boiling in a single microchannel. International *Journal of Heat and Mass Transfer*, **50**, 1049-1060.

50. **Incropera, F. P.,** (1988) Convection heat transfer in electronic equipment cooling. ASME, Transactions, *Journal of Heat Transfer*, **110**, 1097-1111.

51. **Inasaka, F.** and **H. Nariai,** (1989) Critical heat flux subcooled flow boiling with water. *In Fourth International Topical Meeting on Nuclear Reactor Thermal-Hydraulics* (NURETH-4). Proceedings. Vol. 1.

52. **Jang, S. P.** and **S. U. Choi,** (2004) Role of Brownian motion in the enhanced thermal conductivity of nanofluids. *Applied Physics Letters*, **84**, 4316-4318.

53. **Jang, S. P.** and **S. U. Choi,** (2006) Cooling performance of a microchannel heat sink with nanofluids. *Applied Thermal Engineering*, **26**, 2457-2463.

54. **Jiang, L., J. Mikkelsen, J. M. Koo, D. Huber, S. Yao, L. Zhang, P. Zhou, J. G. Maveety, R. Prasher, J. G. Santiago,** and **T. W. Kenny,** (2002) Closed-loop electroosmotic microchannel cooling system for VLSI circuits. *IEEE Transactions on Components and Packaging Technologies*, **25**, 347-355.

55. **Jones, C. D** and **L. F. Smith,** (1970) Optimum Arrangement of Rectangular Fins on Horizontal Surfaces for Convection Heat Transfer, *Journal of Heat Transfer*, **92**, 6-10.

56. **Kandasamy, R., X. Q. Wang,** and **A. S. Mujumdar,** (2007) Application of phase change materials in thermal management of electronics. *Applied Thermal Engineering*, **27**, 2822-2832.

57. **Kandasamy, R., Wang, X. Q.** and **A. S. Mujumdar**, (2008) Transient cooling of electronics using phase change material (PCM)-based heat sinks. *Applied Thermal Engineering*, **28**, 1047-1057.

58. **Kandlikar, S. G.,** (2002) Two-phase flow patterns, pressure drop, and heat transfer during boiling in minichannel flow passages of compact evaporators. *Heat Transfer Engineering*, **23**, 5-23.

59. **Kandlikar, S. G.,** (2005) High flux heat removal with microchannels—a roadmap of challenges and opportunities. *Heat Transfer Engineering*, **26**, 5-14.

60. **Kandlikar, S. G.,** (2006) Nucleation characteristics and stability considerations during flow boiling in microchannels. *Experimental Thermal and Fluid Science*, **30**, 441-447.

61. **Kandlikar, S. G.,** (2012) History, advances, and challenges in liquid flow and flow boiling heat transfer in microchannels: a critical review. *Journal of Heat Transfer*, **134**, 034001.

62. **Kandlikar, S. G.** and **Bapat, A. V.,** (2007) Evaluation of jet impingement, spray and microchannel chip cooling options for high heat flux removal. *Heat Transfer Engineering*, **28**, 911-923.

63. **Kandlikar, S. G.** and **Grande, W. J.,**(2003) Evolution of Microchannel Flow Passages--Thermohydraulic Performance and Fabrication Technology. *Heat Transfer Engineering*, **24**, 3-17.

64. **Kandlikar, S. G., W.K. Kuan, D. A. Willistein,** and **J. Borrelli, (**2006) Stabilization of flow boiling in microchannels using pressure drop elements and fabricated nucleation sites. *Journal of Heat Transfer*, **128**, 389-396.

65. **Kandlikar, S. G.** and **P. Balasubramanian,** (2004) An extension of the flow boiling correlation to transition, laminar, and deep laminar flows in minichannels and microchannels. *Heat Transfer Engineering*, **25**, 86-93.

66. **Kasza, K. E., Didascalou, T.,** and **Wambsganss, M. W.** (1997). Microscale flow visualization of nucleate boiling in small channels: mechanisms influencing heat transfer (No. ANL/ET/CP--92073; CONF-9706130--2). Argonne National Lab., IL (United States).

67. **Kennedy, J. E., G. M. Roach, M. F. Dowling, S. I. Abdel-Khalik, S. M. Ghiaasiaan, S. M. Jeter,** and **Z. H. Quershi,** (2000) The onset of flow instability in uniformly heated horizontal microchannels. *Journal of Heat Transfer*, **122**, 118-125.

68. **Kercher, D. S., J. B. Lee, O. Brand, M. G. Allen,** and **A.,Glezer,** (2003) Microjet cooling devices for thermal management of electronics. *IEEE Transactions on Components and Packaging Technologies*, **26**, 359-366.

69. **Khan, M. G.** and **Fartaj, A.,**(2011) A review on microchannel heat exchangers and potential applications. *International Journal of Energy Research*, **35**, 553-582.

70. **Khodadadi, J. M.** and **S. F. Hosseinizadeh,**(2007) Nanoparticle-enhanced phase change materials (NEPCM) with great potential for improved thermal energy storage. *International Communications in Heat and Mass Transfer*, **34**, 534-543.

71. **Kim, S. J.** and **S. W. Lee,** *Air Cooling Technology for Electronic Equipment*, CRC press, 1996.

72. **Kim, J.,** (2007) Spray cooling heat transfer: the state of the art. *International Journal of Heat and Fluid Flow*, **28**, 753-767.

73. **Koo, J. M., S. Im, L. Jiang,** and **K. E. Goodson,** (2005) Integrated microchannel cooling for three-dimensional electronic circuit architectures. *Journal of Heat Transfer,* **127**, 49-58.

74. **Krishnamurthy, S.** and **Y. Peles,** (2010) Flow boiling heat transfer on micro pin fins entrenched in a microchannel. *Journal of Heat Transfer,* **132**, 041007.

75. **Lafdi, K., O. Mesalhy, and A. Elgafy, (**2008) Graphite foams infiltrated with phase change materials as alternative materials for space and terrestrial thermal energy storage applications. *Carbon,* **46**, 159-168.

76. **Lee, J.** and **I. Mudawar, (**2005a) Two-phase flow in high-heat-flux micro-channel heat sink for refrigeration cooling applications: Part I—pressure drop characteristics. *International Journal of Heat and Mass Transfer*, **48**, 928-940.

77. **Lee, J.** and **I. Mudawar, (**2005b) Two-phase flow in high-heat-flux micro-channel heat sink for refrigeration cooling applications: Part II—heat transfer characteristics. *International Journal of Heat and Mass Transfer,* **48**, 941-955.

78. **Lee, J.** and **I. Mudawar, (**2007) Assessment of the effectiveness of nanofluids for single-phase and two-phase heat transfer in micro-channels. *International Journal of Heat and Mass Transfer,* **50**, 452-463.

79. **Leong, K. C., J. Y. Ho,** and **K. K. Wong,** (2017) A critical review of pool and flow boiling heat transfer of dielectric fluids on enhanced surfaces. *Applied Thermal Engineering*, **112**, 999-1019.

80. **Levin, P. P., A.Shitzer,** and **G. Hetsroni, (**2013) Numerical optimization of a PCM-based heat sink with internal fins. *International Journal of Heat and Mass Transfer,* **61**, 638-645.

81. **Li, D., S. T. Huxtable, A. R. Abramson,** and **A. Majumdar,** (2005) Thermal transport in nanostructured solid-state cooling devices. *Transactions of the ASME-C-Journal of Heat Transfer,* **127**, 108.

82. **Liu, D., P. S. Lee,** and **S. V. Garimella,** (2005) Prediction of the onset of nucleate boiling in microchannel flow. *International Journal of Heat and Mass Transfer,* **48**, 5134-5149.

83. **Mahmoud, S., A. Tang, C. Toh, A. D. Raya,** and **S. L. Soo, (**2013) Experimental investigation of inserts configurations and PCM type on the thermal performance of PCM based heat sinks. *Applied Energy,* **112**, 1349-1356.

84. **Maidi, A., M. Diaf,** and **J. P. Corriou,** (2008) Optimal linear PI fuzzy controller design of a heat exchanger. *Chemical Engineering and Processing: Process Intensification*, **47**, 938-945.

85. **Mala, G. M., D. Li, C. Werner, H. J. Jacobasch,** and **Y. B. Ning,** (1997) Flow characteristics of water through a microchannel between two parallel plates with electrokinetic effects. *International Journal of Heat and Fluid Flow*, **18**, 489-496.

86. **Martínez-Galván, E ., Antón, R., Ramos, J. C.,** and **Khodabandehb, R.,** (2013), Influence of surface roughness on a spray cooling system with R134a. Part I: Heat transfer measurements, *Experimental Thermal and Fluid Science*, **46**, 183-190.

87. **Mathisen, K.W., M. Morari,** and **S. Skogestad,** (1994) Dynamic models for heat exchangers and heat exchanger networks. *Computers &Chemical Engineering*,**18**, S459-S463.

88. **McFarlane, D.** and **K. Glover,** (1992) A loop-shaping design procedure using H1 synthesis. *IEEE Transactions on Automatic Control*, **37**, 759–769.

89. **Mehendale, S. S., A. M. Jacobi,** and **R. K. Shah,** (2000) Fluid flow and heat transfer at micro-and meso-scales with application to heat exchanger design. *Applied Mechanics Reviews,* **53**, 175-194.

90. **Mishima, K.** and **T. Hibiki,** (1996) Some characteristics of air-water two-phase flow in small diameter vertical tubes. *International Journal of Multiphase Flow*, **22**, 703-712.

91. **Morini, G. L.,**(2004) Single-phase convective heat transfer in microchannels: a review of experimental results. *International Journal of Thermal Sciences*, **43**, 631-651.

92. **Mudawar, I.,**(2001) Assessment of high-heat-flux thermal management schemes. *IEEE Transactions on Components and Packaging Technologies*, **24**, 122-141.

93. **Mudawar, I.,**(2013) Recent advances in high-flux, two-phase thermal management. *Journal of Thermal Science and Engineering Applications*, **5**, 021012.

94. **Murshed, S. S.** and **P. Estellé,** (2017) A state of the art review on viscosity of nanofluids. *Renewable and Sustainable Energy Reviews,* **76**, 1134-1152.

95. **Nevriva, P., S. Ozana,** and **L. Vilimec,** (2009) The finite difference method applied for the simulation of the heat exchangers dynamics. *Energy*, **10**, 4.

96. **Nguyen, C.T., G. Roy, C. Gauthier,** and **N. Galanis,** (2007) Heat transfer enhancement using Al2O3–water nanofluid for an electronic liquid cooling system. *Applied Thermal Engineering,* **27**, 1501-1506.

97. **Oktay, S.** and **Kammerer, H. C.,** (1982) A conduction-cooled module for high-performance LSI devices, *IBM Journal of Research and Development*, **26.**

98. **Owhaib, W.** and **B. Palm,** (2004) Experimental investigation of single-phase convective heat transfer in circular microchannels. *Experimental Thermal and Fluid Science,***28**, 105-110.

99. **Ozisik, N.,** *Finite Difference Methods in Heat Transfer*. CRC press, 1994.

100. **Pacheco-Vega, A., C. Ruiz-Mercado, K. Peters,** and **L. E. Vilchiz,** (2009) On-line fuzzy-logic-based temperature control of a concentric-tube heat exchanger facility. *Heat Transfer Engineering,* **30**, 1208-1215.

101. **Pakrouh, R., M. J. Hosseini,** and **A. A. Ranjbar,** (2015) A parametric investigation of a PCM-based pin fin heat sink. *Mechanical Sciences,* **6**, 65-73.

102. **Pakrouh, R., M. J. Hosseini, A. A. Ranjbar,** and **R. Bahrampoury,** (2015) A numerical method for PCM-based pin fin heat sinks optimization. *Energy Conversion and Management,***103**, 542-552.

103. **Pal, D.** and **Y. K. Joshi,** (1998) Thermal management of an avionics module using solid-liquid phase-change materials. *Journal of Thermophysics and Heat Transfer*, **12**, 256-262.

104. **Palm, B.,**(2001) Heat transfer in microchannels. *Microscale Thermophysical Engineering,* **5,**155-175.

105. **Papautsky, I., T. Ameel,** and **A. B. Frazier,** (2001) A review of laminar single-phase flow in microchannels. In ASME, Proceedings of *Int. Mech. Eng Congress Expos Proc (IMECE),*November, **2**, 3067-3075.

106. **Peng, X. F.** and **G. P. Peterson,** (1996) Convective heat transfer and flow friction for water flow in microchannel structures. *International Journal of Heat and Mass Transfer*, **39**, 2599-2608.

107. **Peng, X. F., B. X. Wang, G. P. Peterson,** and **H. B. Ma,** (1995) Experimental investigation of heat transfer in flat plates with rectangular microchannels. *International Journal of Heat and Mass Transfer*, **38**, 127-137.

108. **Phillips, R. J., L. R. Glicksman,** and **R. Larson,** (1990)Forced-convection, liquid-cooled, microchannel heat sinks.*Massachusetts Institute of Technology, U.S. Patent,* **4**,894,709.

109. **Qu, Z. G., W. Q. Li, J. L. Wang,** and **W. Q. Tao,** (2012) Passive thermal management using metal foam saturated with phase change material in a heat sink. *International Communications in Heat and Mass Transfer*, **39**, 1546-1549.

110. **Qu, W.** and **I. Mudawar,** (2002) Prediction and measurement of incipient boiling heat flux in micro-channel heat sinks. *International Journal of heat and mass transfer,***45**, 3933-3945.

111. **Qu, W.** and **I. Mudawar,** (2002) Experimental and numerical study of pressure drop and heat transfer in a single-phase micro-channel heat sink. *International Journal of Heat and Mass Transfer*, **45**, 2549-2565.

112. **Qu, W.** and **I. Mudawar,** (2004) Measurement and correlation of critical heat flux in two-phase micro-channel heat sinks. *International Journal of Heat and Mass Transfer,***47**, 2045-2059.

113. **Reay, D., R.McGlen,** and **P. Kew,** *Heat pipes: theory, design and applications*. Butterworth-Heinemann, 2013.

114. **Roffel, B.,** and **B. Betlem,** *Process Dynamics and Control: Modeling for Control and Prediction.* John Wiley & Sons, 2007.

115. **Rostami, A.A., A. S. Mujumdar,** and **N. Saniei,** (2002) Flow and heat transfer for gas flowing in microchannels: a review. *Heat and Mass Transfer*, **38**, 359-367.

116. **Rowe, D. M.** *CRC Handbook of Thermoelectrics*. CRC press,1995.

117. **Saha, S. K.** and **G. P. Celata,** *Instability in Flow Boiling in Microchannels*. Springer International Publishing, 2016.

118. **Saha, S. K., K. Srinivasan,** and **P. Dutta,** (2008) Studies on optimum distribution of fins in heat sinks filled with phase change materials. *Journal of Heat Transfer,* **130**, 034505.

119. **Sahoo, S. K., M. K. Das,** and **P. Rath, (**2016) Application of TCE-PCM based heat sinks for cooling of electronic components: A review. *Renewable and Sustainable Energy Reviews,* **59**, 550-582.

120. **Sanusi, O., R.Warzoha,** and **A. S. Fleischer,** (2011) Energy storage and solidification of paraffin phase change material embedded with graphite nanofibers. *International Journal of Heat and Mass Transfer,* **54**, 4429-4436.

121. **Sarangi, S., J. A. Weibel,** and **S. V. Garimella,** (2015) Effect of particle size on surface-coating enhancement of pool boiling heat transfer. *International Journal of Heat and Mass Transfer*, **81**, 103-113.

122. **Sato, T.** and **H. Matsumura,** (1964) On the conditions of incipient subcooled-boiling with forced convection. *Bulletin of JSME*, **7**, 392-398.

123. **Shah, R. K.** and **A. L. London,** *Laminar flow forced convection in ducts: a source book for compact heat exchanger analytical data*. Academic press, 1978.

124. **Shao, L., A. Raghavan, L. Emurian, M. C. Papaefthymiou, T.F. Wenisch, M. M. Martin,** and **K. P. Pipe, (**2014) On-chip phase change heat sinks designed for computational sprinting. In *Semiconductor Thermal Measurement and Management Symposium (SEMI-THERM), IEEE,*March, 29-34.

125. **Sharma, A., V. V. Tyagi, C. R. Chen,** and **D. Buddhi,** (2009) Review on thermal energy storage with phase change materials and applications. *Renewable and Sustainable energy reviews,* **13**, 318-345.

126. **Shatikian, V., G. Ziskind,** and **R. Letan,** 2005. Numerical investigation of a PCM-based heat sink with internal fins. *International Journal of Heat and Mass Transfer,***48**, 3689-3706.

127. **Shen, Q., D. Sun, , Y. Xu, , T. Jin, ,** and **X. Zhao,** (2014). Orientation effects on natural convection heat dissipation of rectangular fin heat sinks mounted on LEDs. *International Journal of heat and mass transfer,* **75**, 462-469.

128. **Shen, P., S. K. Aliabadi,** and **J. Abedi,** (2004) A review of single-phase liquid flow and heat transfer in microchannels. Proc. of the *2nd ICMM,* 17-19.

129. **Shoureshi, R.** and **H. M. Paynter, (**1983) Simple models for dynamics and control of heat exchangers. *American Control Conference, IEEE,* June, 1294-1298.

130. **Skogestad, S.** and **I. Postlethwaite,** *Multivariable feedback control: analysis and design,* 2nd ed., John Wiley, NJ, 2005.

131. **Sobhan, C. B.** and **G. P. Peterson,** *Microscale and nanoscale heat transfer: fundamentals and engineering applications*. CRC Press, 2008.

132. **Sobhan, C. B., R. L. Rag,** and **G. P. Peterson,** (2007) A review and comparative study of the investigations on micro heat pipes. *International Journal of Energy Research,* **31**, 664-688.

133. **Steinke, M. E.** and **S. G. Kandlikar,** (2004a) Review of single-phase heat transfer enhancement techniques for application in microchannels, minichannels and microdevices. *International Journal of Heat and Technology*, **22**, 3-11.

134. **Steinke, M. E.** and **S. G. Kandlikar,** (2004b) An Experimental investigation of flow boiling characteristics of water in parallel microchannels, *Journal of Heat Transfer* 126, 518-526.

135. **Steinke, M. E.** and **S. G. Kandlikar,** (2005) Single-phase liquid friction factors in microchannels. In *ASME 3rd International Conference on Microchannels and Minichannels*, January, 291-302.

136. **Stephanopoulos G.**, *Chemical process control*. Prentice hall, New Jersey, 1984.

137. **Sui, Y., C. J. Teo, P. S. Lee, Y. T. Chew,** and **C. Shu,** (2010) Fluid flow and heat transfer in wavy microchannels. *International Journal of Heat and Mass Transfer*, **53**, 2760-2772.

138. **Taler, D.,** (2015) Mathematical modeling and control of plate fin and tube heat exchangers. *Energy Conversion and Management*, **96**, 452-462.

139. **Thome, J. R.,**(2006) State-of-the-art overview of boiling and two-phase flows in microchannels. *Heat Transfer Engineering,* **27**, 4-19.

140. **Triplett, K. A., S. M. Ghiaasiaan, S. I. Abdel-Khalik,** and **D. L. Sadowski,** (1999) Gas–liquid two-phase flow in microchannels Part I: two-phase flow patterns. *International Journal of Multiphase Flow,* **25**, 377-394.

141. **Tsai, C. Y., H. T. Chien, P. P. Ding, B. Chan, T. Y. Luh,** and **P. H. Chen,** (2004) Effect of structural character of gold nanoparticles in nanofluid on heat pipe thermal performance. *Materials Letters*, **58**, 1461-1465.

142. **Tuckerman, D. B.** and **R. F. W. Pease,** (1981) High-performance heat sinking for VLSI. *IEEE Electron device letters*, **2**, 126-129.

143. **Venkatasubramanian, R., E. Siivola, T. Colpitts,** and **B. O'quinn,** (2001) Thin-film thermoelectric devices with high room-temperature figures of merit. *Nature*, **413**, 597-602.

144. **Vinaya, K. V., K. Ramkumar,** and **V. Alagesan,** (2012) Control of heat exchangers using model predictive controller. *In Advances in Engineering, Science and Management (ICAESM), 2012 IEEEInternational Conference* on March, 242-246.

145. **Vlasie, C., H. Macchi, J. Guilpart,** and **B. Agostini,** (2004) Flow boiling in small diameter channels. *International Journal of Refrigeration,* **27**, 191-201.

146. **Voller, V. R.** and **C. R Swaminathan,** (1991) Source-based method for solidification phase change. *Numerical Heat Transfer, Part B Fundamentals*, **19**, 175-189.

147. **Wang, X. Q.** and **Mujumdar, A. S.** (2007) Heat transfer characteristics of nanofluids: a review, *International Journal of Thermal Sciences,***46**, 1-19.

148. **Webb, B. W.** and **C. F. Ma, (**1995) Single-phase liquid jet impingement heat transfer. *Advances in Heat Transfer*, **26**, 105-217.

149. **Weinstein, R. D., T. C. Kopec, A.S. Fleischer, E. D'Addio,** and **C.A. Bessel,** (2008) The experimental exploration of embedding phase change materials with graphite nanofibers for the thermal management of electronics. *Journal of Heat Transfer*, **130**, 042405.

150. **Weng, Y. C., H. P. Cho, C.C. Chang,** and **S. L. Chen,** (2011) Heat pipe with PCM for electronic cooling. *Applied Energy*, **88**, 1825-1833.

151. **Whitaker, J. C.,** *Microelectronics* 2nd Edition 14, CRC Press, 2005.

152. **Winkler, J., J. Killion,** and **S. Garimella,** (2012) Void fractions for condensing refrigerant flow in small channels. Part II: Void fraction measurement and modeling. *International Journal of Refrigeration*, **35**, 246-262.

153. **Wirtz, J.,** *Essentials of Services Marketing*, FT Press,2012.

154. **Wirtz, R. A., N. Zheng,** and **D. Chandra, (**1999) Thermal management using" dry" phase change material. In *Semiconductor Thermal Measurement and Management Symposium*, Fifteenth Annual IEEE March, 74-82.

155. **Wu, H. Y.** and **P. Cheng,** (2003) Friction factors in smooth trapezoidal silicon microchannels with different aspect ratios. *International Journal of Heat and Mass Transfer*, **46**, 2519-2525.

156. **Yang, J., L. Yang, C. Xu,** and **X. Du,** (2015) Numerical analysis on thermal behavior of solid–liquid phase change within copper foam with varying porosity. *International Journal of Heat and Mass Transfer*, **84**, 1008-1018.

157. **Yarin, L. P., A. Mosyak,** and **G. Hetsroni,** *Fluid flow, heat transfer and boiling in micro-channels.* Springer Science & Business Media, 2008.

158. **Yazicioğlu, B.** and **H. Yüncü,** (2007) Optimum fin spacing of rectangular fins on a vertical base in free convection heat transfer. *Heat and Mass Transfer*, **44**, 11-21.

159. **Zalba, B., J. M. Marín, L. F. Cabeza,** and **H. Mehling,** (2003) Review on thermal energy storage with phase change: materials, heat transfer analysis and applications. *Applied Thermal Engineering*, **23,**251-283.

160. **Zames, G.** (1979) Feedback and optimal sensitivity: Model reference transformations, weighted seminorms, and approximate inverses. Proc. *17th AUerton Conf.*, 744-752.

161. **Zebarjadi, M.,** (2015) Electronic cooling using thermoelectric devices. *Applied Physics Letters*, **106**, 203506.

162. **Zhang, W., T. Hibiki, K. Mishima,** and **Y. Mi,** (2006) Correlation of critical heat flux for flow boiling of water in mini-channels. *International Journal of Heat and Mass Transfer,***49**, 1058-1072.

LIST OF PUBLICATIONS

INTERNATIONAL JOURNALS

1. **Indulakshmi, B.** and **Madhu, G.**, (2018), Heat transfer modeling and simulations for electronic cooling systems embedded with phase changing materials, *Heat Transfer—Asian Research,* **47**, 185-202.
   (DOI: 10.1002/htj.21298) *(Published by Wiley Periodicals, Inc.)*

2. **Indulakshmi, B.** and **Madhu, G.**, (2018), Effect of Phase Changing Material Encapsulation on Flow Boiling in a Microchannel Based Electronics Cooling System, *Multiphase Science and Technology*,**30**, 221-237.
   (DOI: 10.1615/MultScienTechn.2018022102) (*Published by Begell House Inc.*)
3. **Indulakshmi, B.** and **Madhu, G.**, (2015), Control Simulation of Heat Transfer in Rectangular Microchannel, *International Journal of Industrial Electronics and Control*, Vol. 7, No. 1, pp. 1-11.
   (www.irphouse.com/ijiec/ijiec7v1_01.pdf)

INTERNATIONAL CONFERENCES

1. **Indulakshmi, B.** and **Madhu, G.**, (2017), Dynamic thermal modeling and simulation of electronics cooling system with latent heat storage encapsulation, *Proceedings of CHT-17, ICHMT International Symposium on Advances in Computational Heat Transfer*, May 28-June 1, 2017, Napoli, Italy.
   (DOI: 10.1615/ICHMT.2017.CHT-7.860) (*Published by International Centre for Heat and Mass Transfer Digital Library)*

2. **Indulakshmi, B.** and **Madhu, G.**, (2017), Modeling and simulation of phase changing material assisted flow boiling in rectangular microchannels, (IHMTC2017-15-0698) *24th National and 2nd International ISHMT-ASTFE Heat and Mass Transfer Conference (IHMTC-2017)*, December 27-30, 2017, BITS Pilani, Hyderabad, India.

3. **Indulakshmi, B.** and **Madhu, G.**, (2018),Dynamic Thermal Modeling and Simulation of Boiling Heat Transfer in PCM Assisted Diverging Microchannels, Paper ID –116, *Asian Joint Workshop on Thermophysics and Fluid Science AJWTF-7*, November 21-24, 2018, Trivandrum, India.

CURRICULUM VITAE

B. Indulakshmi was born in Aluva, Ernakulam District of Kerala, India in 1983. She obtained her B. Tech. Degree in Instrumentation and Control Engineering from N.S S. College of Engineering, Palakkad, (University of Calicut) in 2005 and further obtained M. E. in Control and Instrumentation from Karunya University, Coimbatore in 2007. She has more than 8 years of teaching experience in various engineering colleges in Kerala. Her research interest includes control system design, dynamic system modeling and simulation, and instrumentation. She has so far published four research papers in international journals and presented more than eight papers in international/national conferences. She has participated and presented her research paper in the 7th International Symposium on Advances in Computational Heat Transfer, CHT-17, held in Napoli, Italy, during 28 May - 02 June 2017.